25X1

Approved For Release 2009/05/06 : CIA-RDP80T00246A008200300002-6

INVESTIGATIONAL WORK CARRIED OUT IN THE USSR WITH REGARD TO ICE ENGINEERING PROBLEMS IN HYDRO-ELECTRIC CONSTRUCTION

by

B. V. Proskuryakov

Professor, Doctor of Science

The severe climatic conditions of the Soviet Union left their special mark on the design of hydraulic structures and on the construction and operation methods.

The Soviet design-engineers, constructors, operating personnel of hydro-electric power plants and scientific workers of research institutions had to work hard in order to overcome numerous difficulties which merciless nature created on the way of building and operation of hydraulic structures. This paper presents a brief description of the results achieved by the Soviet ice-engineers.

Main construction methods in winter time. Excavation.

Peculiar are the excavation methods used in the USSR. In view of excavation of frozen soils being immeasurably harder than that of thawy ones, the constructors use as the principal means of warming soils either heat insolation in pre-winter period or special heating of frozen soils. Here, in this country, a number of methods and procedures of heating were developed and necessary equipment was designed for this purpose.

Winter concreting is performed in special housings of different size and forms. Wide use is made in the Soviet Union of the "thermos method" which consists in pre-heating of ingredients of concrete mixture before its pouring in blocks of structures with subsequent warming of concrete by

heat-insolating cover. While concreting in cold weather use is also made of electric heating of placed concrete, either of its exposed surfaces or of the whole mass of interior concrete. In building of industrial structures wide use is made of the method of steam curing of concrete. Within the last few years investigations have been carried out with regard to using in hydro-electric construction the method of cold concrete with chemicals which lower the temperature of water crystallization and provide by this hardening of concrete at low temperatures.

Methods of design of water temperatures in reservoirs and stream flows.

In the 20-ies the Russian researcher Rudovez used the equation of thermal equilibrium for the design of evaporation from the surface of the Caspian Sea. It was the first attempt to establish interrelations between water temperature variations in a reservoir and variations of meteorological factors. This method of temperature design on the basis of thermal equilibrium was further developed by a well known physicist, Professor Academician V. V. Shuleykin, as a result of his investigations on the Kara Sea. A considerable stride forward on this way was made by engineer N. M. Bernadsky who in his works presents the equation of thermal equilibrium in differential form and proposes methods of its integration. Moreover, N. M. Bernadsky's water temperature design accounted for the design of water flows in reservoirs, for which purpose he worked up a method of plotting the stream flow lines. The problems of design of water temperature distribution over the whole depth of stream flows and reservoirs were studied by the B. M. Makkaveev's school by the VNIIG (the All-Union Scientific Research Institute of Hydrotechnics) and by the Hydro-project. The combined efforts of these institutions resulted in solving a number of practically important problems of ice-engineering.

Ice processes in rivers, reservoirs and channels

In the 20-ies large scale development of hydro-electric projects started in the USSR and in connection with this there were carried out field investigations of winter regime in rivers and reservoirs determining the success of hydro-electric power plants operation. We should mark out the investigations carried out at the construction of the Volchov, Svir, Dnieper, Chirchick and other power projects. The results of these investigations are summarized in the works by engineers E.G. Joganson, A.M. Estifeev, F.S. Bydin, V.E. Timonov and others. Later on in the 30-ies an Ice-Engineering Laboratory was organized in the All-Union Scientific Research Institute of Hydrotechnics in Leningrad, of which the engineering staff made a considerable contribution to solving the problems of ice-engineering. Worthy of note are also the works of the State Hydrological Institute (GGL) and the Hydroproject.

As the result of the investigational work carried out by the above institutions, we have available at present the design prediction methods which permit us to solve with an acceptable degree of accuracy the problems pertaining to frazil ice regime, ice jamming and clogging phenomena in rivers. Besides, the above mentioned institutions worked out the methods of combatting ice troubles during the construction and operation of power plants.

Measures were accepted for:

a) controlling of ice processes upstream and downstream of hydro-plants during spring and autumn ice-drift.

b) ice passing through hydraulic structures during the construction and operation periods.

c) preventing metal structures of power house from freezing.

The problems concerning the design of static and dynamic ice pressure against hydraulic structures are also thoroughly studied and recommendations are given. Artificial frost is also widely used in hydro-electric construction.

This large-scale investigational work in the field of ice-engineering permitted also to study in detail the physical constants of natural ice.

The afore-said investigations were widely discussed in the Soviet technical literature - in periodicals as well as in special publications.

ICE AFFECTING ENGINEERING STRUCTURES ON THE SIBERIAN RIVERS DURING ICE-RUN

by

K. N. Korzhavin

Doctor of Technical Sciences

1) Introduction

At the present time in the U.S.S.R. widespread development of hydro electric power projects and transportation facilities is in progress. Particularly in Siberia, the effects of ice on these structures, during construction and operation, require special consideration. In the more severe climates, a considerable thickness of ice usually forms on the rivers, followed by a violent spring break-up, heavy ice runs, and frequent formation of ice jams and packs. The associated problems have been studied extensively, and the results of long-term investigation by the author are contained in this paper.

2) Behaviour and Performance of Bridge Piers during Ice-Run

Field observations of the action of ice on hydraulic structures and bridge piers in Siberia were made between 1934 and 1958, and the process of ice breaking by piers during the 1945-1958 ice runs was filmed. Some of the results noted were as follows:

When an ice cake meets a pier, the vertical face of the pier cuts it for a length of about 0.1 to 0.5 meters causing local compression, and forces are set up which either break the cake or bring it to a stop.

An inclined ice-cutting pier face facilitates break-up of an ice sheet by cutting from below, and reduces the possibility of ice jamming.

The width of a strip cut by the pier in an ice sheet does not exceed the maximum width of the pier.

3) Mechanical Properties of Ice During Ice-Run:

In order to determine ice strength during an ice-run, the author has tested more than 1,500 ice samples, and has drawn the following conclusions:

a) - At the beginning of the spring ice-run, compressive strength and resistance to bending of ice may reduce by as much as three times. 0,5 – 3 times.

b) - Local compression of ice due to pier penetration may increase interaction forces 2 to 2.5 times.

c) - As the rate of deformation of ice increases, the compressive strength decreases. The following relationship was obtained experimentally:

$$R_{com} = \frac{R}{\sqrt[3]{V_o}} \quad - - - \quad (1)$$

which is true when $V_o > 0.1$ m/sec.

Design values for the ultimate strength of ice during an ice-run are given in Table I.

Table I

Design values of ice ultimate strength, t/m^2

Character of Interaction	Rivers of the North and Siberia: Vo = 0.5 m/sec	Vo = 1.0 m/sec	Vo = 1.5 m/sec	Direction of force toward the axis of crystallization
1. Compression	65	50	45	Normal
2. Local bearing	160	125	110	"
3. Bending	60	45	40	"

Character of Interaction	Vo = 0.5 m/sec	Vo = 1.0 m/sec	Vo = 1.5 m/sec	Direction of force toward the axis of crystallization
4. Shearing		30-40		parallel
5. Tension		70-90		"

Tests by the author on 73 ice samples showed that ice-run resistance is influenced greatly by the shape of a penetrating object. The form coefficient (m) for a pier triangular in plan is given by the following equation, confirmed experiementally:

$$m = 0.39\ (1 + \alpha) \quad - \quad - \quad - \quad (2)$$

where α is 1/2 of the pier nose angle.

In the author's opinion, existing standards for determining ice loading upon structures require refinements.

4) Proposed Design Methods:

Assumptions are based on N. A. Rynin's supposition that the maximum possible ice pressure against a structure would be that necessary to break the ice or to bring it to a stop.

a) - Piers with Vertical Cutting Face:

Ice pressure (P) developed at the moment of cutting a large ice sheet by a pier with vertical cutting face is the greatest possible and is given by the equation

$$P = K_p\ b_o\ h \quad - \quad - \quad - \quad (3)$$

where h is ice sheet thickness
b_o is width of pier
K_p is a coefficient for local conditions given by the expression

$$K_p = \frac{2.5\, m\, k\, R_{com}}{\sqrt{V_o}}$$

where 2.5 is local bearing coefficient
m depends upon the form of the pier plan
k is the coefficient of contact
R_{com} is the compressive strength of ice
Vo is the velocity of the ice sheet

b) - Piers with Inclined Cutting Face:

When an ice sheet meets a pier with inclined cutting face, the ice may break due to shear bending. An analysis of observations made during break-up of an ice cover by piers having an inclined cutting fall produced the following relationships for determining ice pressure against piers:

Breaking by Shear

$$P = b_o \; h \; R_s \frac{K}{\sin\alpha} \quad - \quad - \quad - \quad (4)$$

where R_s is ultimate strength of ice in shear

Breaking by Bending

$$P = 0.66 \, R_b \, h^2 \, \frac{\left(\frac{b_o}{h} + 12\cos\alpha\right)}{12\sin\alpha - tg\beta} \quad - \quad (5)$$

where R_b is ultimate strength of ice in bending
β is angle of inclination of cutting face to the horizontal.

The equations for shear and bending were compared with the results of 13 field observations, and in 11 cases showed good agreement.

5) The Method of Determining Ice Pressure in Field Conditions:

When a large ice field is cut by a pier, the pressure (H) against the pier is given by the proposed equation:

$$H = c + fA \, (V_1 - V_o)^2 \quad - \quad - \quad - \quad (6)$$

where c is given by the expression

$$V_1 = V_o - \sqrt{\frac{c}{fA}} \, th \, \frac{(t_1 - t_o)\sqrt{cfA}}{m} \quad - (7)$$

In (6) and (7) above;

f is the coefficient of overall resistance to movement of the ice field
A is the area of the ice field
V_1 is the velocity of the ice field
V_o is the velocity of the flowing water
$(t_1 - t_o)$ is the time of cutting
m is the mass of the ice field.

TABLE II

Comparison of the results obtained by means of equations (6) and (7) with actual measurements are given in Table II.

Comparison of Actual and Design Ice-Pressure
(in tons)

	I C E F I E L D S						
	No. 1	No. 2	No. 3	No. 4	No. 5	No. 6	No. 7
Determined by the Author's method	72.5	25.5	54.5	56.0	66.5	92.0	88.5
Actual Pressure	45.8	17.5	46.4	45.3	21.2	62.6	55.0

Next 16 Page(s) In Document Denied

25X1

PROTECTION DES OUVRAGES HYDROTECHNIQUES CONTRE LA SOUS-PRESSION ENGENDRÉE PAR L'ÉCOULEMENT DE L'EAU

* * *

PROF. R. CEBERTOWICZ & PROF. AGRÉGÉ W. JAROCKI
Laboratoire d'hydraulique et d'hydrologie à l'École polytechnique de Gdansk

* * *

SOMMAIRE

L'article traite des évacuateurs de fond d'un barrage, ainsi que d'un clapet de vanne d'un barrage mobile où, dans certaines conditions, se produit une aspiration d'air, engendrée par l'écoulement de l'eau.

Les conditions dans lesquelles l'aspiration de l'air s'était produite ont été réalisées sur des modèles hydrauliques des ouvrages précités. On y a observé la marche de ce phénomène, ainsi que des phénomènes associés qui étaient accompagnés de bruits et d'ébranlements de la construction.

Afin de protéger l'installation contre l'aspiration de l'air, divers dispositifs ont été aménagés sur modèles hydrauliques; ces derniers étaient destinés à interrompre la couche d'eau afin de faciliter l'accès de l'air à l'espace par en-dessous de la dite couche. L'usage de ces dispositifs n'a pas donné lieu à des solutions générales, vu qu'ils remplissaient leur fonction

uniquement dans des conditions favorables, en dépendance de l'épaisseur de la couche d'eau retombante, de la hauteur de la chute, de la position des dispositifs de fermeture, etc.

Les études réalisées sur modèles réduits ont donné lieu à la conclusion essentielle suivante: dans le cas où l'aspiration se produit il convient tout simplement d'amener l'air d'une manière artificielle à l'espace où a lieu la sous-pression; toutefois, les recherches ultérieures concernant l'aération naturelle des jets d'eau ne sont pas à négliger.

INTRODUCTION

Certains ouvrages hydrotechniques existants en Pologne accusent la naissance de chocs hydrauliques, une déformation des jets d'eau, des ébranlements des constructions, etc. Il a été constaté que lesdits phénomènes se produisent en raison de l'entraînement de l'air par les filets d'eau en écoulement.

L'article présente la description de ces phénomènes en cours d'essais effectuées sur un modèle réduit de pertuis évacuateurs et sur le modèle d'un clapet de vanne d'un barrage mobile, ainsi que l'étude des dispositifs de défense contre les suites nuisibles desdits phénomènes.

ÉTUDE DES ÉVACUATEURS D'UN BARRAGE

Le modèle d'un déversoir de barrage, fermé à l'aide de segments ainsi que des évacuateurs de fond, fermés à l'aide de vannes, a été construit. La hauteur des évacuateurs de fond en nature se chiffrait à 3,5 m. à l'amenée et à 4,75 m. à l'échappement (Fig. 1). L'écoulement maximum à travers le déversoir se montait à 33 m. ^{3}/ sec. par mètre courant du déversoir, tandis que l'écoulement maximum à travers un évacuateur était de 180 m. ^{3}/ sec.

On a constaté qu'en dirigeant l'écoulement de l'eau à travers l'ouverture de l'évacuateur de fond seulement une partie de la section élargie de l'échappement était remplie d'eau, la partie supérieure de la section étant occupée par l'air. Le niveau de l'eau dans la section élargie de l'évacuateur dépendait de la hauteur de l'ouverture de la vanne.

Dans le cas où, au-dessus de l'évacuateur, le segment du déversoir était ouvert, la couche d'eau s'écoulant à travers le déversoir recouvrait complètement l'ouverture de l'évacuateur. Dans ces conditions l'eau s'écoulant à grande vitesse à travers le déversoir et l'évacuateur entraînait par aspiration l'air de l'évacuateur.

Si l'épaisseur de la couche d'eau au déversoir est plus grande que 0,8 m. et la hauteur de l'ouverture de la vanne est inférieure à 20% de sa hauteur totale, alors, au fur et à mesure de l'entraînement de l'air par aspiration dans l'évacuateur, le niveau d'eau commence à monter. Au-dessus de la surface de l'eau dans l'évacuateur il se produit un rouleau hydraulique à axe horizontal (similaire au ressaut de Bidon) qui engendre des chocs hydrauliques et des ébranlements de la construction. La Fig.2 montre le schéma de la formation du rouleau hydraulique, et la Fig.3, les diagrammes de la pression engendrée alors dans l'évacuateur de fond.

Si l'épaisseur de la couche d'eau au déversoir est inférieure à 0,75 m. et l'ouverture de l'évacuateur ne dépasse pas 2,6 m., le rouleau hydraulique ne peut se former au-dessus de l'eau s'écoulant dans l'évacuateur. Cependant à une différence suffisante de pressions d'air à l'intérieur et à l'extérieur de l'évacuateur, l'air extérieur peut faire irruption à travers la mince couche d'eau dans l'évacuateur en y engendrant des vibrations de la construction et des bruits retentissants.

Divers dispositifs ont été aménagés sur le modèle, aux fins d'aération de l'évacuateur. Il s'est trouvé que les interrupteurs des filets d'eau en forme de sauts en ski ou de pyramides, installés au-dessus de l'entrée des évacuateurs, sont les plus avantageux (Figs. 4 et 5).

A l'aide d'interrupteurs en forme de sauts en ski on a été à même cependant d'obtenir l'aération de l'évacuateur pour un écoulement inférieur à 6 m. $^3/$ sec. par mètre courant du déversoir. Aux écoulements plus importants, sur les côtés du jet tombant du saut en ski, de minces couches d'eau se formaient en forme de pellicules qui interdissaient l'accès de l'air à l'évacuateur du côté de l'échappement. Les interrupteurs en forme de pyramides engendraient la rupture de la couche d'eau s'écoulant à travers le déversoir et l'aération de l'évacuateur aux écoulements inférieurs à 20 m. $^3/$ sec. par mètre courant du déversoir (Fig.6). Lors des écoulements plus importants l'eau s'écoulait au-dessus de l'arête supérieure de l'interrupteur en couche d'eau continue, interdisant l'accès de l'air à l'évacuateur.

ÉTUDE DU CLAPET DE LA VANNE AU-DESSUS DU BARRAGE MOBILE

Un clapet à 20 m. de longueur et 1,8 m. de largeur est installé au-dessus de la vanne du barrage. La section du clapet transversal pivotant sur l'axe horizontal a été projetée conformément à la courbe. Divers écoulements d'eau à travers le clapet jusqu'à un volume de 50 m. $^3/$ sec. ont été prévus.

L'étude effectuée sur le modèle d'un clapet de ce genre a montré que l'écoulement d'eau est accompagné d'un entraînement d'air par aspiration par en-dessous du clapet en y produisant une déformation des jets d'eau retombant et engendrant des ébranlements de la construction (Fig. 7). Aux écoulements plus importants les jets d'eau viennent frapper la construction de la vanne et l'eau remplit l'espace à air raréfié.

Deux variantes d'un dispositif d'amenée d'air au-dessous du clapet ont été projetées afin d'assurer l'aération. Une des variantes prévoyait l'installation des interrupteurs à l'extrémité du clapet, l'autre, l'usage d'un clapet à inclinaison variable de ses extrémités (Fig. 8 et 9).

L'étude sur modèle d'un clapet à interrupteurs a démontré leur efficacité lorsque l'épaisseur de la couche d'eau sur le clapet est inférieure à la hauteur des interrupteurs; dans le cas contraire, les interrupteurs donnent lieu à une diminution de l'épaisseur de la couche d'eau; la rupture des filets d'eau ne se produit pas cependant et l'air n'a pas d'accès à l'espace par en-dessous du clapet. L'usage d'interrupteurs à hauteur supérieure, lors de la naissance d'écoulements plus importants, n'est guère possible pour des raisons purement pratiques.

L'usage de clapets à inclinaison variable de leurs extrémités s'imposait, vu la supposition qu'en ce cas une disjonction des jets d'eau tombant du clapet aurait lieu, c'est-à-dire, que dans la partie du clapet à plus forte inclinaison l'eau retomberait plus près, tandis que dans la partie à inclinaison inférieure elle retomberait plus loin de l'ouvrage; entre ces deux jets il se produirait un espace donnant lieu à l'aération par en-dessous du clapet.

L'étude d'un clapet de ce type a cependant démontré que la disjonction de la couche de l'eau retombante ne se produit pas immédiatement, mais à une certaine distance du clapet, relativement à l'épaisseur de la couche d'eau. A une hauteur inférieure de la chute, la disjonction des jets d'eau ne se produit pas et l'espace par en-dessous du clapet n'est pas sujette à l'aération.

CONCLUSIONS

Les études réalisées sur modèles hydrauliques donnent lieu aux conclusions suivantes:

a) lors d'un écoulement d'eau simultané à travers les évacuateurs

et les déversoirs d'un barrage, l'eau en s'écoulant produit une aspiration d'air engendrant une sous-pression dans l'évacuateur;

b) ladite sous-pression engendre dans l'évacuateur un rouleau hydraulique; si la couche d'eau sur le déversoir est suffisamment mince une rupture de la même couche peut se produire donnant accès à l'air dans l'évacuateur; l'air qui fait irruption y restera jusqu'au moment d'une nouvelle aspiration; ces phénomènes sont accompagnés de bruits et d'ébranlements nuisibles à la construction;

c) Le rouleau hydraulique diminue la section utile de l'évacuateur, ce qui donne lieu à un écoulement à grandes vitesses dans l'évacuateur ces vittesses sont quelquefois supérieures à celles qui se produisaient dans l'évacuateur avant la naissance du rouleau hydraulique;

d) à un écoulement d'eau simultané à travers les évacuateurs et les déversoirs, le coefficient de l'écoulement dans l'évacuateur est ordinairement plus élevé, relativement au coefficient de l'écoulement calculé pour le cas d'un déversoir fermé (inactif);

e) l'usage des interrupteurs, resp. d'autres dispositifs d'interruption des jets d'eau et de l'aération, est impropre, car dans ce cas ils ne remplissent que partiellement leurs fonctions, à voir dans certaines conditions, relativement à l'épaisseur de la couche d'eau retombante, de la hauteur de chute, de la disposition des dispositifs de fermeture, etc;

f) il apparaît donc qu'il serait utile, dans le cas où l'aspiration se produit, d'amener l'air par un dispositif spécial à l'espace où la sous-pression a lieu;

g) dans le cas où l'air n'est pas amené au dit espace il conviendrait alors d'éviter l'écoulement simultané de l'eau à travers les évacuateurs et les déversoirs du barrage.

BIBLIOGRAPHIE:

"Ouvrages hydrotechniques mis en lumière en cours d'essais sur modèles reduits" - R. Cebertowicz

"Études des clapets de vannes" - W. Jarocki.
Bulletin du Service hydrologique et météorologique no. 2 Varsovie, 1956.

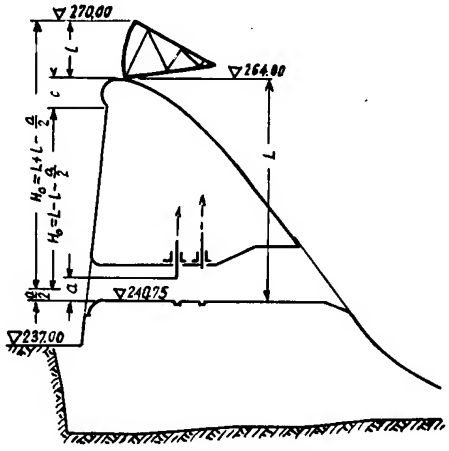

Fig. 1 - COUPE TRANSVERSALE DU BARRAGE.

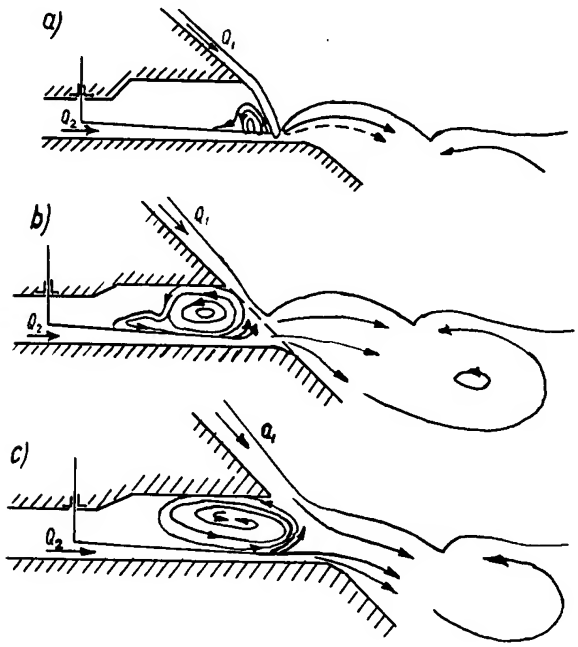

Fig. 2 - ÉCOULEMENT SIMULTANÉ DE L'EAU PAR LE DÉVERSOIR ET LES PERTUIS ÉVACUATEURS DU BARRAGE.

a) début de la formation du rouleau hydraulique,
b) rouleau hydraulique partiel,
c) rouleau hydraulique total.

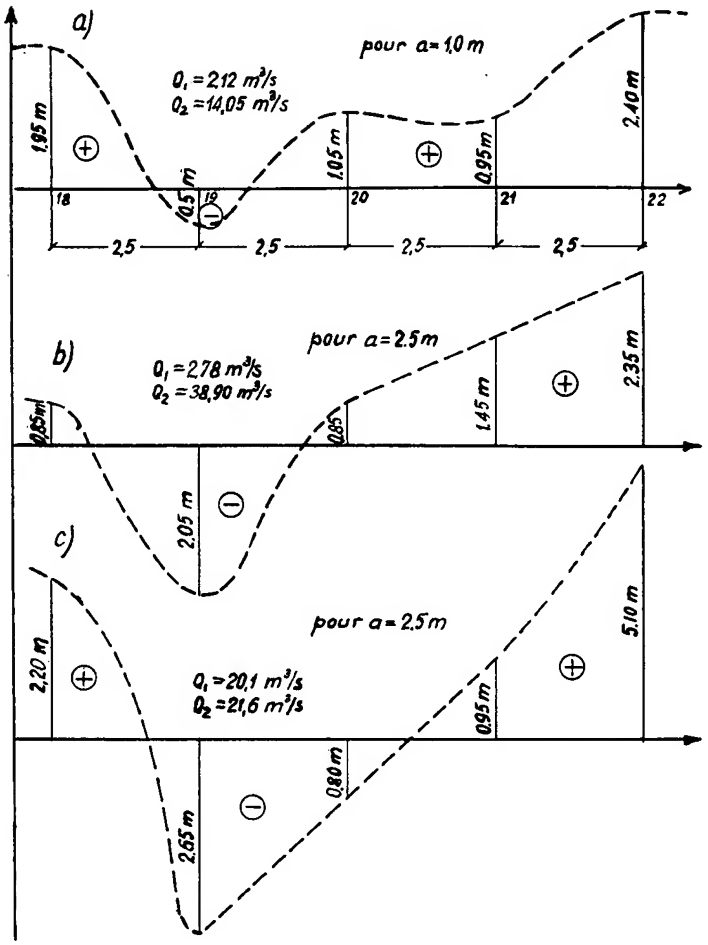

Fig. 3 - PRESSION HYDRAULIQUE SURGISSANT DANS LES ÉVACUATEURS DE FONDS.
a) début de la formation du rouleau hydraulique,
b) rouleau hydraulique partiel,
c) rouleau hydraulique total.

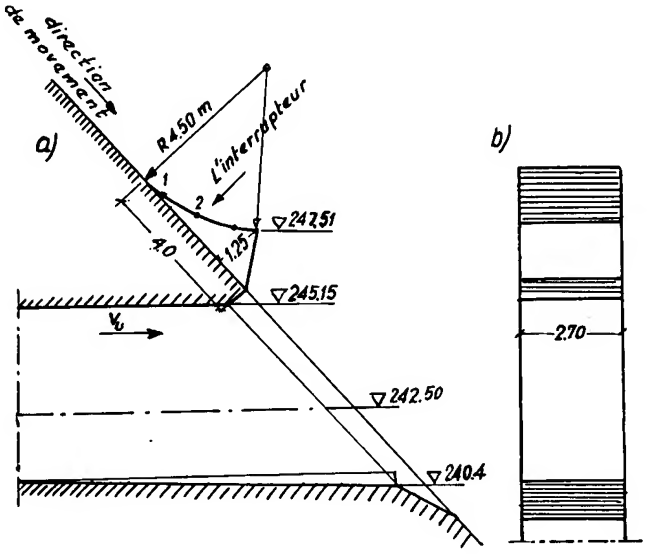

Fig. 4 - DÉTAIL DU DÉVERSOIR EN SAUT EN SKI AU-DESSUS DE L'ÉVACUATEUR.
a) coupe en travers
b) vue d'en face

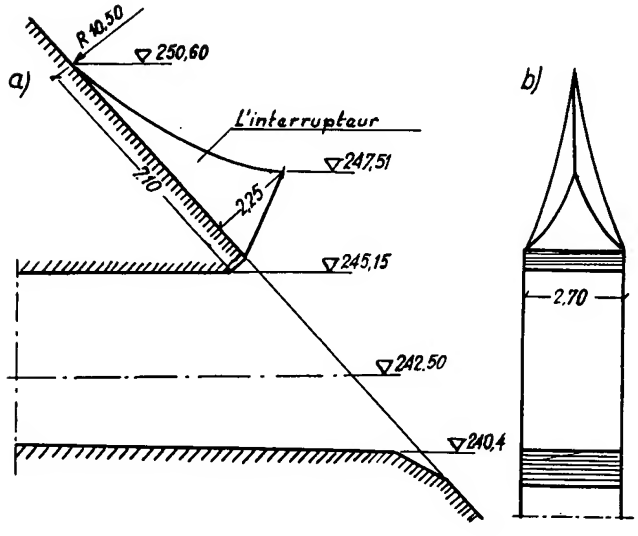

Fig. 5 - INTERRUPTEUR INSTALLÉ AU-DESSUS DE L'ÉCHAPPEMENT DE L'ÉVACUATEUR.
a) coupe transversale
b) vue d'en face

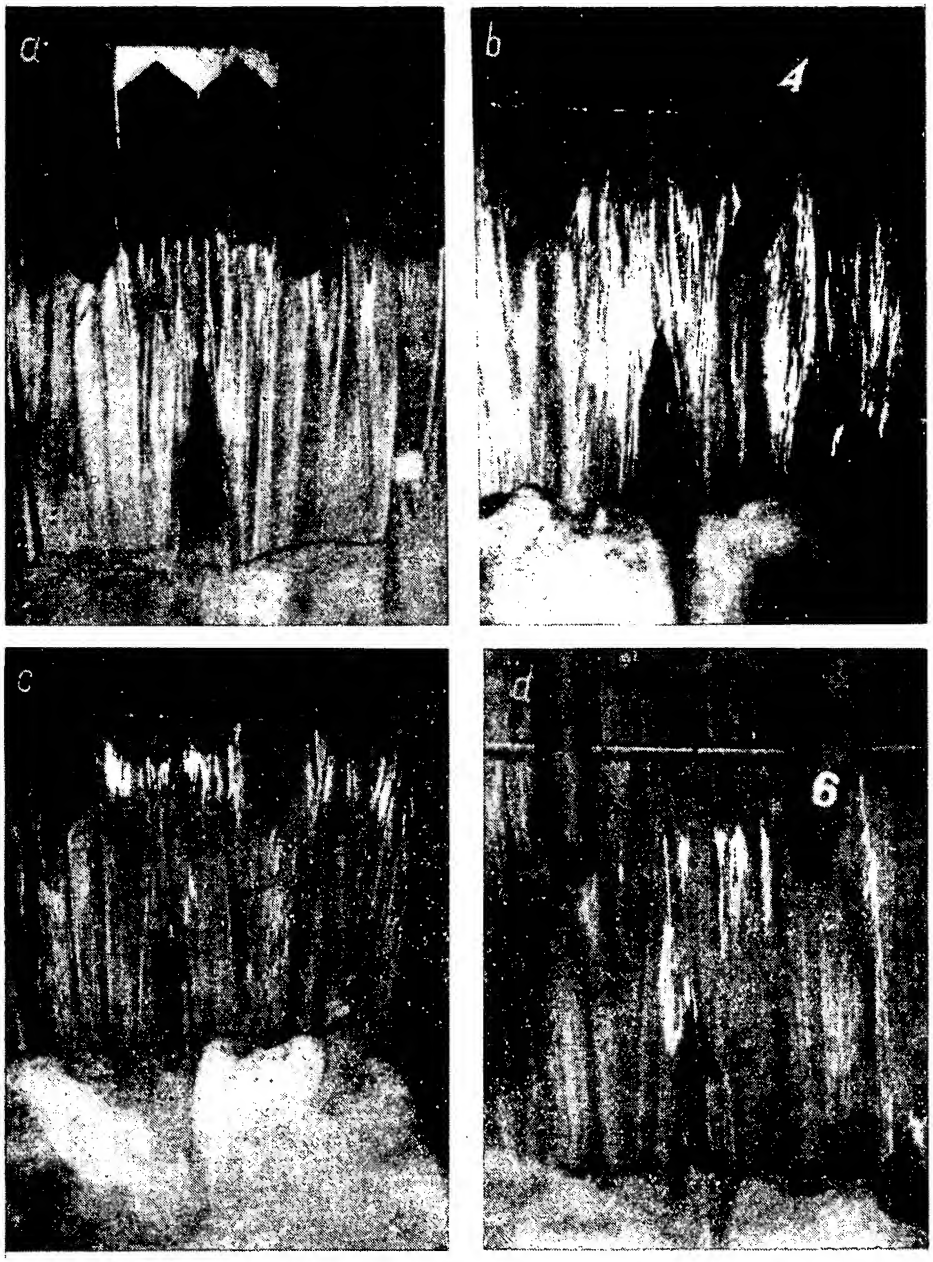

Fig. 6 - FONCTIONNEMENT DES INTERRUPTEURS À DIVERS VOLUMES D'ÉCOULEMENT PAR MÈTRE COURANT DU DÉVERSOIR.

a) 6 m^3/sec. b) 14 m^3/sec.
c) 17 m^3/sec. d) 21 m^3/sec.

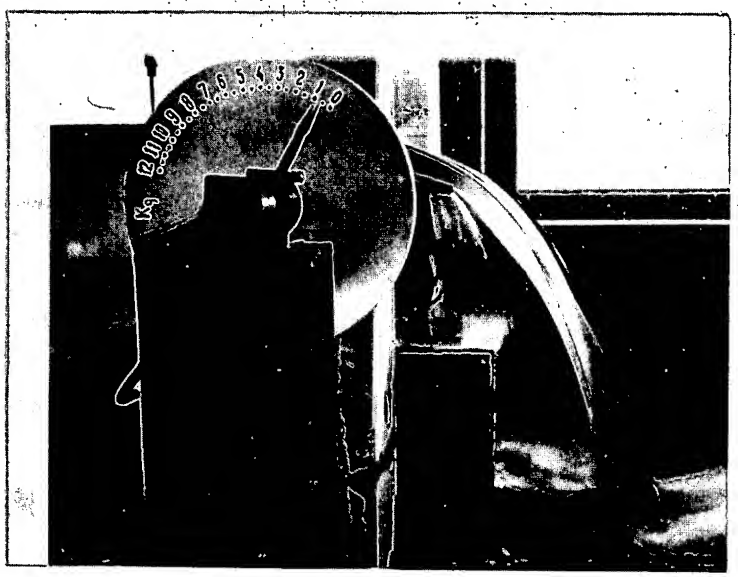

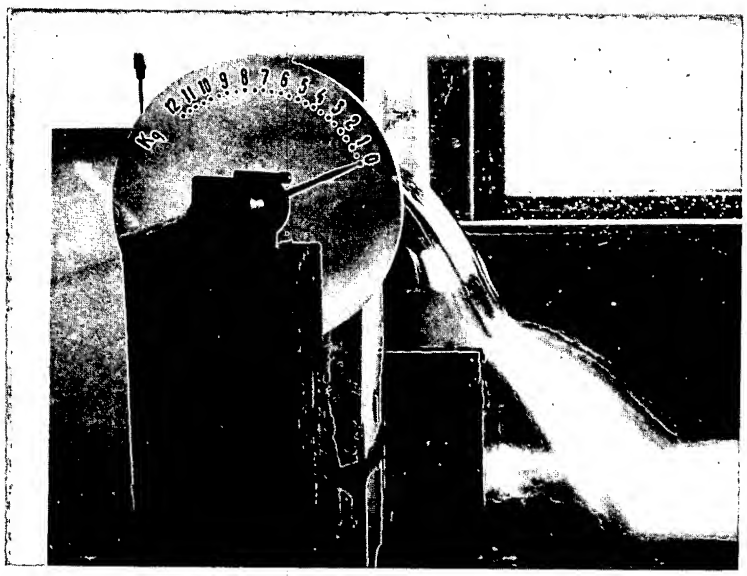

Fig. 7 - ÉCOULEMENT DE L'EAU À TRAVERS LE MODÈLE DU CLAPET DE LA VANNE DU BARRAGE MOBILE.
a) Q 22,8 m^3/sec. b) Q 31,0 m^3/sec.

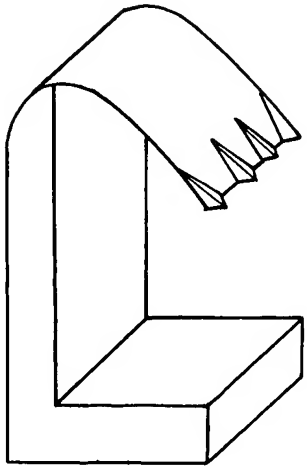

Fig. 8 - MODÈLE DU CLAPET DE LA VANNE À INTERRUPTEURS.

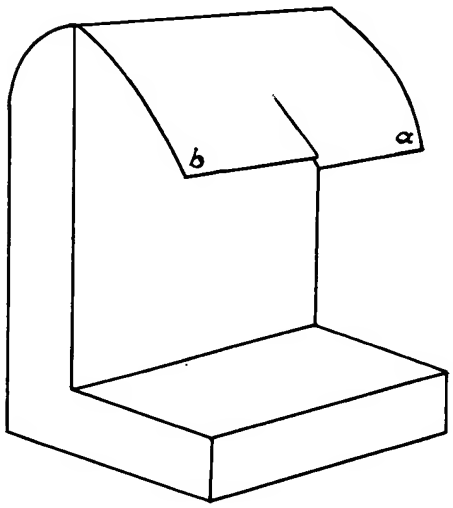

Fig. 9 - MODÈLE DU CLAPET DE LA VANNE À DIVERSES INCLINAISONS DE SES EXTRÉMITÉS.
a) détail d'un clapet à forte inclinaison
b) détail d'un clapet à inclinaison inférieure.

AIR ENTRAINMENT AND VERTICAL DOWNWARD MOTION OF AERATED FLOWS

25X1

* * *

A. G. CHANISHVILI
Master of Science, the Tbilisi Scientific
Research Institute of Engineering Structures
and Hydro-Electric Development

* * *

SUMMARY

The experiments conducted on several models under the conditions of vertical downward motion of liquid with air entrainment yielded the following results.

Within a wide range of the downfall jet velocity variation (I to 15 m/sec) most of the bubbles formed in the flow are 5 - 7 mm. dia. when the normal settling velocity W_o can be considered as a constant value.

An approximate theoretical analysis of the problem concerning the steady air bubble size in water agrees well with the experimental data.

The main reasons for formation of unsteady aerated flows in vertical pipes are insufficient free aeration of downward stream, existence of local obstacles and reverse air flows.

Minimum discharge of entrained air corresponds with uniform motion of the downward aerated flow.

Quantity of air entrained by water falling down the pipe depends upon water discharge, height of fall, etc. The velocity of downward flow causing entrainment of bubbles drops with increasing degree of aeration which is a result of their dynamic interaction under the conditions of decreasing settling velocity.

A similar phenomenon has been observed in liquids with heavy content of solids.

An analysis of the existing methods for taking account of the solids concentration effect on settling velocity shows that determination of the latter by suspending a granular layer in an upward flow yields the results closest to the actual conditions.

Modification of this method for the case of an aerated flow enabled to investigate the effect of the degree of aeration upon settling velocity of air bubbles.

The experimental results within the variation range of the aeration factors A from 0 to 0.30 can be expressed by the following empiric formula:

$$\varkappa = 6.17\ A^2 - 3.72A + 1$$

where $\varkappa = w : w_o$ is relative settling velocity.

SOMMAIRE

Les essais effectués sur plusieurs installations expérimentales en conditions du mouvement de liquide vertical descendant et l'entrainement d'air corrélatif ont donné les résultats suivants.

Dans une large étendue de variation des vitesses de jet (de 1 jusqu'à 15 m/s.), la plupart des bulles qui se forment dans l'écoulement varient en dimensions entre 5 et 7 mm. de diamètre lorsque la vitesse de chute w_o peut être considérée comme une valeur constante.

L'analyse théorique approximative du problème de stabilité des dimensions des bulles d'air dans l'eau est en conformité des essais sur modèles.

L'entrainement d'air dans l'écoulement en conditions insuffisament libres, l'existence des résistances locales et les mouvements d'air inverses sont les causes principales de l'origine du mouvement non-permanent des écoulements aérés.

Le débit minimum de l'air entraîné correspond au mouvement uniforme d'écoulement aéré descendant.

La quantité d'air, entraînée par l'écoulement descendant dans un tube, dépend du débit d'eau, de la hauteur de chute, etc.

La vitesse de l'écoulement descendant, suffisante pour l'entraînement des bulles diminue avec l'augmentation du degré d'aération ce qui est causé par la diminution de la vitesse de chute au cours de leur interaction dynamique.

Le phénomène identique est observé dans les liquides avec des additions importantes de solides.

L'analyse des méthodes existantes de détermination de l'effet de la concentration sur la vitesse de chute des additions, démontre que les résultats les plus rapprochés des conditions réelles sont obtenus par la méthode de détérmination de la vitesse de chute au moyen de suspension de la couche granulée dans l'écoulement ascendant.

La modification de cette méthode pour les cas de l'écoulement aéré a permis d'étudier le problème de l'effet de degré d'aération sur la vitesse de chute des bulles d'air.

Les résultats des essais dans les limites de variation des coefficients d'aération A entre 0 jusqu'à 0.30 peuvent être traduits en formule empirique:

$$\gamma = 6.17A^2 - 3.72A + 1$$

où $\gamma = W : W_0$ - la vitesse de chute relative.

INTRODUCTION

Air entrainment, motion of aerated flows and the process of deaeration are rather complicated and little known physical phenomena.

There is no general theory developed for two-phase or multi-phase systems up to the present. The methods for analytical calculation of the phenomena involving aeration are not reliable and the methods of scale-modelling are little developed. For this reason it is almost impossible to generalize or extrapolate the few experimental results that have been obtained by various researchers at different times as well as to estimate quantitatively the results of theoretical analysis of individual problems.

The problem of aeration is of great importance in hydraulic power engineering. In most cases the aeration process results both for open and closed type hydraulic structures in negative effects causing considerable deterioration of service qualities of the structures and in some cases even leading to serious failures. In pressure type hydraulic structures the effects of the aeration phenomena are usually more pronounced than in pressureless structures.

The problems of the aerated flow motion in hydraulic engineering, particularly the air entrainment phenomena in water flowing down vertical shafts and pipes, were given much consideration at the 5th Congress of the International Hydraulic Research Association in 1953.

Several papers [1), 2), 3)] present the results of extensive research of some air entrainment phenomena and transport of air by water flowing down vertical pipes with flooded outlets. Some conclusions and results of the author's experiments are given in another paper.[4)]

The above-mentioned experimental research enabled to investigate the effect and significance of individual factors in the air entrainment and transport phenomena under specific conditions as well as to establish certain qualitative and quantitative relationships between them.

The model experiments performed at the Tbilisi Scientific Research Institute of Engineering Structures and Hydro-Electric Development are generally similar to the above-mentioned experiments and provide a qualitative confirmation of their results. At the same time, these model experiments enable to define more exactly certain stream and structural peculiarities of a downward aerated flow which can be used to advantage for more profound investigations of the phase interaction phenomenon resulting in varying settling velocity of air bubbles, depending upon the degree of aeration, as well as of other highly significant problems that are outside the limits of the particular case of motion under consideration.

1) Marquenet, G. Entraînement d'air par un écoulement en conduite verticale. - Proceed. Minnesota Intern. Hydraulic Convention, Sept. 1953, p. 489.

2) Kalinske A.A. Hydraulics of Vertical Drain and Overflow Pipes. University of Iowa Studies in Engineering, Bull. No. 26, p. 26.

3) Laushey L.M. and Mavis F.T. Air Entrained by Water Flowing down Vertical Shafts. - Proceed. Minnesota Intern. Hydraulic Convention, 1953, p. 483.

4) Viparelli M. Transporto di aria da parte di correnti idriche in condotti chiusi. -"L'Energia Elettrica", 1954, v. 31, No. 11.

CERTAIN PHENOMENA OBSERVED IN THE CONDUCTED EXPERIMENTS

Detailed description of the experiments and experimental installations omitted, only those results are presented below that are of interest from the viewpoint of defining some aeration phenomena or are directly connected with the problem of settling velocity of air bubbles.

The experiments aimed at the investigation of air entrainment by downward jet and the motion of aerated flow have been carried out under two different types of specific conditions.

1) When the velocities of water flowing down a vertical pipe were considerably less than the settling velocity of the bubbles entrained by falling stream (the experiments designed to investigate the penetration depth of air bubbles inside the liquid);

2) When the liquid phase velocities were commensurate with the settling velocity of separate bubbles (the experiments conducted on vertical pipes with the lower outlet flooded).

The experiments designed to investigate the penetration depth of air bubbles inside water have been conducted under the conditions described below.

A jet of water was run into a vertical cylinder, 30 cm diameter and 3 m high, from two conoid nozzles, 11.1 and 13.2 mm diameter respectively. When striking against water surface, the jet entrained some air. The height of free fall of the water jet varied from zero to 200 cm, rate of water discharge amounted from 0.19 to 2.25 l/sec.

The experiments enabled to establish that under the conditions of air entrainment through jamming, at the atmospheric (gauge) air pressure in the point of contact, the overwhelming majority of air bubbles formed thereby within a wide range of jet velocities (1 to 15 m/sec) are 5 to 7 mm diameter. The aerated flow structure involves uniform distribution of the bubbles by volume.

The penetration depth H_2 of air bubbles entrained by the water jet, with the liquid phase moving through the vertical cylinder and fall remaining constant, increases with the jet velocity and rate of water discharge. With the fall increasing up to a certain value and rate of jet discharge remaining the same, the depth of air penetration suddenly drops, though it begins to increase slowly with further increase of fall.

Use of product $u \cdot d$ as a parameter gives a satisfactory scatter of points along the straight line (I, Fig. 1) expressed by the following equation:

$$H_2 = 0.052\ u \cdot d$$

In fig. 1 are also plotted the straight lines (3 and 2) obtained from the formulae of Abramovitch [1] for the maximum and of Konovalov [2] for mean velocity of a free turbulent jet, assuming that the bubbles penetrate up to the depth where the jet velocity equals the settling velocity of separate particles and introducing some other simplifications.

It is seen from the above figure that the intensity of the vertical flow velocity attenuation in case of air entrainment (non-free turbulent flow) is considerably higher than for a free turbulent stream under the same conditions.

The experimental investigations of air entrainment by water flowing down vertical pipes having different diameters and working with flooded outlets confirm that pulsating motion of air and water mixtures with periodical entrainment of large air volumes is caused by insufficiently free aeration of suction zones as well as existence of local resistances, reverse air flows and so on.

Motion of the mixture becomes steady under the conditions of free aeration and uniform air suction by the flow which is effected by supplying air to the suction zones. A structure formed in this case is characterized by uniform distribution of bubbles which, for the most part, irrespective of the flow fall velocity or other factors, are 5 to 7 mm. diameter, as mentioned above. From the viewpoint of settling velocity such a mixture can be considered uniform (figs. 2 and 3).

Mention should also be made of another property of a uniform downward aerated flow confirmed by our experiments.

It lies in that, with other factors being equal (water discharge, fall etc.), minimum discharge of entrained air corresponds to the uniform motion.

The experiments have shown that at a certain rate of the liquid phase, discharge velocity of liquid flowing down a pipe is such that the flow can ensure through entrainment of air bubbles, that is transport of the whole entrained air.

1) Abramovitch G.H. Free turbulent liquid and gas flows. - Gosenergoizdat, Moscow-Leningrad, 1948.

2) Mackaveyev V.M. and Konovalov I.M. Hydraulics. - Techizdat, 1940.

Air entrainment was observed also with downward flow velocities which were smaller than settling velocity of separate bubbles. Besides it proved to be that the greater was the degree of flow aeration the smaller were these velocities.

This points out to the fact that, similar to the heavy solids content, the entrainment flow ability increases with the degree of aeration due to decreasing settling velocity of the bubbles or increase of actual velocities.

The above-mentioned stream and structural peculiarities of the downward uniform motion of aerated flows somewhat simplify the general pattern of phase interaction, enable to reduce the number of factors to be taken into consideration and, similar to other two-phase flows, offer a possibility to investigate the problems of the settling velocity variation with concentration as well as of sliding between the phases and other phenomena becoming most apparent under specific conditions.

APPROXIMATE THEORETICAL ANALYSIS OF THE PROBLEM CONCERNING STABLE SIZE OF AIR BUBBLES

The problem of size of the air bubbles forming in the water flow aeration is of great significance for determination of the settling velocity, saturation, transport ability and calculation of power balance of the aerated flows.

The attempts at theoretical determination of stable air inclusions known to us [1] have yielded results which are in considerable disagreement with the author's experiments.

Consideration of the bubble stability subjected both to static (P_s) and dynamic pressure P_d heads enables us to work out the following equation:

$$P = P_s + P_d + \Delta P \qquad (1)$$

where $\Delta P = \sigma \left(\frac{1}{R_1} + \frac{1}{R_2} \right)$ is additional pressure due to the surface curvature.[2]

If equation (1) is not observed that would mean transition of the bubble boundary surface to unsteady state.

1) Levitch V. C. Physical and chemical hydrodynamics. - Akademia Nauk USSR, Moscow, 1952.

2) Adam N. K. Surface physics and chemistry. - Gostechizdat, Moscow-Leningrad, 1947.

For approximate determination of the bubble size and its ultimate strain causing damage of the separation surface it can be assumed that the latter phenomenon takes place when the radius of curvature in some point of the surface passes the infinity. In this case an infinitely small variation of the applied force will cause finite strain of the separation surface, that is, application of force will result in unsteady state of the surface.

The point in question will be the lower point located on the vertical axis of symmetry.

If we do not take into consideration the dynamic pressure head and assume that the internal pressure does not depend upon the degree of the bubble strain, the following equation can be drawn from the equation of stability:

$$\frac{R_a}{R_b} = \frac{1 - \frac{\gamma \cdot R_o^2}{2\sigma}}{1 + \frac{\gamma \cdot R_o^2}{2\sigma}} \qquad (2)$$

Assuming $\gamma = 1$ g/cm^3 and $\sigma = 0.075$ g/cm, positive values of R_b and $R_a : R_b$ can be obtained from this formula, with initial radii of an unstrained bubble R_o equalling 0 to 0.38 cm.

Taking into account the hydrodynamic pressure corresponding to a value of settling velocity equalling $W_o \approx 30$ cm/sec. has an insignificant bearing upon finite velocity of a stable bubble. The tests designed to break the bubbles blown out from vertical pipes submerged with their lower ends in water have shown that the adopted hypothesis concerning breakage of the separation surface, when the sign of the curvature varies, is very close to reality.

Therefore, both the approximate theoretical analysis and the experiments confirm that with the air and water mixture in uniform motion and the maximum interphase sliding velocity amounting up to 30 cm/sec. the stable bubble velocities are quite finite.

Within the bubble velocities observed the settling velocity of their isolated motion is constant, i.e., of the order 25-30 cm/sec.[1), 2), 3), 4)], which, from the viewpoint of settling velocity, permits us to consider the air and water mixture under the conditions of our experiments as a homogeneous one.

1) Levitch V.G. Physical and chemical hydrodynamics. - Akademia Nauk USSR, Moscow, 1952.

2) Hasegawa T. USSR Abstracts Journal, Mechanics Series, 1957, No. 4, Abstr. 4212.

3) Kozlov V.K. and Mologin M.A. USSR Academy of Sc., Proceed. Techn. Sc. Dpt., 1951, No. 8.

4) Ladyzhensky R.M., "Journal of Applied Chemistry", 1954, v.27, No.1.

BERNOULLI'S EQUATION FOR TWO-PHASE FLOW MOTION

One of the most convenient and ready means used to determine the relationship between separate factors under the conditions of two-phase liquid flow motion is the Bernoulli's equation. However, correct determination of this relationship depends on the degree of approximation with which this equation was worked out, upon consideration of specific characteristics of the two-phase mixture motion as well as on the fact of how precisely each member of the equation reflects physical nature of the phenomena under study.

Most precise definition of all basic members of the Bernouilli's equation for the two-phase flow motion has been given by M.A. Dementiev (1) who took into account along with other kinds of power the solid phase pressure power absorbed by the flow, when deriving the equation.

The member of Bernoulli's equation that defines the power of the dissipative forces is expressed by various authors by means of three methods differing in their physical nature.

1. If the power losses are related only to the liquid phase unit weight, then the power of the dissipative forces can be expressed as follows:

$$N = \gamma_w \cdot Q_w \cdot h_{ws_1}$$

2. If the power losses are related to the liquid phase unit weight with fictitious discharge equalling the mixture discharge, then:

$$N = \gamma_w \cdot Q_{ws} \cdot h_{ws_2}$$

3. If the losses are related to the unit weight of the mixture, then:

$$N = \gamma_{ws} \cdot Q_{ws} \cdot h_{ws_3}$$

The additional member of Bernoulli's equation will assume different physical meaning and various forms depending on what particular equation of the three given above is used to express the power of the dissipative forces.

It seems to us that from the viewpoint of the phenomena under consideration the third equation is the best one since it allows for a possibility of utilization of the pressure energy and composition of mixtures. The above expression for the losses has also been used by A.N. Klimentov (2).

1) Dementiev, M.A. Proceed. of the All-Union Inst. for Hydraulic Engineering Research, v. 52.

2) Klimentov A.N. "Hydraulic Power Engineering", 1953, No. 9.

If the rotary motion power, non-uniform distribution of velocities and pressures in both phases are not taken into consideration for uniform motion of the two-phase flow, Bernoulli's equation assumes the following form:

$$h_{ws} = H_{ws} - \left(\frac{\gamma_s}{\gamma_w} - 1\right) \frac{Q_s}{Q_w + Q_s} Z \qquad (3)$$

The pressure drop H_{ws} and specific loss h_{ws} related to the unit weight of the mixture are expressed in this formula by the fall of the liquid phase.

If the mixtures are lighter than the medium, for example, air bubbles in water ($\gamma_w > \gamma_a$), Bernoulli's equation for the downward ($Z_1 > Z_2$, $Z = Z_1 - Z_2$) uniform two-phase flow motion is written in the following form:

$$h_{wa} = H_{wa} - \left(1 - \frac{\gamma_a}{\gamma_w}\right) \frac{Q_a}{Q_w + Q_a} Z \qquad (4)$$

or, taking into consideration that $\gamma_a \ll \gamma_w$,

$$h_{wa} = H_{wa} - \frac{Q_a}{Q_w + Q_a} Z \qquad (5)$$

The above equations make it possible to analyze the phenomena in question and establish certain relationships between individual factors peculiar for uniform motion of two-phase flows.

ON SETTLING VELOCITY UNDER THE CONDITIONS OF INTERACTION BETWEEN PARTICLES

The majority of researchers do not take sufficient account of variation of settling velocity of particles under the conditions of interaction between the particles or give erroneous interpretation of the physical and mechanical factors causing this phenomenon.

The existing methods enabling to allow for the effect of concentration of the mixtures, that are heavier than the medium, upon settling velocity as well as physical and mechanical diagrams of the interaction of forces between the mixture phases can be divided into the groups described below.

According to Richards (1) and Karaushev (2), variation in settling velocity is caused by increasing density of the mixture, the latter defined as some fictitious averaged density of a mechanical mixture. In fact, the medium surrounding a particle does not change with concentration, and introduction of the conception of averaged density within the range commensurate with the volumes of separate particles in a mechanical mixture is not rightful.

Finkey, Monroe, (3) Velikanov (4) and Paltchevsky (5) connect variation of settling velocity with increase of the liquid flow rate in the gaps. This diagram is not sufficient to allow for structural peculiarities of a two-phase mixture, the dynamic phase interaction effect developing due to super-imposing of a velocity field forming around each article as well as for a correct estimate of the suspension effect.

Thus, for example, the velocity of fall of suspended particles with respect to a fixed coordinate system under the conditions of dynamic equilibrium of these particles equals zero, though the settling velocity and energy needed for suspension are not equal to zero.

Lyashchenko (6), Mints and Shubert (7) substitute the conditions of the liquid motion through the granular layer in dynamic equilibrium for the conditions of contracted movement of particles and interaction between them.

(1) Lyashenko P. V. Gravity Methods of Separation. - Gostoptechizdat, Moscow-Leningrad, 1940.

(2) Karaushev A. V. "Hydraulics of storage lakes and rivers. - "River Transport", Leningrad, 1955.

(3) Lyashenko P. V. Gravity Methods of Separation. - Gostoptechizdat, Moscow-Leningrad, 1940.

(4) Velikanov M. A. Bed flow dynamics, vol. 11. - Gostechizdat, Moscow, 1955.

(5) Paltchevsky A. P. "Hydraulic Power Engineering", 1953, No. 2.

(6) Idem see p. 15, nl

(7) Mints D. M. and Shubert S. A. Hydraulics of Granular Materials. - Moscow, 1955.

The way this problem is formulated, except for a certain simplification concerning hydromechanical aspects, ensures maximum approximation to actual conditions of the phase interaction and provides extensive experimental possibilities to obtain reliable and physically well-grounded values of settling velocity within a wide range of varying concentrations.

To compare settling velocity in conditions of particle interaction according to the formulae recommended by various authors, in fig. 4 are plotted the curves $\varkappa = \varphi(s)$ for sand possessing different grain size and a volume weight of 2.65 t/m^3.

In case of the contracted fall-out of particles conception of settling velocity assumes somewhat different nature due to lack of coincidence between the absolute and relative velocities of fall-out.

Mints and Shubert determined settling velocity w in their experiments as the averaged velocity of an upward flow $w = v = \frac{q_w}{\omega}$ ensuring dynamic equilibrium of a suspended granular layer.

From the viewpoint of correct allowance for the suspension work in dynamic equilibrium of particles this expression does not give rise to doubt. However, to extend the conception of settling velocity equally well to the uniform upward or downward motion of the mixture, on condition of observing by the above principle, the average velocity should imply the average mixture flow rate:

$$v_{ws} = \frac{Q_w + Q_s}{\omega}$$

Then the settling velocity is determined from an expression:

$$w = v_{ws} - v_s$$

or

$$w = m(v_w - v_s)$$

where m is the volume factor of water content coinciding in meaning with volume porosity which is used with success when considering the problems of flow motion in suspended granular layers or porous mediums to give geometrical characteristics of the particular structure.(1)

In this case the aeration factor is defined by an expression $A = 1 - m$, while the reduced velocity and actual velocity of a liquid (u) are connected by the relationship:

$$v = m \cdot u$$

In a particular case of dynamic equilibrium ($v_s = 0$) these expressions give us $w = m \cdot v_w = v_{ws}$ while for suspending without sliding ($v_w = v_s$) i.e. $w = 0$. The above expressions can be used equally well to determine settling velocity under the intermediate conditions of uniform vertical motion of two-phase liquids.

(1) Idem see p. 16, n. 2.

EXPERIMENTAL INVESTIGATIONS OF SETTLING VELOCITY OF AIR BUBBLES UNDER CONDITIONS OF THEIR INTERACTION

Bernoulli's equation for the uniform vertical motion of an aerated flow (4) or (5) gives an opportunity for experimental determination of settling velocity of air bubbles possessing various degrees of aeration.

If the discharge in individual phases is expressed by appropriate flow velocities: $Q_w = m \cdot \omega \cdot v_w$ and

$Q_a = A\ \omega\ v_a$ then:

$$h_{wa} = H_{wa} - \frac{(1-m)\ \frac{v_a}{v_w}}{m+(1-m)\ \frac{v_a}{v_w}} Z \qquad (6)$$

The condition of dynamic equilibrium for air bubbles in a flow implies that

$$h_{wa} = H_{wa} \qquad (7)$$

If we take for settling velocity the value $w = v_{wa} - v_a$, then formula (6) expressing the relationship between the loss, concentration and flow velocities of individual phases will assume the following form:

$$h_{wa} = H_{wa} - (1-m)^2 \left(1 - \frac{w}{v_{wa}}\right) Z \qquad (8)$$

The conditions most convenient for experimental determination of the degree of aeration are created in case of dynamic equilibrium of the bubbles ($w = v_{wa}$) in a downward flow. Below is given an expression obtained for this case, if we do not consider friction losses between the flow and piping walls as compared to the interphase sliding resistance, and making an assumption that has been confirmed by recent experiments (1) according to which the pressure drop is always equal to the weight of the admixture column, the latter having a cross-section equal to unity.

$$h_{wa} = H_{wa} = (1-m) Z \qquad (9)$$

(1) Idem see p. 16, n 2

Using the above expression, the air content, that is, the aeration factor $A = 1 - m$, can be determined if the values of the pressure drop H_{wa} for the particular region Z are known.

This method can be used equally well with uniform motion of the air and water mixture.

To determine settling velocity of the bubbles in dynamic equilibrium using the formulae given above, experimental determination of the liquid discharge and drop is necessary, and in case of uniform motion air discharge through the particular cross-section should also be known.

Experimental determination of the air bubble settling velocity was carried out using an experimental installation (fig. 5) consisting of a 3 m. high and 10 cm. dia. transparent vertical cylinder. Water was supplied to the upward pipe end while its lower end was lowered in an air trap from which the air evolved was passed through a measuring nozzle (air gauge) calibrated in terms of pressure and provided with a micromanometer.

Every 50 cm. of the cylinder length were mounted piezometers enabling to determine pressure drops on the regions of equal length. The only measurements used to determine settling velocity were those obtained for the lowest region having a depth $Z = 50$ cm. and characterized by uniform flow conditions of the mixture motion to which Bernoulli's equation can be applied without introducing appreciable errors.

Water discharge, as measured for the model, varied from I to 2,85 l/sec. while air discharge varied from zero to 650 cm^3/sec. The aeration factor varied with pressure drop within the range of 0.06 + 0.30.

The following parameters have been determined using the measured values of Q_w, Q_a and H_{wa} :

a) aeration factor,

$$A = 1 - m = \frac{H_{wa}}{Z}$$

b) mixture discharge and flow velocity,

$$Q_{wa} = Q_w + Q_a \quad \text{and} \quad v_{wa} = \frac{Q_{wa}}{\omega}$$

c) velocity of air bubbles.

$$v_a = \frac{Q_a}{A\omega}$$

d) finally, settling velocity,

$$w = v_{wa} - v_a$$

The experimental results (fig. 6) show that with smaller concentrations settling velocity tends to a value of the order 27 cm/sec. which is in good

agreement with the data presented by other authors. With the degree of aeration increasing, the settling velocity gradually drops to 12 cm/sec. when $A = 0.30$.

Thus, within the range of the volume aeration values covered by the above-described experiments settling velocity decreases more than twice, as compared to its value for a separate bubble having the same size.

The reason for such a drop of settling velocity is, as it is well-known, the dynamic interaction between the bubbles caused by the velocity field interference and variation of the flow factor.

In fig. 6 is also plotted an experimental curve expressing the relationship between relative settling velocity and the aeration factor. Settling velocity of separate bubbles is assumed to be $W_0 = 27$ cm/sec. The curve is in satisfactory agreement with the following equation:

$$\chi = 6.17 A^2 - 3.717 A + 1 \qquad (10)$$

The settling velocity drop which, as found out by means of the above experiments, takes place with the degree of aeration increasing, supplies an explanation to a number of phenomena observed in two-phase flow motion, including increase in the transport ability up to a certain limit of saturation.

LIST OF SYMBOLS

H_1 - jet fall, cm.

H_2 - depth of bubble penetration, cm.

H - pressure drop, cm.

h - specific pressure head loss, cm.

γ - volume weight, g/cm^3

Q - volume discharge, $cm^3/sec.$ or litre/sec.

ω - sectional area, cm^2

v - reduced velocity, cm/sec.

u - actual velocity, cm/sec.

The indexes w, s and a denote the liquid, solid and gas (air) phases respectively,

The indexes ws and wa denote a corresponding mixture

d - jet diameter, cm.

D - pipe diameter, cm.

N - dissipated power

P - internal bubble pressure

P_s - external static pressure

P_d - external dynamic pressure

ΔP - pressure due to the surface curvature

$Z = z_1 - z_2$ - difference in the sectional centre of gravity marking, cm.

m - volume porosity or water content factor

$S = A = 1 - m$ - volume concentration of mixtures or aeration factor

w - settling velocity under contracted conditions, cm/sec.

w_0 - normal value of settling velocity (for a separate particle), cm/sec.

$\varkappa = \frac{w}{w_0}$ - relative settling velocity

σ - surface tension factor

R_1, R_2 - main radii of bubble surface curvature in a given point, cm.

R_0 - unstrained bubble radius, cm.

R_a, R_b - curvature radii in the upper and lower points of an unstrained bubble.

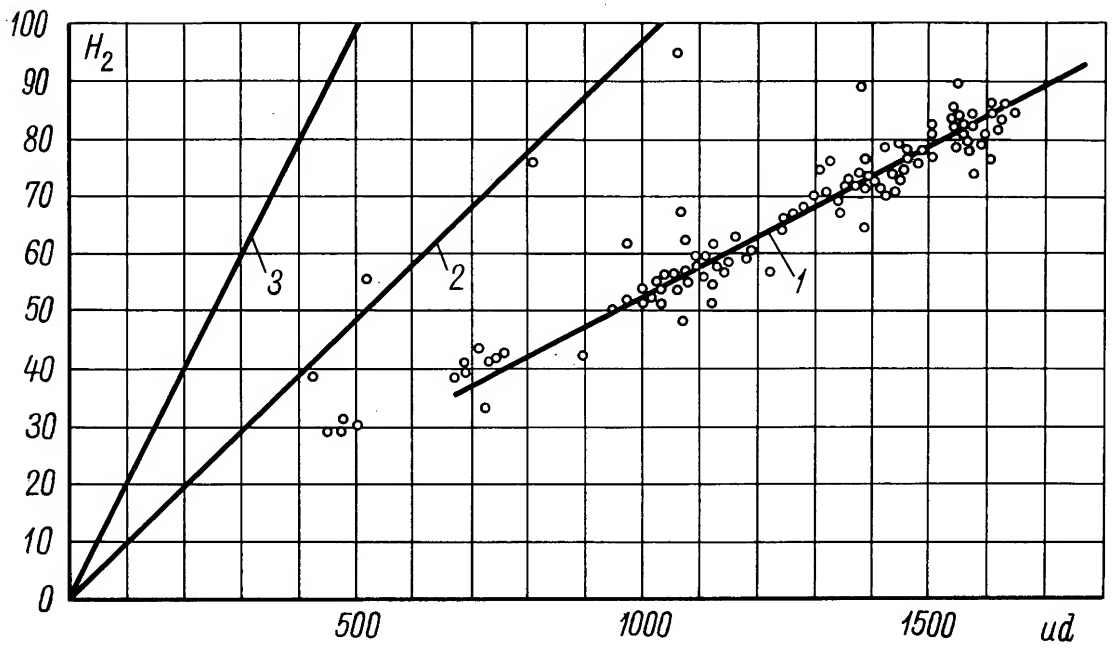

Fig. 1 - EXPERIMENTAL RELATIONSHIP $H_2 = \varphi(u \cdot d)$; STRAIGHT LINES AGREEING WITH THE FORMULAE FOR FREE TURBULENT JET; 2 - ACCORDING TO KONOVALOV; 3 - ACCORDING TO ABRAMOVITCH.

Fig. 2 - STRUCTURE OF A DOWNWARD AERATED FLOW IN UNIFORM MOTION.

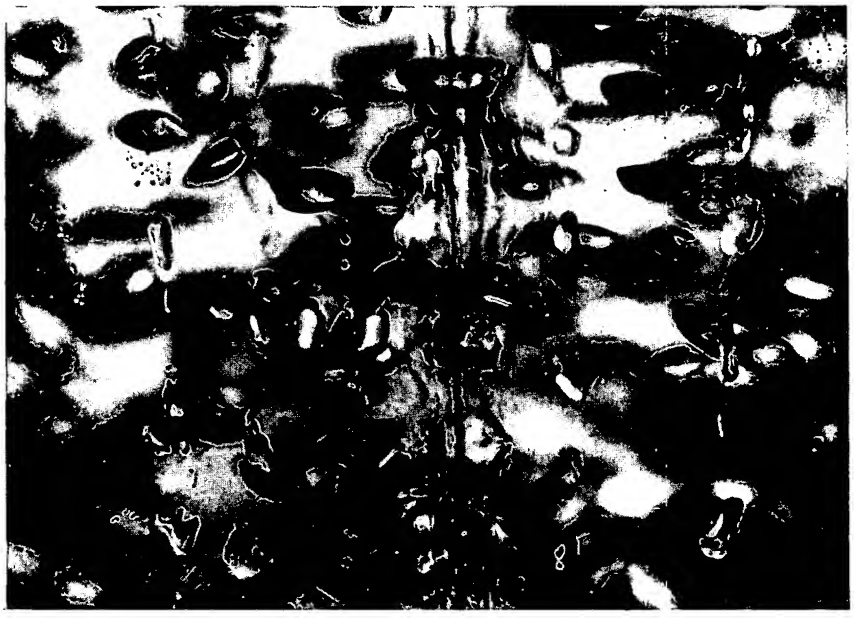

Fig. 3 - SHAPES OF AIR BUBBLES IN A DOWNWARD UNIFORM FLOW.

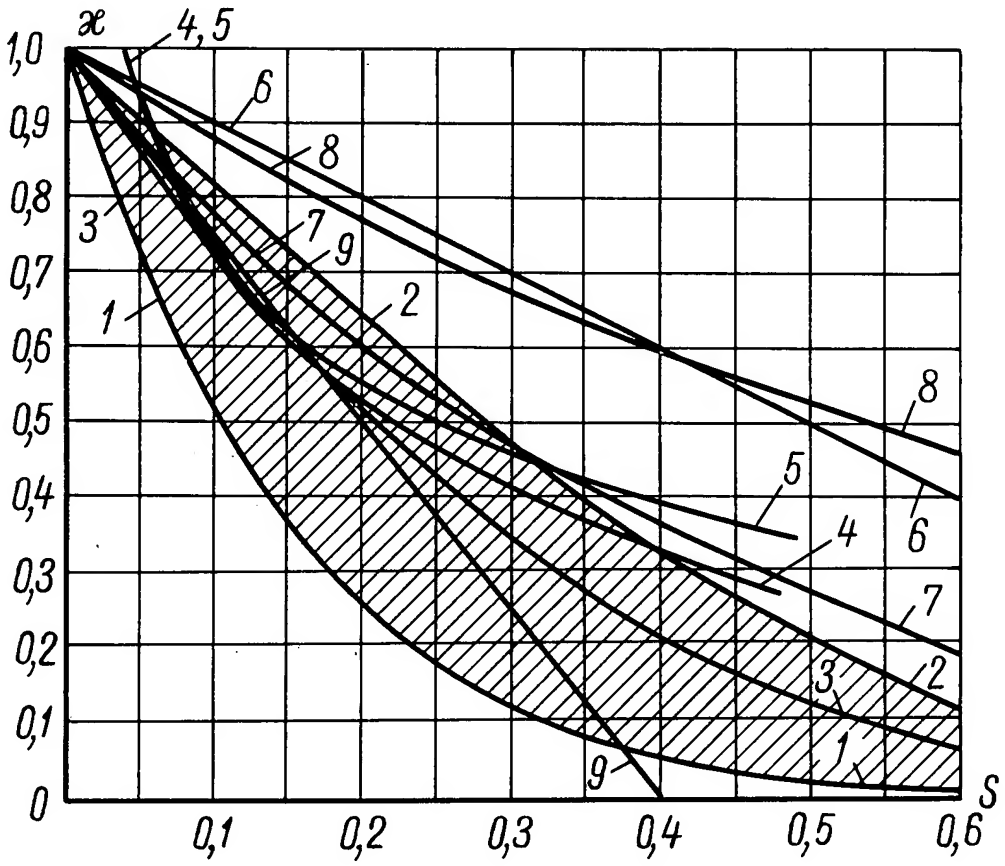

Fig. 4 - RELATIONSHIP BETWEEN RELATIVE SETTLING VELOCITY AND VOLUME MIXTURE CONCENTRATION: 1 AND 2 - MINTS AND SHUBERT EXPERIMENTAL CURVES FOR LAMINAR AND TURBULENT FLOWS (THE REGION OF TRANSITIONAL CONDITIONS SHADED); 3 - LYASHCHENKO EXPERIMENTAL CURVE; 4 AND 5 - CURVES FOR LAMINAR AND TURBULENT FLOWS ACCORDING TO PALCHEVSKY'S FORMULAE; 6 - CURVES AGREEING WITH VELIKANOV'S FORMULA; 7 AND 8 - CURVES FOR LAMINAR AND TURBULENT FLOWS ACCORDING TO KARAUSHEV'S FORMULAE; 9 - CURVE ACCORDING TO ZAGOUSTIN'S FORMULA.

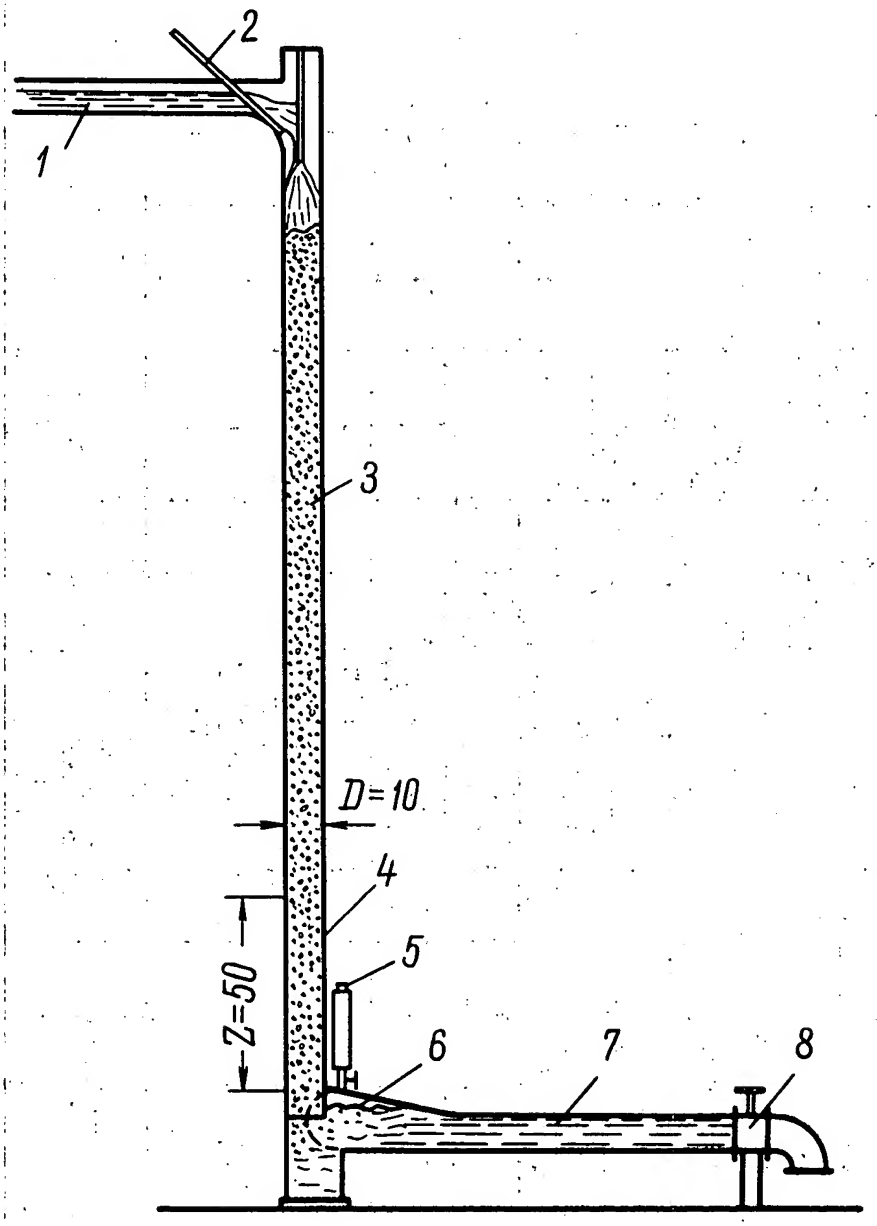

Fig. 5 - SCHEME OF EXPERIMENTAL INSTALLATION DESIGNED TO DETERMINE SETTLING VELOCITY OF INTERACTING AIR BUBBLES; 1 - FEEDING TROUGH; 2 - AERATION TUBE; 3 - VERTICAL TUBE, 10 CM DIA.; 4 - WORKING SECTION; 5 - MEASURING NOZZLE; 6 - AIR COLLECTOR; 7 - HORIZONTAL SECTION; 8 - CONTROL GATE VALVE.

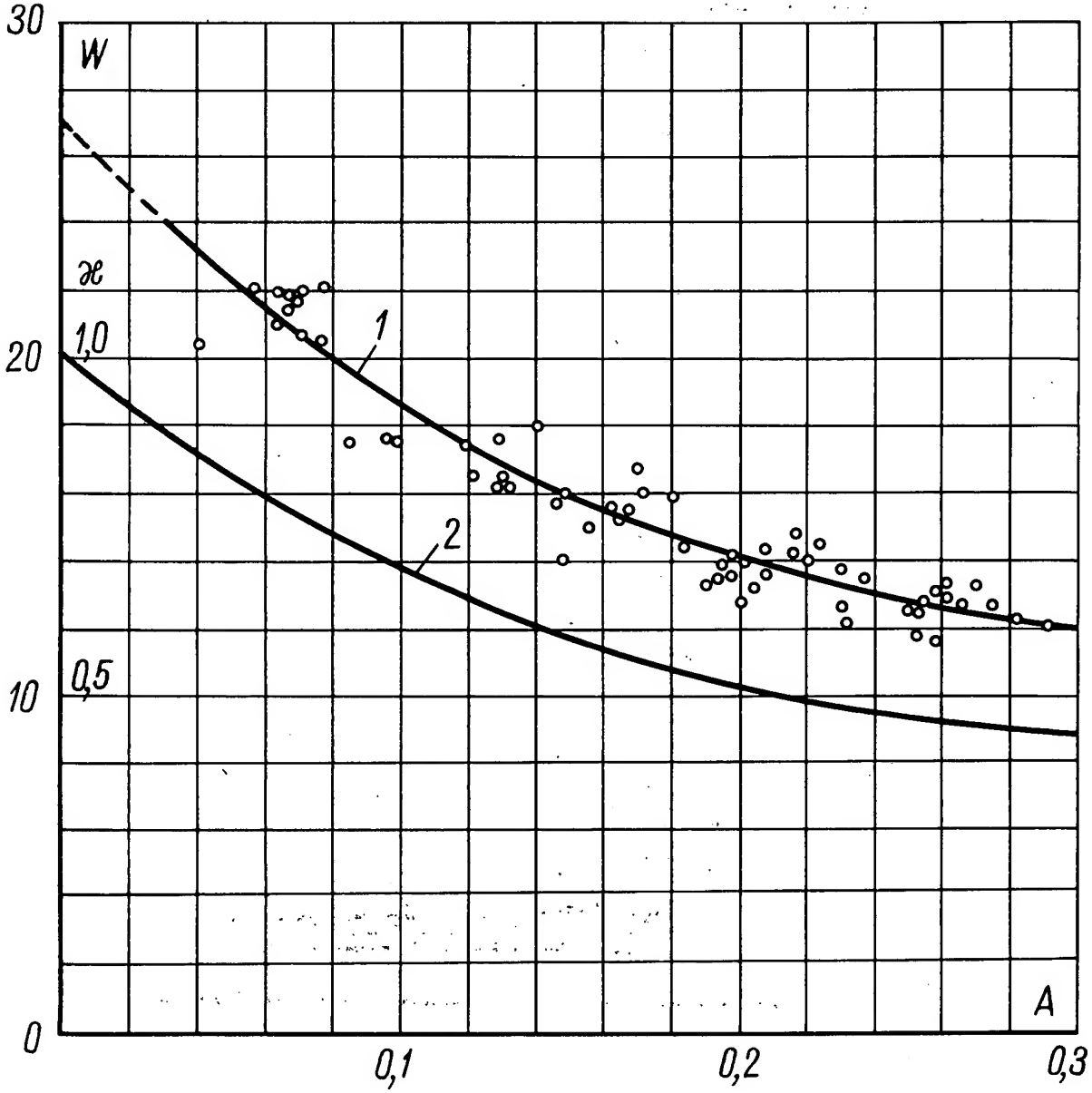

Fig. 6 - EXPERIMENTAL CURVES: 1 - $W = \varphi(A)$

2 - $\varkappa = \frac{W}{W_0} = f(A)$

THEORY OF UNDERFLOWS IN STORAGE RESERVOIRS

* * *

I. I. LEVI
Professor, Dr. Techn. Sciences
The Leningrad Polytechnical Institute named
after M. I. Kalinin

* * *

SUMMARY

The paper deals with theoretical problems of underflows originating in storage reservoirs as a result of considerable quantities of fine alluvium sediment carried by rivers. In actual conditions the regime of the underflow is either non-uniform or unsteady, but in previous investigations this problem has not received the attention it deserves.

An equation is derived in the paper for the non-uniform underflow motion and for plotting curves representing the interface of the underflow and the water filling the reservoir; the equation is integrated for a case of a positive bottom slope and a horizontal channel.

The determination of the value of the total coefficient of resistance λ_c for the underflow is of great importance; experimental studies that were carried out with this aim in view have allowed the establishment of a regular interdependence of λ_c and Reynolds number in the range of the latter's values from 2500 to 35000, at a considerable turbidity (up to 200 kg. per m^3), this fact now allowed the obtainment of a more precise value of this coefficient than those so far obtained.

Section 2 of the paper is devoted to an investigation of the conditions under which an underflow originates.

On the basis of theoretical considerations, as well as the data obtained experimentally a formula is established for the velocity gradient at the upper boundary of the underflow and equation (22) is derived for determining the minimum of turbidity at which the phenomenon becomes unstable.

Section 3 deals with the problem of unsteady motion of the underflow; a system of differential equations is worked out for this case and the term is evolved expressing the velocity of the wave front under the conditions of the interrupted wave which is characteristic of the run-off floods.

SOMMAIRE

Dans ce rapport sont examinées quelques questions de la théorie des courants de fond (underflows) qui se forment dans les réservoirs des rivières saturées par les plus petites particules.

En réalité le régime des underflows est ni uniforme ni permanent; néanmoins dans les recherches précédentes ces problèmes n'étaient pas dûment considerés.

Dans le rapport est déduite l'équation de mouvement non uniforme de l'underflow et sont indiquées les différents formes de l'interface entre l'underflow et l'eau qui remplit le réservoir; l'integration de l'équation est exécutée pour le cas de la pente positive et horizontale.

Pour calculer le phénomène il faut fixer le coefficient total de perte de charge dans le cas de l'underflow; les essais entrepris dans ce but ont donné une fonction régulière λ_c du nombre de Reynolds Re, la valeur duquel était dans les limites de 2500 à 35000; la concentration de vase était assez grande (jusqu'à 200 Kg/m^3); cela a permis de préciser la valeur du coefficient obtenue auparavant.

Le deuxième paragraphe du rapport est consacré aux conditions de la formation des underflows. A la base des considérations théoriques et des essais, l'auteur est arrivé à une formule pour calculer le gradient des vitesses à l'interface de l'interflow et à

l'équation pour définir la concentration minimum avec laquelle le phénomène perd sa stabilité.

Le mouvement non permanent de l'underflow est examiné dans le troisième paragraphe; l'auteur a établi pour ce cas le système des équations différentielles et la formule pour déterminer la vitesse du front d'onde qui se forme dans le cas de l'onde interrompue qui est caractéristique pour les grandes crues d'ondée.

INTRODUCTION

The experience accumulated in the course of the last twenty years in operating storage reservoirs on the rivers possessing a high degree of sedimentation has led to the discovery of underflows in reservoirs.

A turbid flow possessing a density considerably greater than that of water descends to the lower water layers and moves there in the direction of the dam. The peculiarity of this phenomenon is that the underflow is capable of transporting the finest particles suspended in water ($d < 10\text{-}20\,\mu$) across the total length of the reservoir regardless of how great this length is (up to 150 km).

The described phenomenon, which has been named the density current, was made an object of a number of field and laboratory investigations conducted in France, USA, Yugoslavia, Chinese People's Republic and USSR[1), 2), 3)]. The obtained data were used by Raynaud, Blanchet and Villatte in working out an approximate solution to the problem of a uniform steady underflow with a homogenous density fluid, moving in the water medium, as the base of the concept of the density currents. Under the conditions of turbulence an intermediate layer(y) is formed between this dense fluid and water, within the boundaries of which the velocity and density gradients are quite considerable (fig. 1).

---

1) H. Duquennois. New methods of sediment control in reservoirs. Water Power. May, 1956.

2) Étude des courants d'eau boueuse dans les retenues (underflow). 4 Congrès des Grands Barrages New-Delhi; 1951, Question n° 14. Rapport n° 48.

3) I. I. Levi. "Laws of a high turbidity flow motion in reservoirs." Reports of the High School, Construction, No. I, 1958.

4) C. Blanchet et H. Villatte. Courants de densité. Études expérimentales en canal vitré. Conférence technique régionale. Tokio, 1954. Laboratoire Dauphinois. Neyrpic, Grenoble, France.

Proceeding from these assumptions Blanchet and Villatte produced the following equation[4)]

$$(\gamma_1 - \gamma) h I_o = \left[\frac{\gamma_1}{C_o^2} + \frac{\gamma H}{C_1^2 (H-h)} \right] \qquad (1)$$

In actual conditions the regime of the underflow is unsteady during 4-5 months; run-offs are of a rain-water variety and are characterized by a few waves of high intensity. The process of sedimentation of reservoirs in such or similar hydrological conditions can be conceived as follows: in the upper parts of the reservoir a cone of alluvium is formed consisting of the largest size sand particles transported by the river (mainly of particles d $>$ 0.02 - 0.05 mm. Zone I); as soon as the cone of alluvium reaches sufficient height there appears an underflow; the finest sediment (d $<$ 0.01 mm)[1)] particles are carried downstream unobstructed, while intermediate size particles are deposited a considerable distance below the cone of alluvium (Zone 2) (fig. 2).

Due to accumulated flood waters, large masses of turbid water with high content of the finest particles of silt and clay come together in the lower depths of the reservoir; with the end of the rainy season, when underflows are formed no longer, these masses of turbid water flow down towards the dam, their level becoming horizontal and the sediment beginning gradually to settle down. Just this kind of situation can be observed in the reservoirs on Lake Mead on the Colorado River, in the Kwan-Ting reservoir in China and in a number of reservoirs in Algeria.

The presence of a clearly defined change of the shape of the bottom slope, in passing from Zone 2 to Zone 3, results in a non-uniform current regime coinciding with those periods of the year in which the river discharges become sufficiently steady, - a drop appears in the horizontal section and a backwater in the section upstream. In case of a speedy increase of the discharge and turbidity of the stream, the run-off water is propagated in the form of an interrupted wave and, in a short period of time, reaches the dam; here the wave is reflected, this phenomenon being accompanied by a sharp rise of the turbid current at the dam. The narrower the river cross section

---

1) According to the opinion of French scientists the maximum diameter of the particles transported by the underflow reaches 12-20.

and the greater the accumulated discharge of the river - the greater will be the rise of the turbid current at the dam.

This general outline of the process of underflow formation in reservoirs should be supplemented by an investigation of the conditions of the non-uniform and unsteady regime of the density currents, since only such an investigation would furnish the data necessary to form a correct idea of the current mean velocities for the total length of the reservoir, of the speed of the run-off wave front propagation, of the height of the density flow rise at the dam at the moment of the wave reflection, and of the nature of the accumulation process. Solution to these problems is absolutely indispensable for the purpose of designing the process of the reservoir sedimentation and of determining forces acting upon the structures.

It is at the same time necessary to make a thorough study of the conditions under which the bottom current is originated; observations prove that this phenomenon occurs only when a definite amount of sediment S_{min} is present in the river. Sedimentation being a known factor, the duration of the period can be determined, in which the underflow will be extant, and the finest sediment particles carried down to the tail race.

The present investigation is devoted to studying the problems indicated. The experiments described below were accomplished under the author's guidance in the Laboratory of River Hydraulics of the Leningrad Politechnical Institute by N. P. Kulesh, Master of Tech. Sciences, L. N. Alexandrov, Assistant, and A. K. Khapayeva, Senior Engineer.

1. Non-uniform Motion of the Underflow

In working out the equation for the non-uniform underflow, we shall proceed from the same postulates that Blanchet and Villatte had put at the base of their analysis; tangential stresses at the outer boundaries of the current would be $\tau = \gamma_1 \frac{\lambda_i v^2}{2g}$ while λ_o would represent the bottom resistance coefficient and λ_1 - the upper boundary resistance coefficient.

The slope of the boundary separating the underflow from the rest of the fluid mass will be

$$I = I_o - \frac{dh}{ds}$$

where I_o = the bottom slope.

Summing up all the acting forces including the force of inertia, and referring it to the unit volume (fig. 1, section 1-1 - 2-2) the following equation is arrived at:

$$(\gamma_1-\gamma)\left(I_0-\frac{dh}{ds}\right)=\gamma_1(\lambda_0+\lambda_1)\frac{v^2}{2gh}+\gamma i+\gamma_1\alpha\frac{d}{ds}\left(\frac{v^2}{2g}\right) \quad (2)$$

where i is the gradient of the reservoir free surface. Member is to be excluded from equation (2). For this purpose the theorem of pulses is applied to the flow as a whole, including the inverse current (section 1-A-B-2, Fig. 1) and the result referred to the unit volume:

$$(\gamma_1-\gamma)\left(I_0-\frac{dh}{ds}\right)=\gamma_1\lambda_0\frac{v^2}{2gh}+\gamma\frac{H}{h}i+\gamma_1\alpha'\frac{d}{ds}\left(\frac{v^2}{2g}\right) \quad (3)$$

here $\alpha'=\frac{\int_0^H u^2dy}{v^2h}$, u - is local velocity.

If the inverse current velocity in the upper layers of the reservoir is negligible α' differs little from α; assuming $\alpha'=\alpha$ in the first approximation and substracting (2) from (3):

$$\gamma i=\gamma_1\lambda_1\frac{v^2}{2g(H-h)} \quad (4)$$

whereupon equation (2) is transformed to appear:

$$\gamma'\left(I_0-\frac{dh}{ds}\right)=\left(\lambda_0+\lambda_1\frac{H}{H-h}\right)\frac{v^2}{2gh}+\alpha\frac{d}{ds}\left(\frac{v^2}{2g}\right) \quad (5)$$

Here $\gamma'=\frac{\gamma_1-\gamma}{\gamma_1}$

Substituting v by $\frac{q}{h}$ where q is discharge per channel unit width (rectangular bed being assumed) we have:

$$\frac{dh}{ds}=\frac{\gamma' I_0\left(\lambda_0+\lambda_1\frac{H}{H-h}\right)\frac{q^2}{2gh^3}}{\gamma-\frac{\alpha q^2}{gh^3}} \quad (6)$$

Equating the denominator to Zero the critical depth of the bottom flow is found:

$$h_c=\sqrt[3]{\frac{\alpha q^2}{g\gamma'}} \quad (7)$$

Critical Velocity:

$$v_c = \sqrt[3]{g q \gamma'} \tag{8}$$

Depth of reservoir $H=H + I_o S$; thus, in the given conditions the uniform flow regime is impossible.

Equating $\frac{dh}{ds}$ to zero the minimum (or maximum) value of function h is determined and the following formula obtained:

$$\varphi(h_o) = \left(\lambda_o + \lambda_1 \frac{H}{H-h} \right) \frac{h_c^3}{h^3} 2\alpha I_o \tag{9}$$

where h_o - minimum depth, $\lambda_o + \lambda_1 \frac{H}{H-h_o} = 2\lambda_c$

To characterize λ_c graph $2\lambda_c = \varphi$ (Re) (fig. 3) is given from which it is clearly seen that the resistance coefficient decreases regularly as Reynolds number grows; in the experiments density was as high as 200 kg. per $m.^3$; this fact permitted to establish value in a sufficiently wide range of Reynolds Number.

Values of Re $>$ 24000 can be considered as related to the quadratic zone. This assumption, however, is subject to additional confirmation. Since H = f(s), also h_o = f(s); variation of h_o is negligible, however. Line h may change its curvature; equating the second derivative $\frac{d^2h}{ds^2}$ to zero, the value of dh/ds at the point of inflection D is determined:

$$\left|\frac{dh}{ds}\right|_{\mathfrak{D}} = -\frac{dH}{ds} \frac{\lambda_1 (h^3 - h_c^3)}{(H-h)^2 h \left[6(\lambda - \alpha I_o) - \frac{\lambda_1 H (h^3 - h_c^3)}{h_o^2 (H-h_o)^2} \right]} \tag{10}$$

and since $\frac{dH}{ds} > 0$, with $h > h_c$, $\left|\frac{dh}{ds}\right|_{\mathfrak{D}} < 0$.

It may be inferred from this formula that should a curve of drop be formed the curvature of line h is subject to variations.

Configuration of the interface will vary depending on the correlation of h_o and h_c (I_o and I_c).

These configurations for $I_o < I_c$ are shown in fig. 4. Lines N-N and K-K define three zones of the interface curves:

Zone A, where backwater is observed,

Zone B, where drop is seen, and

Zone C, where there is backwater.

In the horizontal section interface curves of only B and C types are possible.

The task is now to integrate the equation for the case of a positive slope of the bottom of the reservoir. New variables $\eta = \frac{h}{h_c}$ and $\sigma = \frac{s}{h_c}$ are introduced. Equation (1) will then appear

$$\frac{d\eta}{d\sigma} = I_o \frac{1 - \frac{A}{\eta^3}}{1 - \frac{1}{\eta^3}} \qquad (11)$$

where $A = \frac{\lambda_c}{\alpha I_o} = \frac{(b-\eta)\lambda_o}{2\alpha I_o (a-\eta)}$

$a = \frac{H}{h_c}$; $b = a\left(I + \frac{\lambda_1}{\lambda_o}\right)$

Since $H = f(s)$, quantity $A = f(\eta, \sigma)$; solving equation (11) becomes very difficult. An approximated solution is, however, possible with A assumed being constant within the boundaries of the investigated area of the reservoir. It is thus necessary to divide the whole of the upstream water into several areas in whose boundaries variations of quantity A are but negligible.

Separating the variables and integrating equation (7) we have

$$I_o \sigma + K = \eta + (A-1) \frac{d\eta}{\eta^3 - A} \qquad (12)$$

Integral $\int \frac{d\eta}{\eta^3 - A}$ is easily reduced to integral $\varphi(z) = \int \frac{dz}{z^3 - 1}$ well known in the theory of non-uniform motion, by substituting $\eta = \sqrt[3]{A}\, z$

$$\int \frac{d\eta}{\eta^3 - A} = \frac{1}{\sqrt[3]{A^2}} \varphi(z) \qquad (13)$$

We obtain the final solution in the following form:

$$I_0 \frac{S_2 - S_1}{h_c} = \eta_2 - \eta_1 + \frac{A-1}{\sqrt[3]{A^2}} \left[\varphi(z_2) - \varphi(z_1) \right] \tag{14}$$

In the process of the silting of the reservoir the river bed in front of the dam spillway openings is levelled and becomes horizontal; the case of the bottom flow moving over the horizontal bed is, therefore, of a particular interest from the practical viewpoint. The equation of motion will in the case take the following form:

$$\frac{d\eta}{d\sigma} = - \frac{b - \eta}{2(\eta^3 - 1)(a - \eta)} \tag{15}$$

In the studied problem quantity H can be regarded as being constant since the river bottom is horizontal while the gradient i of the free surface is insignificant.

Separating the variables from the following equation and integrating equation (15) we have:

$$K - \frac{\lambda_0 \sigma}{2} = \varphi(\eta) = \int \frac{(\eta^3 - 1)(a - \eta)}{b - \eta} d\eta \tag{16}$$

$$\varphi(\eta) = \frac{\eta^4}{4} - \eta - (b-a) b^3 \left[\zeta + \frac{\zeta^2}{2} + \left(1 + \frac{1}{b^3}\right) \ln\left(1 - \zeta\right) \right] \tag{17}$$

where $\zeta = \frac{\eta}{b}$

In the first approximation the method of summation can be applied in designing

$$\frac{\lambda_0 \sigma}{2} = \sum_1^n \frac{f(\eta_i) + f(\eta_{i+1})}{2} \Delta\eta \tag{18}$$

$f(\eta)$ - sub-integral function

Fig. 5 illustrates an experimentally plotted curve of a drop that was observed in one of the experiments conducted in the laboratory of the Leningrad Polytechnical Institute; there is, in the same graph, another curve plotted by designing with

$$\lambda_0 = 0.005 \text{ and } \lambda_1 = 0.006.$$

2. Factors contributing to the underflow formation

A steady bottom current can be formed only if certain definite conditions are extant; these prerequisite conditions are: depth h must be considerably less than H; since quantity h depends upon the flow discharge and its turbidity, it can be asserted that the turbidity should exceed a certain minimum quantity S_{min} if an underflow is to be formed.

Should depth h of the flow be comparatively small, velocity u of the inverse current will be low as compared to velocity $\mathfrak{v}$ of the density flow, while the intermediate zone will become negligible (fig. 1). With decreased turbidity and increased h the inverse current velocity will grow, gradually approaching $\mathfrak{v}$; simultaneously, the intermediate zone thickness y will increase. Finally, the inverse current velocity gradients will approximate each other and the turbulence will spread to the total depth of the reservoir; at this moment the underflow will become unsteady. On the basis of this condition we shall proceed now to determine the minimum density at which the underflow is formed.

The experiments conducted by Blanchet and Villatte, on one hand, and by Kulesh on the other prove that the velocity curve in the intermediate zone is approximating the straight line; this is in full accord with the deductions of the turbulent stream theory, so that it can be assumed by analogy that

$$\frac{d\upsilon}{dy} = \text{Const} = \frac{\upsilon_h}{y} \qquad (19)$$

since the intermediate layer thickness y, provided $\mathfrak{v} = u$, is equal to $\frac{H-h}{2}$, $\frac{d\upsilon}{dy} = \frac{2\upsilon_h}{H-h}$; here υ_h is the velocity at the upper boundary of the underflow (at height h).

The distribution of velocities in the underflow is ruled by the Logarithmic Law[1]; the variation of velocity in the central body of the cross-section is therefore insignificant so that υ_h can be assumed to be proportional to the mean velocity $\mathfrak{v}$, which is equal to $\sqrt{\frac{g h \gamma' I_o}{\lambda_c}}$. On equal grounds quantity $\frac{d\upsilon}{dy}$ can be considered as directly proportional to $\sqrt{\gamma'}$ and inversely proportional to $\sqrt{h}$

---

1) Idem, p. 3, N. 4

In order to verify these assumptions special experiments were carried out at the Laboratory of River Hydraulics of the Leningrad Polytechnical Institute. The results obtained are shown in fig. 6; two points related to the experiments of Blanchet and Villatte and borrowed from their paper have been plotted against this graph.

On the basis of these data the rated correlation for $\frac{dv}{dh}$ can be represented as

$$\frac{dv}{dh} = 2{,}5\left(\sqrt{\gamma'} - 0{,}03\right)\sqrt{\frac{g}{h}} \qquad (20)$$

We shall now introduce (20) into (19) and express v_h in the term of v:

$$v_h = Cv \text{ , where } C < 1.$$

$$\frac{2v_h}{H-h} = \frac{2C}{H-h}\sqrt{\frac{g\,h\,I_o\,\gamma'}{\lambda_c}} = 2{,}5\left(\sqrt{\gamma'} - 0{,}03\right)\sqrt{\frac{g}{h}}$$

reducing the expression we have

$$\frac{h}{H-h}\sqrt{\frac{I_o}{\lambda_c}\gamma'} = \frac{1{,}25}{C}\left(\sqrt{\gamma'} - 0{,}03\right) \qquad (21)$$

Using formula (9) to determine h we write down the final equation to find γ_{min}.

$$\sqrt{\gamma'_{min}} - \frac{0{,}8\,C\,f\sqrt[6]{\frac{I_o\,\gamma'_{min}}{\lambda_c}}}{1 - f\sqrt[3]{\frac{\lambda_c}{I_o\,\gamma'_{min}}}} = 0{,}03 \qquad (22)$$

where $f = \sqrt[3]{\frac{q^2}{g\,H^3}}$

In this equation q, H, I_o and λ_c are given quantities; hence γ_{min} is a function of q, H, I_o and λ_c. Values of γ_{min} and S_{min} for two values of $\frac{I_o}{\lambda_c}$: 1.0 and 0.1 are given in Table No. 1: quantity "C" is taken as being equal to unity, which constitute a calculation reserve.

TABLE No. 1

f	$I_o/\lambda_c = 1$		$= 0.1$	
	$\gamma_{min.}$	$S_{min.}$ kg/m.^{3}	$\gamma_{min.}$	$S_{min.}$
0.01	0.0011	1.85	0.001	1.7
0.02	0.0014	2.4	0.0013	2.2
0.03	0.0017	2.9	0.0017	2.9
4.04	0.0022	3.7	0.0025	4.25
0.05	0.0029	5	0.0038	6.5
0.06	0.0039	6.6	0.0056	9.5

We are thus convinced that with an increase of f, i.e. with an increase of discharge q or with a decrease of H, turbidity necessary to maintain the steady motion of the underflow must grow; the effect of I_o/λ_c is slight.

To corroborate these theoretical assumptions corresponding experiments were conducted, of which the first series was for the purpose of qualitative verification of the phenomenon and provided an evidence confirming the variation of the regime of motion in the spatial conditions on a plot of 10 x 13 m.^{2} (S. J. Goriunov, Master of Techn. Science, The All-Union Scientific Research Institute of Hydrotechnics, named after B. E. Vedeneev), turbidity being 2-4 kg. per m.^{3} and f being equal to 0.02 - 0.04. The experiments of the second series (N. P. Kulesh, Master of Techn. Sciences), were to establish the greatest depth of the underflow, at which it becomes unsteady; value of $\frac{h}{H}$ fluctuated within 0.35 - 0.45, turbidity being about 2.5 - 5 kg. per m.^{3}; obtained by calculation, are shown in Table No. 2.

TABLE No. 2

$\frac{I_o}{\lambda_c}$	f	S_{exp}	S_{calc}	$\frac{S_{calc}}{S_{exp.}}$
1	0.04-0.045	2.5 - 3	3.7-5	1.5-1.7
2.5	0.065-0.08	4 - 5	6.5-8.5	1.625-1.7

From the data shown it can be seen that with C=1 the calculation furnishes a value of S_{min} which is in excess by 50-70%, this constituting a calculation reserve; it would naturally be impossible to expect the calculated and experimental values of S_{min} to tally completely in the case under investigation.

3. Unsteady Motion of the Underflow

The system of equations for unsteady motion of fluid as applied to the conditions of the underflow in reservoirs should be corrected in view of the fact that the density of a flow is a quantity variable in time.

With variable γ' introduced in the calculation our equations will take the following form:

$$\left.\begin{aligned}(\gamma'-\gamma)\left(I_0-\frac{\partial h}{\partial s}\right)&=\gamma_1\lambda_c\frac{v^2}{gh}+\frac{\alpha v}{g}\frac{\partial(\gamma_1 v)}{\partial s}+\frac{1}{g}\frac{\partial}{\partial t}(\gamma_1 v)\\ \frac{\partial(\gamma_1 Q)}{\partial s}&+\frac{\partial(\gamma_1\omega)}{\partial t}=0\end{aligned}\right\}\quad(23)$$

Characteristic equation $\gamma_1 = f(t, s)$, which determines density variation in time and over the current field, should be included in the system; as a rule, the density in the upper boundary cross-section is predetermined.

Going over to the new independent variables h and t (as is usual with the analysis of an unsteady regime) and transforming the equations we arrive at the formula for the velocity of the wave fron propagation $\frac{ds}{dt}$:

$$(\gamma_1-\gamma)g\frac{\omega}{B}-\gamma_1\left(v-\frac{ds}{dt}\right)^2=0$$

hence,

$$C=\frac{ds}{dt}=v\pm\sqrt{\frac{(\gamma_1-\gamma)}{\gamma_1}g\frac{\omega}{B}}\quad(24)^{1)}$$

1)

S. Angelin and K. Flikstad determine quantity "C" by an analogical formula, but without the first summand.

S. Angelin and K. Flikstad. An investigation of intake arrangements for cooling water supply stratified Seawater. Alokarleby, Sweden VII Congress IAHR (Lisbon) C-13.

The second equation will take the following form:

$$(\gamma_1 - \gamma) I_o gh = \gamma_1 \lambda_c v^2 + \gamma_1 h \frac{dv}{dt} + \gamma_1 \left(v - \frac{ds}{dt}\right)\frac{dh}{dt} + h\left(\frac{\partial \gamma_1}{\partial t} + v \frac{\partial \gamma_1}{\partial S}\right)\frac{ds}{dt} \quad (25)$$

(equation (25) is given for a rectangular channel).

In case of turbidity γ_1 being constant the equation is reduced to complete differentials and is solved in finite differences in conjunction with (24):

$$d(\gamma_1 v) = \pm d(\gamma_1 h)\sqrt{\frac{g(\gamma_1 - \gamma)}{\gamma_1 h}} + \left[g(\gamma_1 - \gamma) I_o - \gamma_1 \lambda_c \frac{v^2}{h}\right] dt \quad (26)$$

where $\gamma_1 v$ and $\gamma_1 h$ are variables.

As can be seen from formula (24) the velocity of propagation of the wave front depends, to a considerable measure, on the turbidity of the flow. Together with the increased flood discharge and turbidity the velocity of the flood wave propagation will also be increased.

Since the turbidity of the flow increases several times during rain falls (5-10 times on the Huang Ho river for instance) while at the same time the depth of the underflow substantially increases, the flood wave, gently sloping in the beginning, will rapidly increase its slope and will break. This entitles us to regard the rain flood wave as an interrupted wave. The above was confirmed by calculations carried out for a large storage reservoir (150 km. in length), on the Huang Ho River; these calculations proved that the flood wave is transformed but little and reaches the dam in no less than 12 hours, the duration of the flood being 5-8 days.

In analysing the problem of the underflow motion in the form of an interrupted wave (fig. 7) we shall apply the Law of Quantities of Motion to fluid section I-I ÷ II-II; it can be assumed then that during the period of time Δt the section will shift to position AA - BB.

As a result of this shifting the increment to the fluid mass will be equal to AA' - CC' (shaded):

$$\Delta M = \frac{\gamma_1}{g}(\Delta S - v_1 \Delta t)(h_2 - h_1)$$

where v_1 and h_1 = initial velocity and depth of fluid respectively,
v_2 and h_2 = velocity of wave front propagation,
$C - v_1 = a$, $q_1 = v_1 h_1$, $q_2 = v_2 h_2$.

The velocity acquired by this mass $\Delta v = C - v_2$; hence the increment of the section quantity of motion during Δt will take the form of:

$$\Delta M \Delta v = \frac{\gamma_1}{g} a (h_2 - h_1)(c - v_2) \Delta t$$

Substituting a and $h_2 - h_1$ for $C - v_2$ we have:

$$C - v_2 = a \frac{h_1}{h_2}, \quad v_2 - v_1 = a \frac{h_2 - h_1}{h_1}$$

Hence, the increment of the quantity of motion will appear as

$$\frac{\gamma_1 (h_2 - h_1)}{g h_2} \quad h_1 a^2 \quad \Delta t$$

The impulse of the acting forces, with the bottom of the reservoir being horizontal, will be:

$$P < \Delta t = (\gamma_1 - \gamma) \frac{h_2^2 - h_1^2}{2} \Delta t$$

Equating it to the increment of the quantity of motion we arrive at the final relationship:

$$\frac{\gamma_1 (h_2 - h_1) h_1}{g h_2} a^2 = (\gamma_1 - \gamma) \frac{h_2^2 - h_1^2}{2} \qquad (27)$$

and hence

$$C = v_1 \pm \sqrt{g \gamma' \frac{(h_2 - h_1) h_2}{2 h_1}} = v_1 \pm \sqrt{g h_1 \gamma' \left(1 + \frac{3}{2} \frac{z}{h} + \frac{z^2}{2 h_1^2} \right)} \qquad (28)$$

With z being small, as compared with h_1 ($\frac{z}{h_1} < 0.4$), quantity $\frac{z^2}{2 h_1^2}$ can be ignored.

Formula (28) differs from that of the interrupted wave velocity in open channels by factor $\sqrt{\gamma'}$ only.

Formula (28) has been derived with the assumption that the thickness of the intermediate layer between the underflow and inverse current of clear water is relatively small. In cases when this assumption is impossible the calculated formula for the interrupted wave velocity will

take the following form:

$$c = v_m \pm \sqrt{g h_m \gamma' \left(1 + \frac{3}{2} \frac{z}{h_m}\right)} \qquad (29)$$

where $h_m = h_1 + y$, $\gamma'_m = \gamma' \left(1 - \frac{y}{2h_m}\right)$ and

$$v_m = v_I \left(1 - \frac{y}{2h_m}\right);$$

in deriving formula (29) the distribution of velocities and density in the interrupted layer is taken as variable in accordance with the Linear Law.

In the event of the fluid discharge accumulation, the flood wave, reaching the dam, will be reflected from the construction, the height of the return wave will depend on the quantity of the accumulated discharge. In order to determine the height of the reflected wave we shall use the method of approximation offered by M. D. Chertoussov; the velocity of the front wave propagation will be determined in this case from formulae (28) or (29), the minus sign to be placed before the term which is under the radical sign (photograph 8). The accumulated discharge ΔQ being known, we can determine the height of the wave in front of the construction at the initial moment of its formation from formula

$$\Delta Q = Q - Q_2 = \left[\sqrt{g\gamma' \frac{\omega}{B_1}\left(1 + \frac{3}{2}\frac{zB}{\omega}\right)} - v_2\right] Bz \qquad (30)$$

where B is the channel width in front of the construction at the height and B_1 - width across the bottom. Velocity v_2 is dependent upon the conditions of the flow approach to the construction; since the flood is propagated in the form of an interrupted wave, we have to calculate v_2 from formula (28); this calculation should be performed before the reflected wave is designed. It is obvious that this case will give the maximum possible value for Z.

It should be borne in mind that the channel in front of the construction is usually considerably narrower than the channel of the upper pool; the reflected wave, therefore, in its subsequent movement, widens the plan and its height decreases. The filling of the bottom layers of the reservoir is rapid due to repeated reflections; the final level of the underflow depends on the total volume of the accumulated discharge

W and the form of the reservoir between the initial and final level[1] of the underflow which may be considered as being horizontal. The level of the free surface of the reservoir, which can also be regarded as being horizontal, will rise at the same time.

In order to compute ΔZ and Δy the balance equation is to be used in its integrated form, worked out separately for filling the bottom and surface layers of the reservoir. For the bottom layers (turbid flow) we have:

$$\int_{t_0}^{t_1} \gamma_1 Q\,dt = \int_{0}^{t_1} \gamma_1 Q\,dt + \gamma_1 \int_{z_1}^{z_2} \Omega_z\,dz \qquad (31)$$

where Ω_z = bottom area at level Z, variable with increase of Z

Q = inflow discharge

Q_2 = discharge to the tail race

Similarly, for the surface layers:

$$\int_{t_0}^{t_1} \gamma_1 Q\,dt = \int_{t_0}^{t_1} \gamma_1 Q_2\,dt + \gamma \int_{y_1}^{y_2} \Omega\,dy \qquad (32)$$

where Ω = area of the reservoir water surface at level y.

Since Ω is considerably greater than Ω_z, the level rise of the free surface is much smaller than the rise of the bottom current level. With the channel in front of the construction sharply narrowing, the initial rise of the bottom current level may prove to be the greatest and will not be exceeded in the process of discharge accumulation. In view of this fact the problem of the reflected wave calculation at the moment of its inception is of great practical interest. To ascertain the validity of the assumptions the Laboratory of River Hydraulics of the Leningrad Polytechnical Institute undertook a number of experimental studies in the course of which the relationship between the accumulated (Q) and spilt (Q_2) discharges was modified and so was the turbidity of the flow. Distribution of turbidity by depth was non-uniform; due to this the turbidity in the reflected wave was much lower than it was in the direct, and its velocity was low (fig. 9); by

---

1) Initial level is determined by calculation, in accordance with the formulae of non-uniform motion at the discharge proceeding the flood.

this fact high values of $\frac{z}{h_2}$, observed in the experiments, can be explained. With uniform distribution of turbidity by depth, values of $\frac{z}{h_2}$ are found to be within the range of 0.5 - 1.5, depending on quantity $\frac{v_2}{\sqrt{g h_2 \gamma'}}$. The results of the comparison of the calculated value of $\frac{z}{h_2}$ with the results obtained experimentally are given in (fig. 10) where calculated and experimental values of $\frac{z}{h_2}$ are shown on the abscissa and ordinate axes respectively; the velocity of the flow at the approach was near the critical velocity. Thus, the data obtained by calculations based on formula (28) are satisfactory enough, accuracy of the result ebing within 10%. In most cases the values obtained by computation are exaggerated, the excess constituting a reserve of accuracy.

CONCLUSIONS

The obtained calculated formulas supply means for determining the main hydraulic characteristics of the underflow originating in reservoirs, provided there is a certain definite amount of sediment present in the river.

These characteristics are: mean values of velocity (regime of the flow being steady), velocity of the flood wave front propagation, height of the rise wave in front of the dam with the flood waters partial accumulation, and the general rise of the underflow levels in the process of the flood waters accumulation.

These characteristics being known one is able to design the process of the reservoir sedimentation proceeding from the scheme described earlier and to determine the quantity of fine suspended sediment that can be discharged into the tail race of the hydro-electric station.

For this purpose it is first of all necessary to establish the minimum turbidity at which formation of underflow is possible; the duration of the period will thereby be determined, in which the fine suspended sediment may be discharged into the tail race. In the remaining part of the year all the sediment will settle in the reservoir proper since velocities of the current will be very low.

It is further necessary to analyse the problem of the volume of the accumulating flood waters, which is of importance in controlling floods

on one hand and in the matter of a more complete utilization of the water discharge at the hydro-electric stations on the other, and for the purposes of irrigation.

The underflow velocities in flood periods are perfectly sufficient for silt and clay particles to be easily transported by the current; in the time intervals between the floods and at the time following their passage the current velocities will be considerably lower and especially so at the time when deposits of the finest sediment particles will be settling in front of the dam (Zone 3). The deposits will cause a backwater in the upper areas, where current velocities may become so low that even the finest sediment particles will begin settling; it has been observed that settling begins at velocities lower than 10-15 cm per sec.

Making use of the equation for the non-uniform motion of the underflow in the horizontal area of the reservoir the zones and volumes can be designed of probable deposition of silt and clay particles, forming in the result of the backwater mentioned.

Owing to the above calculation methods it becomes possible to draw up a general picture of the underflow formation, to establish the degree of intensity of the wave phenomena and the volume of sedimentation that will be carried by these currents into the river tail race.

Designers will thus be enabled to determine, with sufficient degree of certainty, the date of the reservoir sedimentation and pressures borne by hydrotechnical constructions when waves of the rising turbidity flow appear at the site of the hydro-electric station.

SYMBOLS

v - mean velocity of underflow

h - depth of underflow

H - depth of reservoir

γ_1 - specific gravity of underflow

- specific gravity of water

C_o and C_1 - Chezy Coefficients for lower and upper boundaries of underflow

λ_o and λ_1 - coefficients of resistance for the same boundaries

τ - tangential stresses

α and α' - correctives of quantity of motion

h_c and v_c - critical depth and velocity

$\eta = \frac{h}{h_c}$, - $\sigma = \frac{s}{h_c}$, q, specific discharge $q = \frac{Q}{B}$

B - channel width

Ω_z - reservoir bottom area

Ω - reservoir water face area

v_1 and v_2 - velocities of current in the range of interrupted wave front

C - velocity of interrupted wave front

h_2 - depth after wave passage

Z - height of wave: $z = h_2 - h_1$

BIBLIOGRAPHY

1 H. Duquennois, New methods of sediment control in reservoirs. Water Power, May, 1956.

2 I. P. Raynaud, Étude des courants d'eau boueuse dans les retenues (underflow). 4 Congrès des Grands Barrages. New Delhi. Quest. N14, rapp. N 48.

3 I. I. Levi, Laws of a high turbidity flow motion in reservoirs. Reports of the High School, Construction, N№ 1, 1958.

4 C. Blanchet et H. Villatte. Courant de densité. Études expérimentales en canal vitré. Conférence technique régionale. Tokio, 1954.

5 S. Angelin and K. Flikestad. An investigation of intake arrangements for cooling water supply stratified Seawater. Alvkarleby, Sweden. VII Congress I.A.H.R. (Lissbon) C-13, 1957.

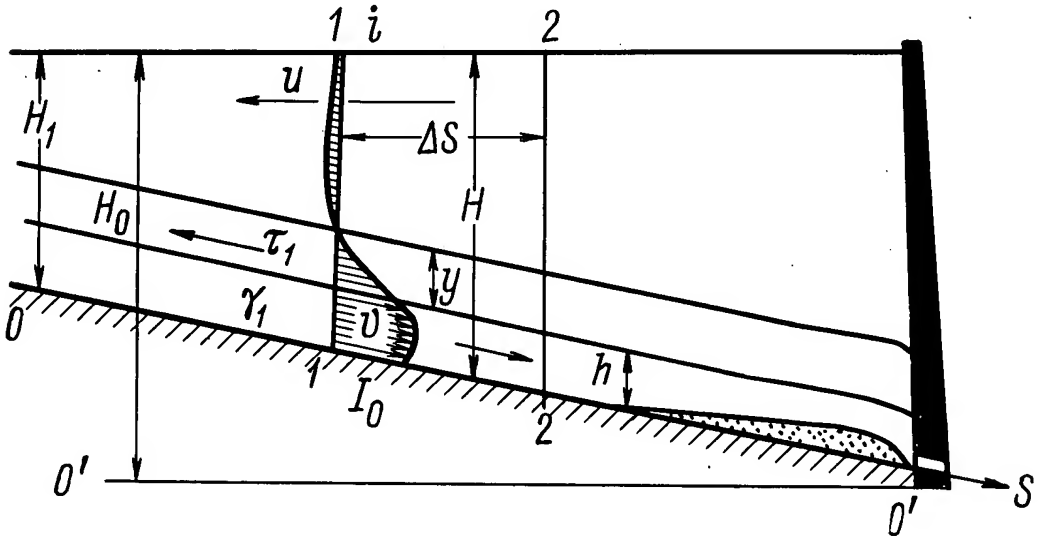

Fig. 1
Hydraulic scheme of underflow.

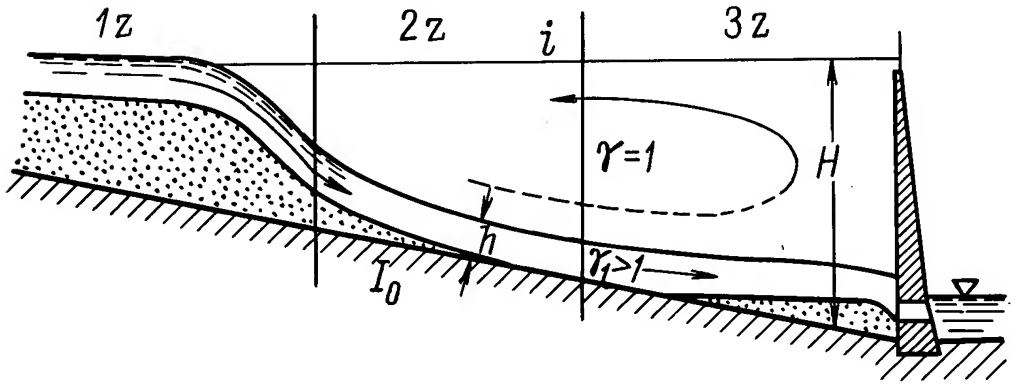

Fig. 2
Motion of high turbidity flow in reservoir and silting of reservoir.

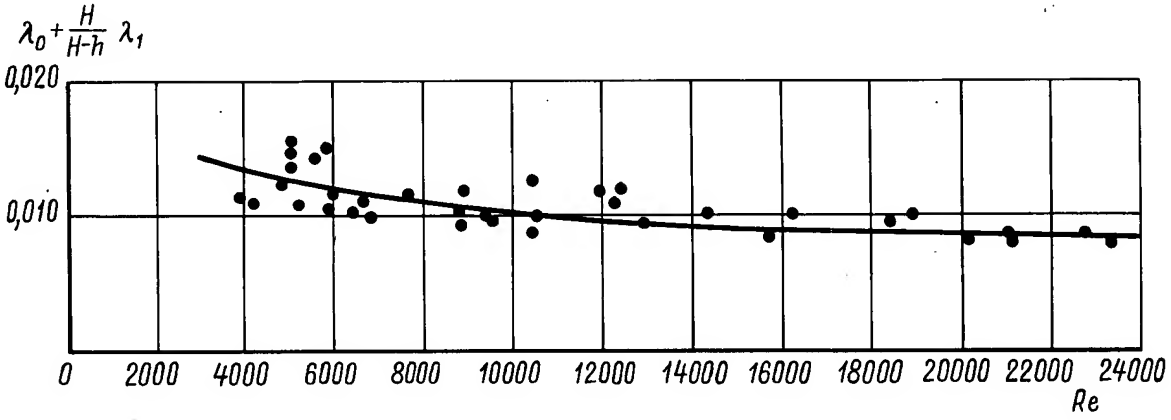

Fig. 3
Correlation $\lambda_c = \varphi(Re)$

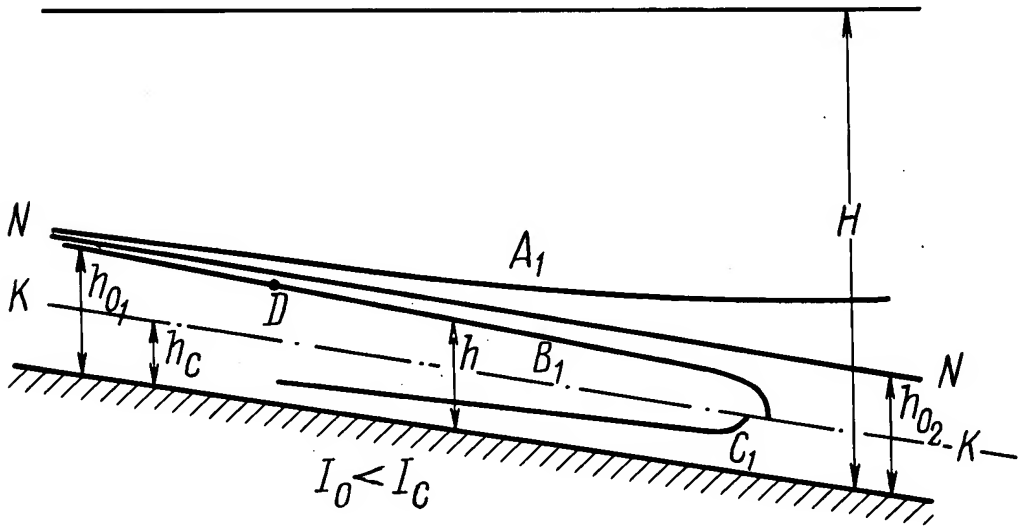

Fig. 4
Curves of underflow interface.

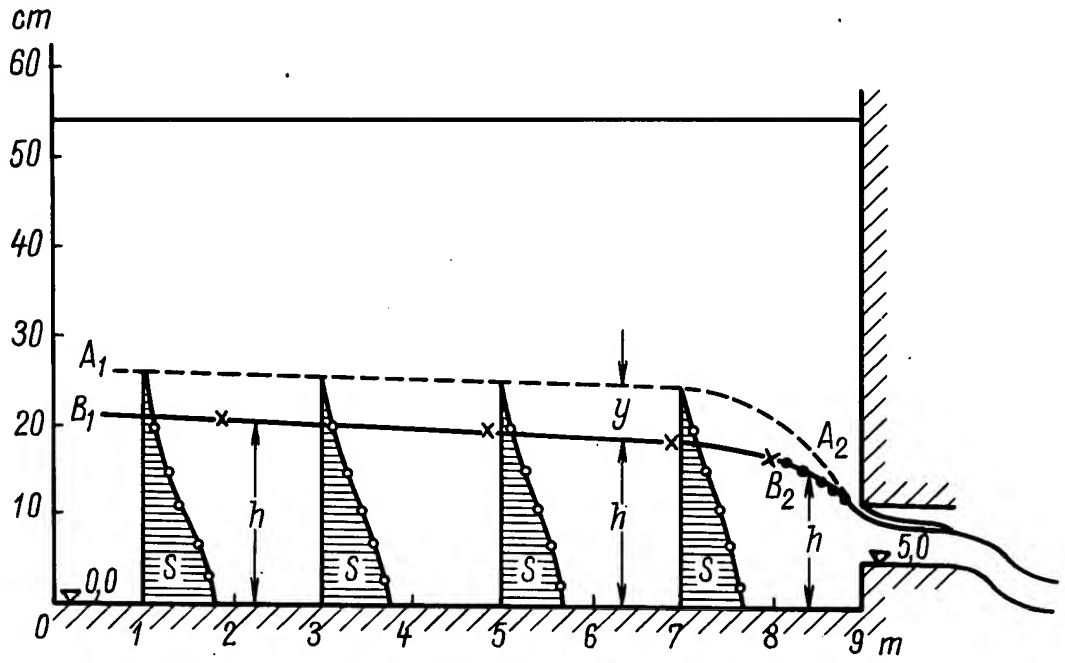

Fig. 5
Computed curve of type B underflow interface in horizontal flume, $\lambda_0 = 0.005$;
comparison with experimental data: o - empiric points
x - computed points

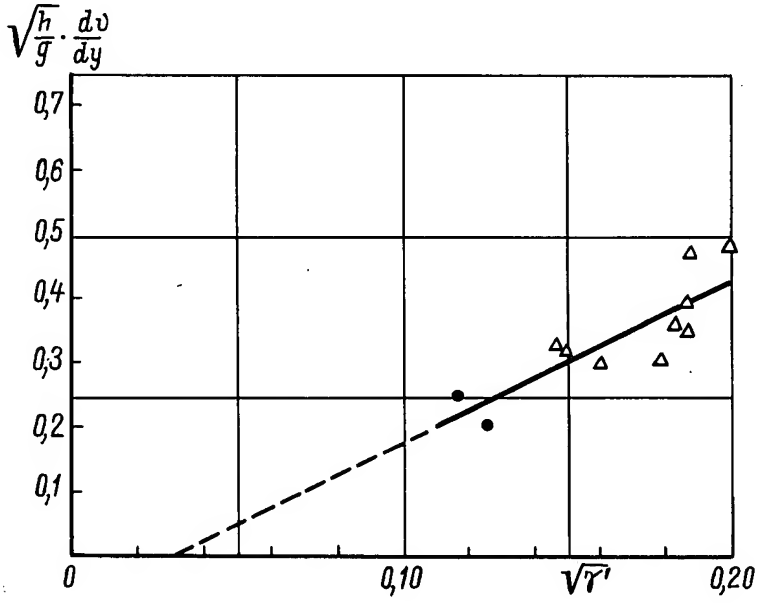

Fig. 6
A graph for determination of $\frac{dv}{dy}\sqrt{\frac{h}{g}}$

△ - Levi points; ● - Blanchet points.

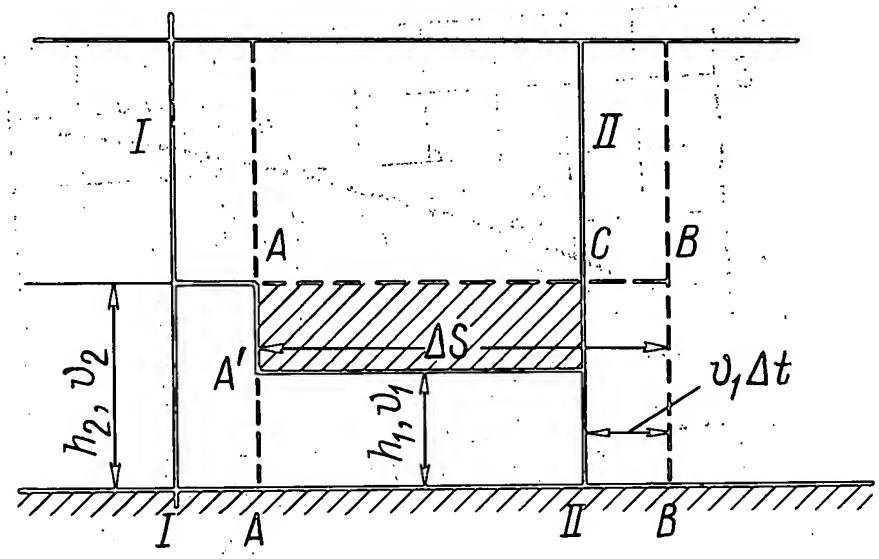

Fig. 7
Computed table for interrupted wave of filling.

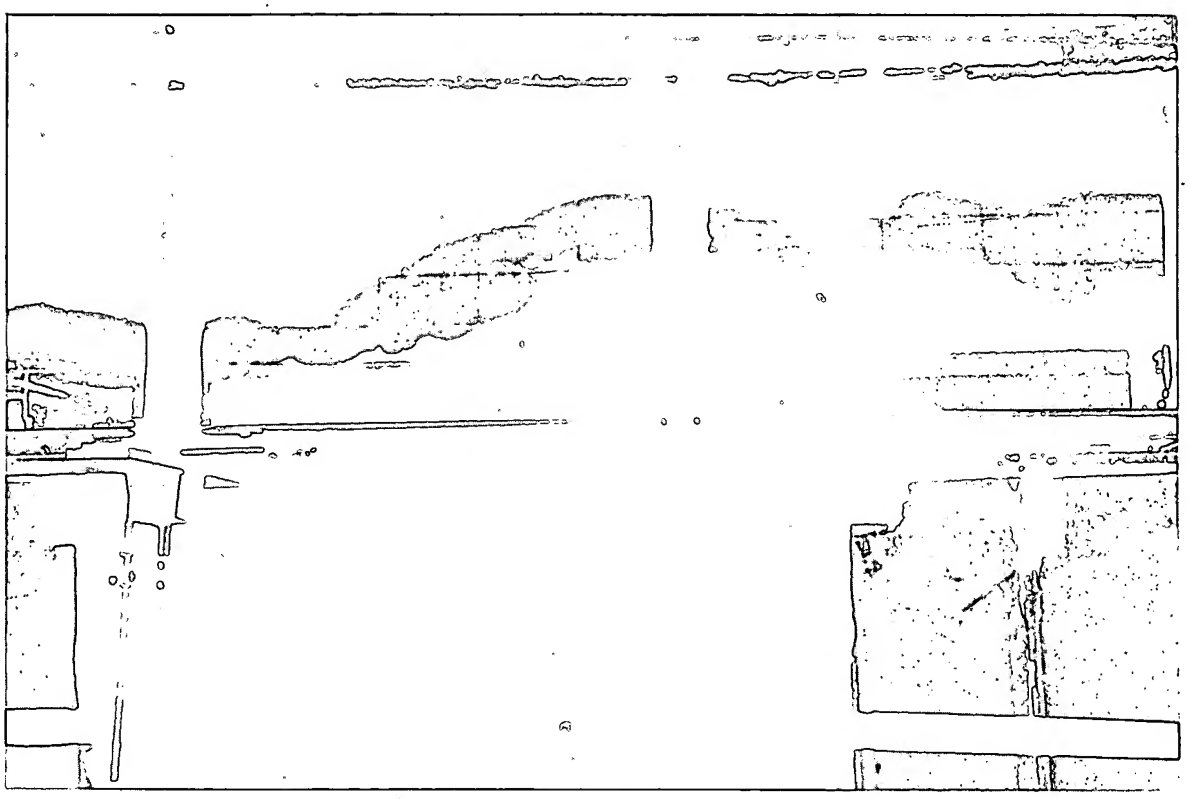

Fig. 8
Photograph of the wave of rising in front of the structure when discharge water accumulates (an experiment).

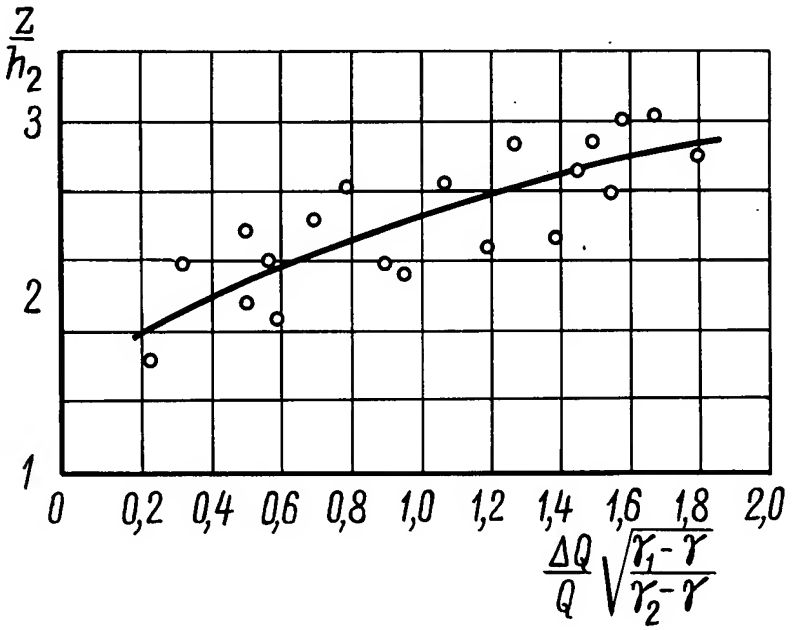

Fig. 9
Dependence of the wave rising on discharge accumulation (experiments). $\frac{z}{h_2} = \varphi\left(\frac{\Delta Q}{Q}\right)$

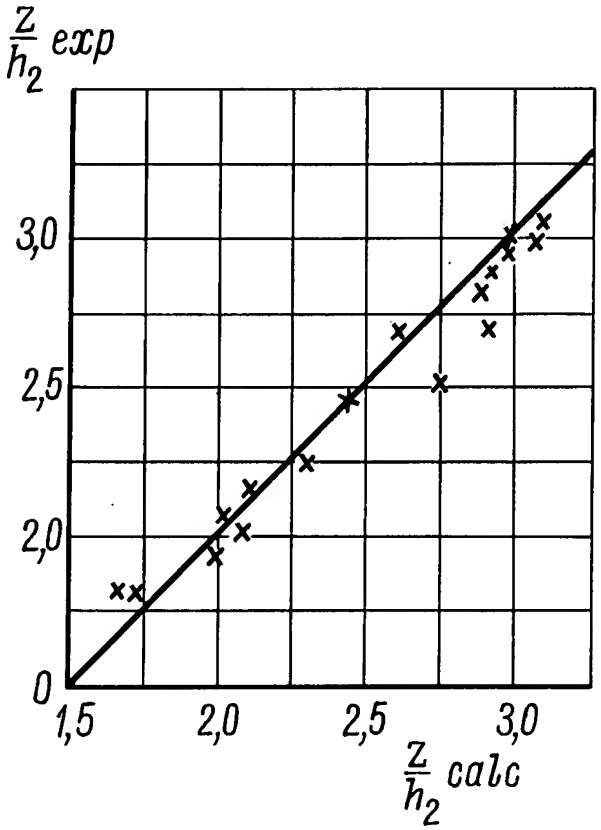

Fig. 10
Comparison of the empiric data with designed wave of rising.

HYDRAULIC INVESTIGATIONS OF NAVIGATION LOCKS IN THE VOLGA RIVER BASIN

25X1

* * *

KHALTURIN A. D., Engineer
LYUBIMOV A. I., Engineer
MIKHAILOV A. I., D. Sc.
ONIPCHENKO G. F., Engineer

* * *

SUMMARY

The majority of navigation locks built during the last years in the Volga River basin were preliminarily tested in hydraulic laboratories, as many problems of their hydraulics cannot be solved only by calculations and on the basis of theoretical analysis.

Laboratory tests included mainly the following problems:

a) Determination of hydraulic characteristics of the lock culvert system;
b) Determination of hydraulic and operation conditions of vessel lying at the time of the locking and in approach canals;
c) Improvement of the initial design supposition and lock structures on the basis of laboratory testing and checking.

Field observations have been performed on several constructed and working locks, having as their aim the following:

a) Determination of actual hydraulic and operation characteristics of built structures for their further use in future projects;
b) Derivation of data for comparison of results of laboratory

tests and theoretical calculations with actual values for improving the procedure of laboratory tests and theoretical calculations.

All laboratory and field observations carried out on locks were performed according to specially worked out procedure with the application of unique measuring apparatus.

The paper contains the main results of tests of upper head and distribution systems for filling and emptying lock chambers, as well as their comparison with the results of field observations. Besides, the paper describes the methods of laboratory tests and field observations. In particular it is shown that during dynamometric measurement in mooring tackle, variation in mooring conditions introduces many uncertainties, while the application of the longitudinal trim of the vessel, as one of the principal factors of lying conditions gives reliable and certain data.

The paper shows that as a result of research work certain relations have been determined between the conditions of vessel lying and the nature of wave phenomena, especially in approach canals, as well as several general conclusions on operation and hydraulic characteristics for various lock culvert systems.

SOMMAIRE

La majorité des écluses de navigation récemment construites dans le bassin de la Volga furent l'objet de recherches préalables dans des laboratoires hydrotechniques, certains aspects hydrauliques des problèmes les concernant n'ayant pu être résolus uniquement par des calculs.

Le programme des recherches en laboratoire portait essentiellement sur les questions suivantes:

a) Détermination des caractéristiques hydrauliques des systèmes d'alimentation de l'écluse;
b) Détermination des conditions hydrauliques et d'exploitation des bateaux en attente durant l'éclusage et dans les larges aval ou amont;
c) Amélioration, à la base de la documentation obtenue en laboratoire, des impératifs d'étude et des systèmes constructifs des écluses.

Des recherches sur place furent entreprises sur certaines écluses réalisées et exploitées, ayant pour but de:

a) Fixer des caractéristiques hydrauliques et d'exploitation

réelles des ouvrages déjà réalisés afin de les utiliser dans les projets ultérieurs;

b) Acquérir des données afin de confronter les résultats des recherches obtenues en laboratoire et des calculs théoriques avec les résultats réels pour améliorer les méthodes des recherches en laboratoire et des calculs théoriques.

Toutes les recherches sur les écluses en laboratoire et sur place furent effectuées d'après des méthodes spécialement étudiées avec emploi d'appareils de mesure originaux.

Le rapport expose les principaux résultats des recherches sur les systèmes de tête et de distribution, de remplissage et de vidange des sas et les confronte avec les résultats des recherches effectuées sur place. Le rapport expose en outre les méthodes des recherches faites en laboratoire et sur place. Il est noté en particulier que lors des relevés dynamométriques dans les amarres, la diversité des conditions d'amarrage introduit de nombreux facteurs d'indétermination et la différence du bateau, en tant qu'un des indices fondamentaux de son comportement, permet d'obtenir des données plus concrètes auxquelles on peut se fier davantage.

Le rapport note que les recherches ont permis d'établir des relations déterminées entre le comportement du bateau et le caractère des ondes, surtout dans les larges. Ces recherches ont permis de tirer certaines conclusions générales sur les caractéristiques de service et les caractéristiques hydrauliques de différents systèmes d'alimentation des écluses.

INTRODUCTION

During the last 30 years in the basin of the Volga River and in artificial water-ways connecting it with the White, Baltic and Black Seas, over 50 navigation locks have been built, including eleven locks on the Volga River proper. Ten more locks have already been designed and are now under construction.

Several hydraulic problems which have arisen during the design of these locks cannot be solved only by theoretical calculation methods. Therefore, all culvert systems of these locks were tested (to different extent) on models in hydraulic laboratories.

To find the degree of conformity of the model testing results with actual conditions, and also to obtain data on the actual hydraulic conditions of lock operation and conditions of vessel lying in chambers and in approach canals, field observations were performed on several locks with specially designed and built apparatus.

Because of the wide amount of investigation material this paper is limited by the description of procedure and principal results of hydraulic tests carried out for the typical feeding systems of locks, not touching upon the investigation of operation of hydro-mechanical equipment (lock gates, culvert gates, guard gates, etc.)

All locks working with water heads in the chamber up to 13 m were designed with head feeding systems.

In case of small variations of water level in the upstream of the mentioned locks, it was typical to fill the chambers through lifting lock gates located on the drop wall. The energy of the stream is dispersed in the chamber formed by shaped baffles (Fig. 1).

For large variations in upstream water level and low drop walls the chambers are filled in most cases through short by-pass culverts located in the abutments leading into the baffle chambers and being closed by flat or cylindrical gates.

At lock heads over 9 - 10 m, either multi-speed or variable accelerated opening of culvert outlets is widely used.

The chambers are emptied, as a rule, through short by-pass culverts closed by flat gates and water discharges through outlet culvert sections, partially or completely embedded into the lock bottom (see Fig. 1).

At high water heads reaching 18 to 21 m in single-chamber locks and up to 27 m in the middle head of the double-chamber locks the large two-line Volga locks have distribution culvert feeding systems.

Most of these locks are filled through longitudinal bottom culverts (Fig. 2). When these locks are located on derivation canals the water is also discharged downstream through a system of distributing culverts. When the locks are placed right next to the river bed there are two cases of water intake and discharge through the side structure from the chamber: in one case separately, i.e. the water intake is separated from water discharge; in the other, combined in a separate structure adjoining the spillway dam.

The general problem of hydraulic laboratory tests of each lock is the improvement of the designed feeding system and the determination of such dimensions of separate parts of this system, which ensure filling and emptying of the chambers during a certain time conforming with the required capacity of lock. In this case satisfactory operation conditions of vessel lying during locking and satisfactory operation of individual parts of the lock should be fulfilled.

The conditions for vessel lying in the chambers during locking and at the approaches are estimated by the hydrodynamical forces acting on the vessel and actually taken by steel ropes, used for mooring the vessel in the lock.

The allowable values of the longitudinal and transverse components of hydrodynamical forces are standardized in the USSR in relation to the displacement of the vessels passing through the locks

$$\left(\frac{S}{W} = \frac{1}{1.000} \quad \text{to} \quad \frac{1}{2.500}\right).$$

The maximum (average by section) water velocities in approach canals to the locks are limited by a value of 0.7 to 0.8 m per sec.for ensuring safe movement and manoeuvrability of vessels during filling and emptying of the chambers.

On the basis of these requirements for the lock feeding systems the following principal problems arise, which may be solved by hydraulic tests on lock models:

1. Conditions of lock filling (direction and velocity of flow, shape of guide structures, limits of reinforcing and structure of the water intake itself).
2. Duration of filling and emptying of chambers for the one or the other water distribution system in the chamber for various velocities and graphs of gate opening.
3. Hydrodynamical forces acting on the vessel during filling and emptying of the chambers and their dependence on the speed and graphs of gate opening, discharge distribution system by length and width of the chamber, location and displacement of the vessel.
4. Conditions for discharge of water downstream (distribution and value of flow velocity, shape of bank joints reinforcing limits, water discharge structure).
5. Conditions of vessels lying at downstream approach of lock.
6. Wave phenomena in approach canals and between lock canals.

2. LABORATORY TESTING METHODS AND MEASURING APPARATUS

A. Testing methods. Laboratory tests of navigation locks and approach canals were performed in the hydrotechnical laboratory of GIDROPROJECT and in the laboratories of other scientific - research institutes on models of various scale.

For solving individual problems by testing locks, for example, determination of the outline of the culvert and baffle chambers, determination of

the flow discharge coefficients of the system, etc., tests were performed on fragmentary models reproducing usually to the scale of 1:40 the required parts of the structure. This allowed a timely introduction of the necessary correctives into the design of the lock, using them to build the complete lock model.

The scale of complete models for testing locks were taken in the range of 1:20 to 1:40. Models built according to these scales were employed for finding the principal operation characteristics: duration of water levelling, conditions of vessel lying in the chamber and at the approaches, operation of lock gates and culvert gates. Smaller models built to the scale of 1:100 were used for preliminary testing of the operation of discharge outlets downstream and water intakes upstream.

Together with the development of laboratory research work, testing methods and measuring apparatus were also constantly improved.

At present the hydraulic laboratory of the Scientific - Research Sector of GIDROPROJECT employs the following methods for testing locks:

1. Determination of the hydraulic characteristics of the designed feeding system. Thus, the graph for water level variations is plotted, as well as the graph for gate operation and flow discharge coefficients changing with time.
2. Evaluation of vessel lying conditions in the chamber during locking, being performed by two mutually controlled methods: determination of forces by the dynamometric device of Prof. V.M. Mackaveyev and determination of vessel trim by a trimograph. The latter method proposed by engineer A.D. Khalturin has been found very successful both for laboratory and especially for field observations.
3. Determination of wave phenomena in approach canals during locking.
4. Introduction of required changes in the lock feeding system, determination of the best conditions for gate operation from the point of view of favourable conditions for lying of vessels in the chamber and at the moorage on the approach sections.

Laboratories are equipped with the installations usually employed for such tests and devices containing a number of weir chutes with large spillway front. Upstream and downstream are constantly fed for preventing variations in water level during intake and discharge of flow in the process of locking.

In the process of model tests it was found that the water outlet conditions reproduced on models with different length of modeling sections for downstream approach canals show different effect on conditions of vessel lying not only in the canal but also in the chamber when it is being emptied, due to the fact that the wave phenomena in the canal depends on the length of the latter.

In view of this a series of purely methodical tests were performed and measures were chosen allowing to get closer agreement of data and to create in the approach canals shortened on the model the conditions of wave phenomena approaching the actual conditions. These tests allowed by means of inclination of the chute water level regulator to obtain on the model any coefficient of wave reflection, both positive and negative. With the aid of these chutes it was found possible to disperse the discharge wave, having obtained on the model conditions corresponding to a canal of infinite (great) length, i.e. the case when this wave reflected from the canal outlet into the river bed does not have enough time to return to the lock during locking.

The results of tests are preliminarily plotted as curves for water level time as well as flow discharge-time relations, hydrodynamical forces and speed of gate lifting, vessel position in a chamber, its displacement, initial depth in a chamber. This procedure for performing tests excludes possibility of accidental mistakes, as individual faulty tests are immediately discovered by the deviation of test points from their general disposal order.

The comparison of records received on the trimograph and on the Mackaveyev device have shown that the vessel trim value, while the chamber is being filled changes similar to the readings on the Mackaveyev device, but with the advantage that the trim does not depend on the mooring system; this permits to use the trimograph readings for determination of the longitudinal forces for any system of vessel mooring.

When choosing the water discharge method into approach canals tests were performed on models of two scales; preliminary tests on models made to a scale 1:100 and then on the main model of the lock to a scale of 1:40. Velocity in the approach canals was measured both for steady hydraulic conditions conforming with the maximum flow discharge and for unsteady conditions during emptying of the chamber. On the basis of these measurements the water discharge system was chosen and the required reinforcing limits of the canal bottom were determined.

The comparison of test results obtained on models of various scales allowed to find the acceptable scale of the model for solving one or the other problem. Thus, it has been found that the solution of problems connected with wave phenomena, distribution of water velocity in canals is possible on models of a scale 1:100 and even 1:150, while the determination of operation characteristics of the lock (gate operating conditions, filling duration, conditions for vessel lying) are best of all found on models of a scale 1:40.

B. Measuring apparatus. For studying the above mentioned phenomena the GIDROPROJECT laboratory has new unique apparatus allowing to

carry out automatic and high accuracy recording of rapid water level variations, changes in forces on vessels; values of instantaneous and average velocities, hydrodynamic pressures, etc.

Most of the apparatus newly applied in the hydraulic laboratory have been worked out and made in the design department and shops of the Scientific - Research Sector of GIDROPROJECT under the guidance of V. P. Bombtchinsky.

For recording the water level variations in the chambers float lymnigraphs have been used, selfwriting on paper with the aid of a constantly beating high-frequency striker. Similar apparatus register the lifting of gates. Small fluctuations of water level are registered by special optical or pneumatic wave-meters.

The forces acting on vessels while lying were previously measured by the Mackaveyev devices with spring-type dynamometers. At present a new device is being employed for evaluation of the conditions of vessel lying with dynamometers having induction pick-up units, their readings being recorded on an oscillograph (Fig. 3). The new device has stiff springs of low strain, this almost entirely excluding longitudinal movement of the vessel during operation of the dynamometers, which could reach a significant value (10 - 20 mm) when measuring by the Mackaveyev device.

The velocity of steady water movement is registered by water-vanes and the usual plan photographing of illuminated floats. For unsteady water movement the surface velocity is fixed by a moving picture camera, or rapid photography with multi-frame film cameras, while the velocity in the water is fixed by a special ball-type probe with optical registration of the two plane velocity components on the moving picture camera film.

For recording the trim of the vessel the laboratory employs a mechanical trimograph, which registers on smoked paper in an increased scale the half difference of the altitude position of the vessel fore and aft, being transmitted to the instrument by thin metal threads.

Hydraulic hoists are employed for lifting the gates, allowing to change the lifting speed in a wide range.

All apparatus are controlled automatically from a special control board.

This control board has two attachments with stop watches and a time-marker, allowing to synchronize registration on all apparatus, obtain special signals at the important moments of the test and to register automatically the time of gate lifting and equalization of water levels.

3. PRINCIPAL RESULTS OF LABORATORY TESTING

A. Head water feeding systems. Initially, by testing the first locks on general models these systems were chosen both according to the predetermined conditions of lying of vessels during locking as the main dimensions of the designed water feeding system, duration and speed of opening the culvert gates, and also according to the type and dimensions of dissipating devices, which determine as well as the hydraulic characteristics the time of filling-emptying of the chambers. This required, with a large amount of variables, many tests, which reached over a thousand in case of multispeed opening of the gates.

Later, on the basis of analysis of extensive test data and obtained relations between the maximum hydrodynamic force on vessels in locks and at approaches to them and the hydraulic values characterizing filling and emptying of chambers, A.V. Mikhailov had worked out methods of hydraulic calculations of lock head feeding systems according to the allowable conditions of vessel lying during locking.[2] These methods of calculation, confirmed by a series of methodical tests, allow theoretically to determine the principal dimensions and maximum speed of opening culvert gates for the designed water feeding system, to plot their hydraulic characteristics and, finally, to find the minimum time required for filling and emptying chambers depending on operation conditions.

The formulas derived by V.M. Mackaveyev and I.M. Konovalov [3] and confirmed during tests also allow to determine the pressure drop behind water-tight culvert gates and those located in open shafts.

Due to this, hydraulic testing of the Volga-Don locks performed by the laboratory of GIDROPROJECT from 1949 to 1951 corroborated the principal dimensions of the water feeding system and speed of culvert gate opening, which were determined by theoretical calculations on the basis of the predetermined time of filling-emptying the chambers and allowable longitudinal hydrodynamic forces on the vessel in the chambers and at approaches. These overall dimensions were used for designing the structures proper and main equipment and mechanisms for lifting and lowering upper lock gates and for culvert gates of lower lock head were ordered on the basis of the designed speed for opening the water outlets.

In the hydraulic laboratory fragmentary models reproducing parts of locks and general models were also used for finding only the shape and

2) A.V. Mikhailov, Head Feeding Systems for Navigation Locks and their Calculation, 1951.

3) V.M. Mackaveyev and I.M. Konovalov, Hydraulics, 1948.

size of baffling and stilling structures when filling the chambers, for which the hydrodynamical forces on vessels in the chamber during water discharges increasing with time do not exceed the designed values of the first peak, caused at the beginning of filling mainly by wave phenomena in the chamber.

The problem was studied of replacing the curvilinear and multi-speed opening of gates by the installation of slot sills before the gates lifted at uniform speed (proposed by the personnel of the hydraulic laboratory A. D. Khalturin, V. S. Mikhailovsky and N. V. Khalturina). The piers of the slot sill during the first period of chamber filling obstruct the opening (disclosed under the gate), thus allowing to receive the effect of the multi-speed curve for gate lifting by a simple single-speed mechanism (see Fig. 4). Making attempts to lower the time for filling the chambers in comparison with the designed height of the slot sill piers (0.75 m), the investigators began to lower the pier height on the general model of the lock without changing the speed of gate lifting. It turned out that lowering of the pier height to 0.25 m did not increase the maximum longitudinal hydrodynamical forces on the designed vessels during locking, while the time for filling the chamber decreased significantly (up to 17%). Further lowering of the pier height lead to rapid increase of forces (by 1.7 times) at the same gate lifting speed without the slot sill.

The principal reason causing the rise of direct longitudinal forces acting on the vessel during lock filling is the wave phenomena in the chamber. The analysis of laboratory test data has shown that the smallest required time for filling the chambers may be obtained when the gate reaches the top of the piers when the wave front, being formed at the beginning of water feeding into the chamber, moving along the chamber and vessel inside of it is reflected from the lower lock gate.

The time of wave run through the chamber with the vessel in it determined theoretically agrees well with test data. This has allowed in the future to find by calculation the pier height conforming to the given gate lifting speed.

Slot sills are made on all standard locks on the Lenin Volga-Don Canal.

The design of the baffle chamber at the lock head, consisting of a screen and beam-type baffle wall, was chosen mainly according to the conditions of lowering the maximum of reverse forces to a value not exceeding the first maximum of direct forces.

When emptying the chamber through designed shape and size by-pass culverts and designed speed of gate lifting, in the laboratory were chosen the grate obstructions increasing towards the lock center line above the

discharge culverts, and also the shape of the mooring structures at the approaches providing the best conditions of lying and manoeuvring of vessels at the approach to the lock.

A solid wall is built across the water discharge culverts along the lock center line.

This measure allows to obtain satisfactory water spreading in the canal even when emptying the chamber through one by-pass culvert.

It should be noted that the performance of model investigations of the conditions of vessel lying in the chamber and downstream approaches when emptying the chamber has allowed to come to the conclusion that opening of the culvert gates should be always designed with uniform speed for the head feeding systems, being opened during $t_3 = (0.5-0.7)T$ - duration of chamber emptying.

B. Distribution feeding systems. The design of distribution feeding systems for two-line large-size Volga locks with heads in the chamber up to 18 m, due to the presence of large and rapidly growing load capacity should conform with the following important operation requirements: a) filling and emptying of chambers should not exceed 8 minutes and b) the maximum longitudinal hydrodynamical forces on the largest vessels should not exceed 1/2,500 of their displacement and for medium-size vessels correspondingly 1/1,500 of their displacement; the highest transverse forces should not exceed 50% of the longitudinal forces.

Conformance with these requirements in the conditions when the maximum discharges of water entering the chamber during filling and discharged during its emptying exceeded 500 cu.m.per sec.with gradual and slow opening of culvert gates required long duration and extensive laboratory tests. These tests were performed initially in relation to the conditions of vessel lying during filling and emptying of chambers in the hydraulic laboratory of the Leningrad Polytechnic Institute (under the guidance of M. D. Chertousov and B. D. Khachanovsky), and then on the general models of locks and approach canals in the hydraulic laboratory of GIDROPROJECT under the guidance of A. D. Khalturin.

The performed tests of several different schemes of distribution feeding systems have shown that at great length and width of the lock chambers: a) the simple types of these schemes with short outlets from the longitudinal culverts distributed along their entire length may comparatively slightly improve the conditions of lying of vessels during locking and slightly lower the time required for filling the chambers in comparison with the best modern schemes of head water feeding:
b) for filling the chambers of the Volga locks with the volume of water

in the chambers up to 170,000 cu.m.for a short period of time at rigid conditions of vessel lying in the locks each of the longitudinal culverts should feed water only for a certain part of the length of the chamber through the discharge openings of the short transverse culverts.

As a result of further laboratory tests the system for flow discharge distributing along the length and width of the chamber ensuring the given conditions was chosen (see Fig. 2).

Regulation of water inflow along the length of the chamber is made in these locks by the corresponding location of inlet and outlet openings along the length of each culvert and time shifting of the beginning of gate lifting in various culverts (gate lifting advance).

The distribution of flow across the chamber is performed by a system of transverse outlets formed between each pair of concrete distribution I-beams (see Fig. 2).

Water discharge into the downstream approach canals was also designed of the distribution type.

The measurement of velocities in the approach canals was performed during laboratory tests both for steady-hydraulic conditions conforming with maximum discharge and unsteady conditions when emptying the chambers.

On the basis of these tests a scheme of discharge culverts was chosen, as well as the required limits of reinforcement of the canal bed determined.

4. FIELD OBSERVATION METHODS AND MEASURING APPARATUS

For obtaining data on the actual hydraulic conditions of lock operation and vessel lying in chambers and approach canals, and also for checking the degree of conformance of model test results with actual data, the GIDROPROJECT laboratory had carried out field observations of some of those navigation locks which were designed on the basis of laboratory tests.

For these field observations a method was worked out similar to that of laboratory tests; special apparatus have been designed and made.

During field observations, work was performed on the following principal problems:

1. Determination of hydraulic characteristics of lock operation, by recording of water level change in the chamber with time and calculation of flow discharges according to the increment of water level for each short period of time;

2. Investigation of conditions of vessel lying in the chamber during filling and emptying and also in the approach canal by the determination of forces on the moorings, trim and longitudinal shifting of the vessel;
3. Study of the mutual influence of two-line lock chamber operation with a common emptying system;
4. Study of wave phenomena in the canals between the locks and at the downstream approach canals of the locks;
5. Measurement of flow velocity in the canal at the end reinforced section.

For measuring of water levels in chambers and canals the following apparatus were used:
a) Lymnigraphs with four scales for measurement of water level and with four time scales;
b) Suspended 15-meter metal rods for readings of the position of water level in the chamber; the time of the reading was registered by radio signals sent every 15 seconds;
c) Portable 1.5 m fixed rods installed on the canal slopes for studying the wave phenomena in the canal; the time of the reading was registered by synchronous stop watches, also every 15 seconds.

The use of rods was very reliable and sufficiently precise; they allowed to organize observations in the most variable conditions, while their results completely coincided with the control records of the lymnigraphs.

The evaluation of the conditions of vessel lying in locks was carried out by two methods: by determination of the vessel trim, and by direct measurement of the forces on the mooring ropes.

The trim was registered by means of two systems of measuring units:
a) Trimograph with heavy-weight pendulum and optical mirror system of registration of deviations in relation to its base plate;
b) Trimograph with precise level guage and continuous photography of its position on a moving film.

The comparison of records on these apparatus is given in Fig. 5. Both apparatus are placed on the deck of the vessel.

The greatest difficulties were met with when measuring the forces on the vessels and transmitted to the mooring ropes. The actual system of vessel mooring cannot be performed in the same way as in the laboratory and the conditions of measuring these forces must be adapted to the mooring conditions usually employed during operation (mooring by two ropes at one board). The forces were measured by spring-type

dynamometers included in the mooring tackle with remote registration of their readings on an oscillograph; the trim of the vessel was registered at the same time as the forces measured by the dynamometers.

The trim, not depending on the vessel mooring system, may be directly compared with the trim recorded on the model. Simultaneously, the trim in combination with the data on longitudinal vessel shifting allows to obtain material for control of the dynamometer readings in the mooring tackle, thus permitting to analyze the causes of separate jerks marked by the dynamometers. This comparison allows to judge whether the jerks were caused by filling or emptying of the chamber or whether it was caused by insufficiently tight mooring and sagging in the ropes or jamming of the mooring rings. In the first case maximum trim coincides with maximum force; in the second case the forces increase in the ropes only at small changes of the trim and significant shifting of the vessel.

The device for recording the longitudinal shifting of the vessel during locking was either placed on the parapet of the chamber or on the board of the vessel. The device has a movable sighting carriage and rod with a centimeter scale.

Common water wheels were used for registering the velocity in the canal and lock culverts. The direction of flow is registered by indicators set on the water wheel rods designed in the same way as wind vanes with electrical contacts. The lighting of lamp on the control panel allows to judge the presence of direct or return velocity.

5. RESULTS OF FIELD OBSERVATIONS

These observations have allowed to find the actual values of the flow discharge coefficient for various systems of filling and emptying of chambers and to compare them with the data of laboratory tests; besides, it enables to compare the data on hydrodynamic forces registered by the dynamometers in the mooring ropes with the forces calculated according to the trim, and directly compare the trim records obtained in the field and in the laboratory. An example of these comparisons is given in Fig. 6. Though the last curve of vessel displacement on the model and in the field somewhat differs, the general conformance of the trim changing can be well seen. When filling Volga-Don locks there is some difference probably connected with the different type of seal work when the gate passed through the slot sill piers on the model and in the field and with the presence of slight distortion of the gate in the field.

During the testing of one of the locks, due to the presence of a permanent test vessel with the principal apparatus located on it, the con-

ditions of operation of mooring tackle were checked when mooring the vessel by two ropes at one board and four ropes at both boards. In the latter case the lengths of all ropes were made exactly equal and two ropes were placed on winches for adjusting the rope tension.

These tests have shown that for normal operating conditions two-sided mooring by four ropes does not achieve any advantage, first of all, because it is impossible to place the center line of the vessel parallel with the center line of the chamber, the forces are taken by any one fore or aft rope, but the friction of the vessel board against the chamber wall, which improves the lying conditions, is not used. For methodical mooring tests on four ropes there are some advantages, as this avoids the friction of the vessel against the side of the chamber.

Besides the field observations on filling of locks and vessel lying conditions in the chambers and approach canals, the wave phenomena were studied in canals adjoining the locks. These observations were performed for canals of various length and different shapes in plane with one end at the river bed or reservoir or for those having locks at both ends.

The obtained field data on waves phenomena in locks of canals of different length and shape allowed critically to evaluate the conditions of laboratory tests of locks, where due to limited space the approach canals were not fully reproduced on models.

These field observations have shown that during laboratory testing it is necessary to consider the nature of wave phenomena which actually arise in the approach canals of the model, as these phenomena may in some cases be superimposed and alter the conditions of vessel lying not only in the approach canals but also in the lock chambers.

When performing field observations of wave phenomena in navigation canals the coefficient of wave deflections was determined at the entrance of the navigation canal into the wide river bed at an angle of 30° to 40°. The obtained deflection coefficient was K=0.35-0.37. The actual velocities of the waves were obtained for canals having several small shallow one-sided widenings by length. The speed of wave propagation in canals conforms with the Lagrange formula.

The most suitable conditions for lock operation were determined in the field with the locks being located at the end of short canals between locks, eliminating the possibility of swinging them, measures being advised allowing during lock operation to take these swingings into account. On structures observations took place with oscillations varying in the range of 0.7 to 0.5 m. It should be noted that the evaluation of the con-

ditions of vessel lying in the field is more complex than in the laboratory. The dynamometric measurement of forces on mooring tackle takes into account phenomena which do not take place in the laboratory tests (speeding-up of the vessel, friction against the chamber walls, jamming of floating mooring rings insufficient rigidity of mooring rope fastenings on the vessel cleats, etc.).

Therefore, field dynamometric measurements should be accomplished simultaneously by registration of the trim of the vessel and combined consideration of the obtained results, each of them correcting the other.

The longitudinal incline of the vessel (the trim) may be recommended as the main qualitative index for field study of the conditions of vessel lying in lock chambers and approach canals.

Of special importance for the trim is its independence of the conditions of vessel mooring and the possibility of direct comparison of model and field data.

The field observations showed some of the complications in lock operation obtained due to the presence of an emptying system common for both chambers. The combined system of water discharge was accepted owing to the considerations of obtaining the most uniform distribution of velocities in the canal when emptying any of the chambers.

However, experience has shown that the combined water discharge system for lock lines introduces more complications into lock operation than unequal distribution of velocity in plane and it is not reasonable to achieve uniform distribution of velocity in this manner.

BIBLIOGRAPHY

1. Building Design Code, 1954.

2. A.V. Mikhailov, Head Feeding Systems for Navigation Locks and Their Calculation, 1951.

3. V.M. Mackaveyev and I.M. Konovalov, Hydraulics, 1948.

SYMBOLS

H - Lock head

ho - Initial water depth in chamber

h - Head before upper lock gate

S - Total longitudinal forces acting on vessel, tons metric

W - Vessel displacement, tons metric

t_3 - Duration of gate lifting

T - Duration of filling or emptying

I - Longitudinal incline of vessel

t - Variable time during process of filling or emptying chamber

K - Coefficient of wave reflection when reflected from wide river bed

u - Gate lifting speed, m.per min.

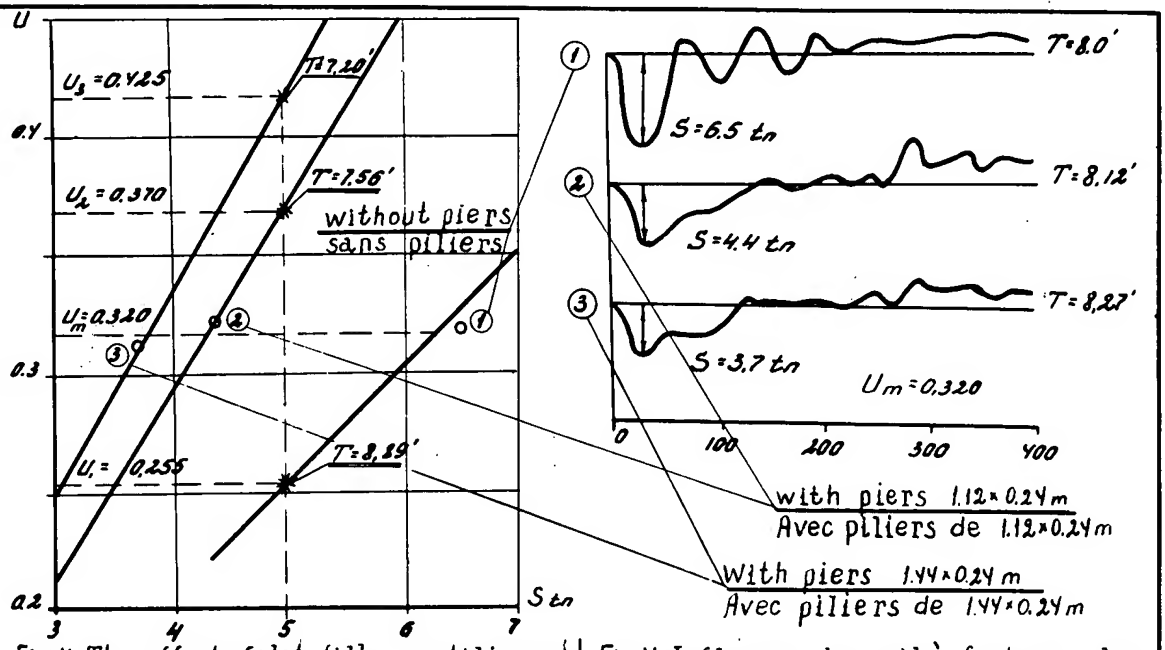

Fig.4. The effect of slot fill on rectilinear longitudinal forces acting on vessel lockage.

Fig. 4. Influence du seuil à fente sur les sollicitations directes longitudinales subies par le bateau éclusé.

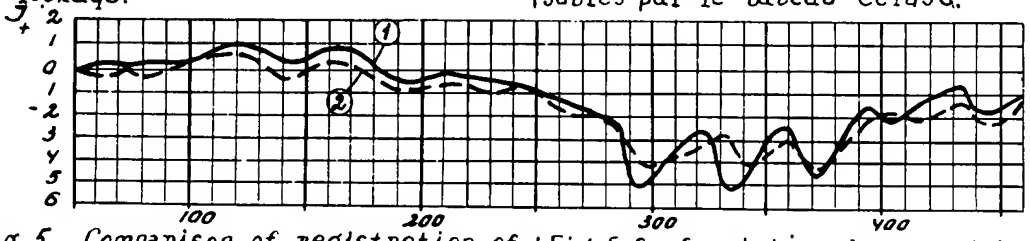

Fig 5. Comparison of registration of vessel tpim in field on two instruments of various types /average values/
1-with heavy pendulum.
2-with precise water level.

Fig. 5 Confrontation des enregistrements de la différence du bateau faits sur place par deux appareils de typs divers
1- à balancier lourd.
2- à niveau précis.

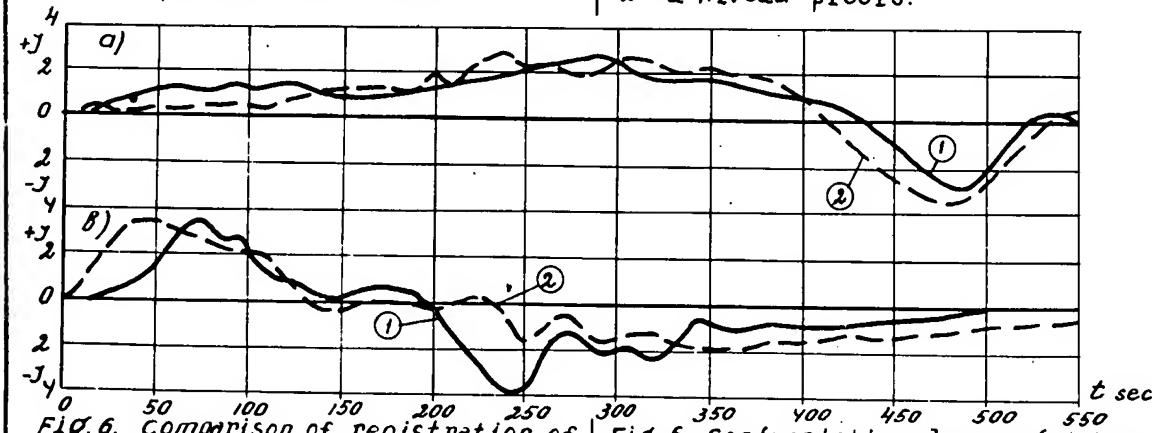

Fig. 6. Comparison of registration of vessel trim. a) During emptying of chamber. b) During filling of chamber.
1. Trim in field. 2. Trim of model.

Fig. 6. Confrontation des enrégistrements de la différence du bateau; a) Lors de la vidange du sas; b) Lors du remplissage du sas. 1. Différence sur place. 2. Différence sur modèle.

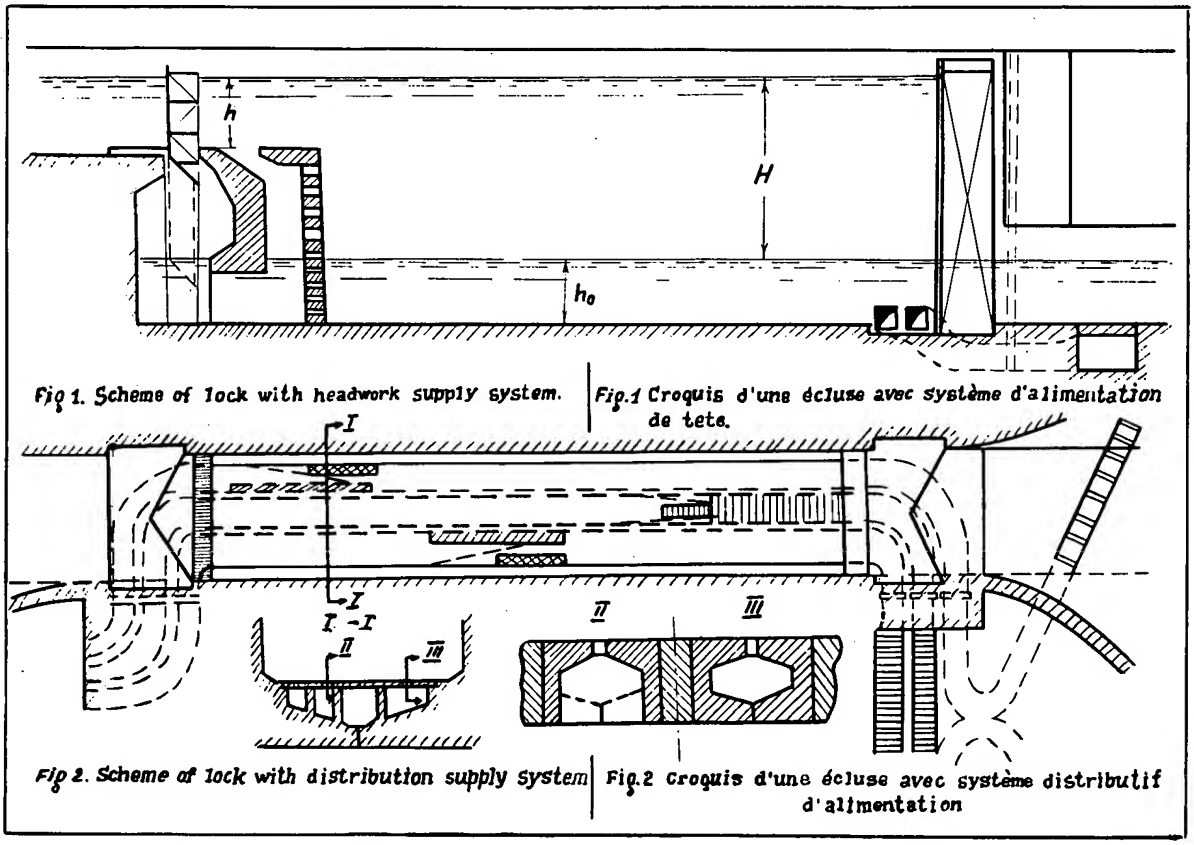

Fig 1. Scheme of lock with headwork supply system.

Fig.1 Croquis d'une écluse avec système d'alimentation de tete.

Fig 2. Scheme of lock with distribution supply system

Fig.2 Croquis d'une écluse avec système distributif d'alimentation

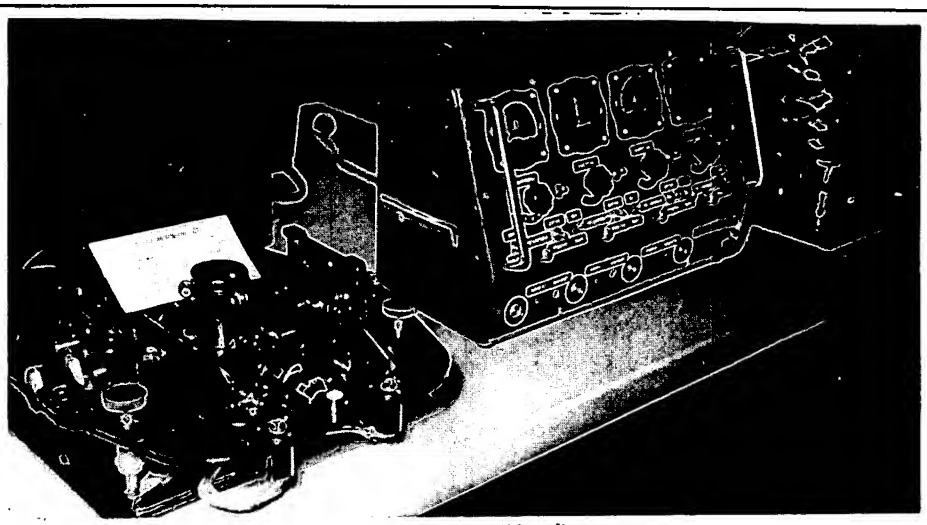

Fig.3
View of new measuring apparatus for evaluation of forces acting on model of vessel during locking.

Fig.3
Appareils nouveaux permettant d'enrégistrer les sollicitations agissant sur les modèles des bateaux lors de l'éclusage.

WATER SURFACE FLUCTUATIONS IN LOCKS AND INCLINED SHIP ELEVATORS AND THE CONDITIONS OF SHIP STAY

25X1

* * *

O. F. VASILIEV

Candidate of Engineering Sciences,
Assistant Professor at the Moscow Institute of Civil Engineering

* * *

SUMMARY

We present here an approximated theoretical investigation of the fluctuations of water and of the conditions of ship stay in the chambers of locks and inclined ship elevators. Both these problems have much in common and are solved here by the same method.

The problem of fluctuations in lock chambers and in approach channels is treated in the first part of the report. Differential equations, with some restrictions, have been derived for water surface fluctuations in a linearised form, with an approximate account for the movement of the ship itself. An example is worked out for the initial stage of the filling up of a head-fed lock chamber. As a result, the wave force acting upon the ship is determined.

The problem of the inclined ship elevator is considered in the second part of the report. Approximated differential equations have been derived for the water surface fluctuations in the boat-carrying tank. The equations are integrated and the forces acting upon the ship are analysed.

SOMMAIRE

Cette communication est consacrée à l'étude théorique des flottements de l'eau et aux conditions de stationnement des bateaux dans un sas de l'écluse ou d'un ascenseur en pente. Ces deux problèmes étroitement liés sont résolus par l'auteur à l'aide d'une même méthode.

Le problème des flottements dans un sas (chambre) et dans les canaux de l'écluse est exposé dans le premier chapître. On donne ici des équations différentielles linéarisées de flottements de surface de l'eau en tenant compte de la présence du bateau. A la fin du chapître est donné un exemple de la solution de ces équations pour le premier moment de remplissage du sas de l'écluse (par amont). Comme résultat de calculs on obtient la force qui agite le bateau.

Le problème hydraulique de l'ascenseur de bateaux est étudié dans le deuxième chapître. En se servant de la même méthode d'analyse on obtient des équations différentielles approximatives des fluctuations de niveau dans la chambre de l'ascenseur. On effectue l'intégration de ces équations et on analyse la valeur des forçes agissant sur le bateau stationnant dans la chambre de l'ascenseur.

Many works have been dedicated throughout the world to the hydraulic theory of locks; however, up to the present time it is still insufficiently elaborated. The theory of inclined ship elevators was hardly even touched upon. At the present time the latter problem is of considerable interest to Soviet hydraulic engineers, in connection with the design of large ship elevators for the Bratsk and Krasnoyarsk hydroelectric power projects.

I. THE PROBLEM OF OSCILLATIONS IN LOCK CHAMBERS

1. Approximate Differential Equations for Water Surface Oscillations in Chambers and in Approach Channels

It is known that the tension of a ship's mooring ropes is, in the main, determined by the wave action of a fluid upon the ship, due to the oscillations of the surface of the fluid when the chamber is either filled or emptied.

When the ship is moored in a lock-chamber, the maximal tension of a mooring rope is registered usually in the initial period of chamber filling. 1/ To simplify calculations, it may be assumed that for the initial period of chamber filling (or emptying), which is of the greatest practical interest, the depth in the chamber varies but little from the initial depth (h).

In analysing the unsteady movement of water and the conditions of ship stay in approach channels the surface fluctuations may also be considered to be small as compared with the initial depth, in this case, during the entire locking period.

1/ This has been shown in the works of A. V. Mikhailov.

These circumstances permit us to simplify substantially the investigation of the most important phases of lock operation.

For the calculation of the unsteady movement of water both in locks and in approach channels, with ships in them, A. V. Mikhailov applied the theory of shallow - water waves in its general form, i.e., using non-linear equations, which were integrated by the method of characteristics. We think that, in these most important cases of hydraulic calculation of locks, the shallow - water wave theory may be applied in its simplified form, by the use of linearised equations, which greatly simplify calculations. That is all the more so as the non-linear theory is only an approximation, since the calculations of the ship vibrations oscillations are approximate.

Let us consider the lock-chamber to be a prism with a horizontal floor. Let us also consider the approach channels of prismatic sections with horizontal floors.

Let us so arrange the xyz system of coordinates that the xy plane should coincide with the fluid surface in a state of rest; let us place the x-axis parallel to the lock axis (or to the approach channel axis) and let us arrange the origin of coordinates "0" at that lock head, from which the lock (Fig. 1) is being filled (or emptied).

Since in both the lock and in the approach lock channel water surface fluctuations may be only small, the solution may be based on a system of assumptions which are usually made in the theory of long wave of small amplitude. For this reason we will consider that ship oscillations are also small. Considering only longitudinal waves, we may regard the component of the fluid particle velocity u_x to be considerably larger than the u_y and u_z components.

Ignoring water viscosity and the lesser members in the equations of fluid dynamics we obtain:

$$-\frac{1}{\rho}\frac{\partial p}{\partial x} = \frac{\partial u_x}{\partial t}, \qquad /1.1/$$

$$g + \frac{1}{\rho}\frac{\partial p}{\partial z} = 0 \qquad /1.2/$$

(quadratic velocity members are cast off, since the undulations are considered to be small).

From equation /1.2/ we obtain:

$$p = p_0 + \rho g(\zeta - z) = p_0 + \gamma(\zeta - z). \qquad /1.3/$$

Substituting this expression into the equation /1.1/ we obtain:

$$\frac{\partial u_x}{\partial t} = -g\frac{\partial \zeta}{\partial x}. \qquad /1.4/$$

In addition to the dynamic equation obtained let us derive an equation of continuity.

Let us separate out a section by transverse cross-sections I and II (Fig. 2), with a distance dx between them. Let the free surface curve occupy the position a-a in the time instant t and the position a'-a' in the time instant t + dt; at the same time the ship bottom gets displaced from position b-b into position b'-b'.

During the time dt into the section under consideration through cross-section I there is an inflow with a volume $u_x \omega\, dt$. At the same time through cross-section II there is an outflow with a volume

$$\left[u_x \omega + \frac{\partial (u_x \omega)}{\partial x} dx\right] dt.$$

Due to the inflow of water through the longitudinal culvert, there will be delivered a volume qdxdt, where q = q (x, t) is the rate of flow entering the chamber (or channel) per unit of time and per unit of length. 1/

Thus, the increment of the volume of water in the section during the time interval dt will be:

$$-\frac{\partial (u_x \omega)}{\partial x} dx dt + q\, dx dt. \qquad /1.5/$$

This volume increment in the section of the lock free from the hull is due to the surface undulation while in the section of the lock occupied by the boat's hull also by the change of its position. It is equal to:

$$\frac{\partial \omega}{\partial t} dt\, dx \qquad /1.6/$$

Equating expressions /1.5/ and /1.6/ we get the continuity equation:

$$\frac{\partial \omega}{\partial t} = -\frac{\partial (u_x \omega)}{\partial x} + q \qquad /1.7/$$

1/ The longitudinal gallery outlets are usually arranged sufficiently frequently, and therefore the rate of flow entering along the length may be presented as a continuous function q of x. When water flows out through the gallery q is negative.

Let us note that in the free sections of the prismatic chamber $\omega = \omega(\zeta)$ while the sections occupied by ships $\omega = \omega(x, \zeta, \eta)$, where η is the ordinate of the ship's waterline equal to the rise of the waterline with relation to its initial position. Therefore, for free sections

$$\frac{\partial \omega}{\partial t} = \frac{\partial \omega}{\partial \zeta} \cdot \frac{\partial \zeta}{\partial t} = b_k \frac{\partial \zeta}{\partial t} \qquad /1.8/$$

and for sections occupied by the ship's hull

$$\frac{\partial \omega}{\partial t} = \frac{\partial \omega}{\partial \zeta} \cdot \frac{\partial \zeta}{\partial t} + \frac{\partial \omega}{\partial \eta} \cdot \frac{\partial \eta}{\partial t} = b \frac{\partial \zeta}{\partial t} + b_c \frac{\partial \eta}{\partial t} \qquad /1.9/$$

where $b = b_k - b_c$: the width of the free surface of the fluid on a section occupied by the hull.

It is easy to notice that the expression /1.9/ is more general than /1.8/ and contains it as a special case. Therefore, let us perform the further transformations with the aid of the expression /1.9/, i.e., for a section of a chamber occupied by a ship.

The continuity equation will be represented thus:

$$b \frac{\partial \zeta}{\partial t} + b_c \frac{\partial \eta}{\partial t} = - \frac{\partial (u_x \omega)}{\partial x} + q. \qquad /1.10/$$

In analysing the relative motion of a ship moored in a lock on ropes, the longitudinal shifting of the boat may be disregarded, since they are of no great importance but the mooring ropes have practically no effect either on the longitudinal oscillations of the boat about its transverse axis (the pitching motions) or the vertical oscillations. Therefore, the vertical and longitudinal oscillations of the boat have to be taken into account.

In calculating vertical and longitudinal ship oscillations, which, as aforesaid, are considered to be small we shall regard each of these oscillations as a sum of two kinds of oscillations:

1) forced - with a period equal to the period of oscillation of fluid in the lock;

2) natural - with a period equal to the period of the free oscillations of the ship.

The period of the natural oscillations of boats may be evaluated by formulae known from the general theory of ship design (see, for inst., /3/, pages 13-15)

Both theoretical and experimental analyses have shown that for ordinary practical conditions the oscillation period of a fluid in a chamber exceeds many times the period of the natural oscillation (both vertical and longitudinal) of the ship itself. For such a correlation of periods of oscillation of the fluid surface and of the ship natural oscillation, as is regarded in the theory of ship design (see, for inst., /3/, pages 13-15), the amplitude of ship oscillations is close to the amplitude of water surface oscillations, i.e., the ship follows after the movement of the water surface.

That circumstance logically leads to an assumption, which greatly facilitates the solution of the problem: LET US ASSUME THAT THE ORDINATE OF THE WATER LINE η AT ANY INSTANT OF TIME IS ON THE AVERAGE EQUAL TO THE ORDINATE OF THE FREE SURFACE OF THE FLUID ζ : 1/

$$\eta \approx \zeta \qquad /1.11/$$

By bringing /1.11/ into the continuity equation /1.10/ we will receive its approximate expression:

$$b_k \frac{\partial \zeta}{\partial t} = - \frac{\partial (u_x \omega)}{\partial x} + q \qquad /1.12/$$

Let us note that, for free sections of the chamber, this equation, not being tied up with the assertion /1.11/, may be regarded to be precise.

Let us exclude u_x from the equations /1.4/ and /1.12/, for which purpose we will represent the first equation in the form

$$-g\omega \frac{\partial \zeta}{\partial x} = - \frac{\partial (u_x \omega)}{\partial t} , \qquad /1.13/$$

differentiate it along x and add to the second, which is differentiated along t. As a result we will obtain:

$$b_k \frac{\partial^2 \zeta}{\partial t^2} = g \frac{\partial}{\partial x} \left(\omega \frac{\partial \zeta}{\partial x} \right) + \frac{\partial q}{\partial t} . \qquad /1.14/$$

If the area of the cross-section of the fluid in the chamber, which is in a state of rest, is a constant quantity (ω = constant), then the equation /1.14/ gets transformed into an ordinary wave equation.

$$\frac{\partial^2 \zeta}{\partial t^2} = c^2 \frac{\partial^2 \zeta}{\partial x^2} + \frac{1}{b_k} \cdot \frac{\partial q}{\partial t} , \qquad /1.15/$$

where the celerity of wave distribution along the chamber length

$$c = \sqrt{g \frac{\omega}{b_k}} . \qquad /1.16/$$

1/ A more rigid analysis of this assumption shows that it practically is equivalent to the omission of the inertia of the ship. A more precise theory of fluid and ship oscillations without any assumptions /1.11/, is now being developed by the author. In this case the problem is resolved to integral-differential equations.

The equation /1.15/ may be applied directly to free lock sections; here $\omega = \omega_K$ and the celerity of waves

$$c_K = \sqrt{g \frac{\omega_K}{b_K}}. \qquad /1.17/$$

If, in order to simplify the solution of the problem, we consider that the transverse cross-section of the submerged portion of the ship does not change along its length and that ω_o = const. and b_c = const., then the equation /1.15/ may also be applied to lock sections occupied by the hull; here $\omega = \omega_K - \omega_c$ and the celerity of waves 1/

$$c_c = \sqrt{g \frac{\omega_K - \omega_c}{b_K}} = c_K \sqrt{1 - \frac{\omega_c}{w_K}}. \qquad /1.18/$$

The relation of the kind of /1.18/, V. M. Makkaveev and A. V. Mikhailov obtained by another method. In the present work this relation, in the author's opinion, was founded with greater precision.

When the differential equations obtained here are applied to lock chambers (or channels) with concentrated systems of supply, these equations get simplified, since then q = 0. In calculating oscillations in locks with distributional sluicing systems the function q = q(x, t) must be first established, based on the calculation of the insteady flow in the distribution system itself (in the longitudinal culvert).

Let us formulate the boundary conditions for the integration of the equation /1.14/ in analysing oscillations in lock chambers, whereby, for simplicity, we shall limit ourselves to the case when there is only one boat in the chamber (Fig. 1).

1/ In deriving equations /1.14/ and /1.15/ and transforming /1.13/, we considered $u_x \frac{\partial \omega}{\partial t} \approx 0$, based on the accepted assumption that the oscillations are small. Let us note that the range of application of these equations in calculating oscillations in lock chambers, due to the smallness of the quantity $\partial\omega/\partial t$ (because of the slowness of the process of filling the chamber), may be somewhat extended, if we consider the celerity of the distribution of waves C to be a function slowly varying with time, for which ω_K should be considered to be a time variable: $\omega_K = f/h(t)/$.

Nevertheless, these equations will only be true till

$$\omega \frac{\partial u_x}{\partial t} \gg u_x \frac{\partial \omega}{\partial t}, \quad \text{or} \quad \frac{\partial Q}{\partial t} \gg u_x \frac{\partial \omega}{\partial t},$$

where Q is the discharge of flow in the transverse cross-section of the chamber.

With relation to the distributional sluicing systems we may write down for the extreme cross-sections:

$$u_x(0,t) = u_x(l_K, t) = 0,$$

whence, with the aid of /1.14/, may be obtained

$$\frac{\partial \zeta(0,t)}{\partial x} = \frac{\partial \zeta(l_K,t)}{\partial x} = 0. \qquad /1.19/$$

In the head supply system for the extreme cross-sections we may write down:

$$\omega_K u_x(0,t) = Q(t), \qquad u_x(l_K,t) = 0,$$

where Q (t) is the discharge of water delivered into the chamber.

Hence, it follows:

$$\omega_K \frac{\partial \zeta(0,t)}{\partial x} = -\frac{1}{g} Q'(t), \quad \frac{\partial \zeta(l_K,t)}{\partial x} = 0 \qquad /1.20/$$

Let us denote the values ζ and ω on the section $(0_1, l_1)$ through ζ_1 and ω_1, on the section (l_1, l_2) through ζ_2 and ω_2, on the section (l_2, l_k) through ζ_3 and ω_3. Then the conditions, which must be observed in the intermediate sections $x = l_1$ and $x = l_2$ may be written down in the following way:

$$\zeta_i(l_i,t) = \zeta_{i+1}(l_i,t), \quad \omega_i \frac{\partial \zeta_i(l_i,t)}{\partial x} = \omega_{i+1} \frac{\partial \zeta_{i+1}(l_i,t)}{\partial x}$$

$$(i = 1,2) \qquad /1.21/$$

The first of these conditions follows from the Bernoulli equation, if it be written for cross-sections arranged at a small distance either to the left or to the right from the separating $x = l_i$ and if velocity heads are neglected because of their smallness. The second condition may be obtained by the aid of /1.4/ from the continuity equation written down for the same cross-sections.

If a concentrated supply is realized in any one of the intermediate cross-sections of the chamber $x = l_j$, where the discharge of water $Q_j(t)$ is delivered, then this cross-section is subject to the following conditions:

$$\zeta_j(l_j,t) = \zeta_{j+1}(l_j,t),$$

$$\omega_j \frac{\partial \zeta_j(l_j,t)}{\partial x} - \omega_{j+1} \frac{\partial \zeta_{j+1}(l_j,t)}{\partial x} = \frac{1}{g} Q_j'(t),$$

/1.22/

where ζ_j and ω_j belong to the section to the left of the cross-section under consideration, while ζ_{j+1} and ω_{j+1} belong to the section to the right.

Since at the initial instant of time the fluid is at rest, the initial conditions are:

$$\zeta(x,0)=0, \qquad \frac{\partial \zeta(x,0)}{\partial t}=0. \qquad /1.23/$$

When problems are solved for approach channels, boundary conditions are set up similarly. Let us note, however, that for the open end of the channel with a length l, opening into a large water basin, the boundary condition is

$$\zeta(l,t)=0, \qquad /1.24/$$

When local changes of the cross-section of the channel are confronted with, in particular, directly in front of the lock, then /1.21/ must also be applied.

Thus, the calculation of unsteady fluid movements in locks and their approach channels in the indicated characteristical cases is brought down to linear wave problems of the simplest type, the mathematical apparatus for the solution of which has been well developed and is classical in essence (problems on the transverse vibrations of a string, longitudinal vibrations of a bar etc.).

In analysing fluid oscillations in locks it often becomes necessary to determine the distribution of longitudinal velocities along the length of the lock (for inst., for the determination of the forces acting upon the ship). To that end, after the expression $\zeta(x,t)$ is established, equations /1.4/, or /1.12/ may be intergrated.

Let us set up an expression for the wave force acting on the ship. In practical lock calculation, the wave force P_b is known as the longitudinal horizontal component of forces of fluid pressure acting upon the ship:

$$P_b = \iint_{S_c} p \cos(n,x)\, ds, \qquad /1.25/$$

where S_c is the submerged surface of the hull, n is the direction of a line interior normal to the surface S_c. The analysis shows that as the oscillations, both of the fluid surface and of the ship, are small the wave force may be determined by integrating the formula /1.25/ for the submerged hull surface S_c^o in a state of rest (1) (the error is of the second order of smallness). Considering, in addition, here and further on the submerged portion of the hull to be close to a rectangular

(1) In the case of calculation of locking in a chamber, it is appropriate to consider the boat's water-line as coinciding with the mean position of the level in the chamber.

parallelepiped in shape, we will obtain:

$$P_b = \int_{\omega_c} p(l_1,t)d\omega - \int_{\omega_c} p(l_2,t)d\omega = \int_{\omega_c} [p(l_1,t) - p(l_2,t)]\,d\omega,$$

thence, utilising /1.3/, we get:

$$P_b = \gamma \int_{\omega_c} [\zeta(l_1,t) - \zeta(l_2,t)]\,d\omega =$$

$$= \gamma [\zeta(l_1,t) - \zeta(l_2,t)]\,\omega_c .$$

/1.26/

Let us note that in the expressions presented, a reduced length of the ship is being considered:

$$l_c = \frac{W}{\omega_c},$$

/1.27/

where ω_c is the area of the middle cross-section of the ship.

We will demonstrate the application of the expressions obtained here by a practical solution in the case of a head-on type of water supply.

2. Calculation for the Initial Stage of Lock Chamber Filling with an End-on System of Supply.

Let there be one boat in the chamber. In this case the level fluctuations are determined by integrating /1.14/ with q = O, boundary conditions /1.20/, /1.21/ and initial conditions /1.23/.

Practically it may be considered /1/, that at the initial stage of chamber filling

$$Q'(t) \approx Q' \quad (O) = \text{constant.} \quad /2.1/$$

Integrating by the Fourier method and presenting the solution with the aid of dimensionless quantities, we get

$$\zeta = \frac{Q'(0)}{l_k b_k} \left(\frac{l_c}{c_c}\right)^2 \left\{ \frac{1}{2} \left(\frac{c_c}{l_c} t\right)^2 + \bar{\delta}(\bar{x}) - \right.$$

$$\left. - 2\,\bar{l}_k \sum_{n=1}^{\infty} \frac{1}{\nu_n^2 \bar{N}_n} \cos \frac{c_c}{l_c} \nu_n t X_n(\bar{x}) \right\}, \qquad /2.2/$$

where $$\bar{N}_n = \bar{l}_1 + A_{2n}^2 + B_{2n}^2 + (A_{3n}^2 + B_{3n}^2)\,\bar{l}_2', \qquad /2.3/$$

$$X_n(\bar{x}) = \begin{cases} \cos \sigma \nu_n \bar{x} & \text{at } 0 \le \bar{x} \le \bar{l}_1, \\ A_{2n}\cos \nu_n(\bar{x}-\bar{l}_1) + B_{2n} \sin \nu_n(\bar{x}-\bar{l}_1) & \text{at } \bar{l}_1 \le x \le \bar{l}_2, \\ A_{3n} \cos\sigma \nu_n (\bar{x}-\bar{l}_2) + B_{3n}\sin\sigma\nu_n (\bar{x}-\bar{l}_2) & \bar{l}_2 \le x \le \bar{l}_K. \end{cases} \qquad /2.4/$$

For these same three sections (i = 1, 2, 3) :

$$\bar{\mathcal{R}}_i(\bar{x}) = \bar{\mathcal{R}}(\bar{l}_{i-1}) - \frac{\omega_K - \omega_c}{\omega_i}\bar{l}_K(\bar{x}-\bar{l}_{i-1})\left(1 - \frac{\bar{l}_{i-1}}{\bar{l}_K} - \right.$$

$$\left. - \frac{\bar{x}-\bar{l}_{i-1}}{2\bar{l}_K}\right),$$

where $\bar{l}_0 = 0$, $\bar{\mathcal{R}}(0) = 2\bar{l}_K \sum_{n=1}^{\infty} \frac{1}{\nu_n^2 \bar{N}_n}$.

Coefficients

$$\left.\begin{aligned} A_{2n} &= \cos\sigma \nu_n \bar{l}_1, & B_{2n} &= -\frac{1}{\sigma} \sin\sigma \nu_n \bar{l}_1, \\ A_{3n} &= \begin{vmatrix} A_{2n} & -B_{2n} \\ \sin \nu_n & \cos\nu_n \end{vmatrix}, & B_{3n} &= -\sigma \begin{vmatrix} A_{2n} & B_{2n} \\ \cos\nu_n & \sin \nu_n \end{vmatrix} \end{aligned}\right\} \qquad /2.5/$$

The spectrum of values ν_n is determined by the transcendental frequence equation:

$$\sigma^2 + \sigma \cot\nu\,(\tan\sigma\bar{l}_1\nu + \tan\sigma\bar{l}_2'\nu) -$$

$$- \tan\sigma\bar{l}_1\nu \cdot \tan\sigma\bar{l}_2'\nu = 0, \qquad /2.6/$$

where values ν_n are connected with natural frequencies γ_n and corresponding periods of water oscillation T_n in the chamber by the following relation:

$$\nu_n = \gamma_n \frac{l_c}{c_c} = \frac{2\pi}{T_n} \frac{l_c}{c_c}. \qquad /2.7/$$

Substituting from formula /2.2/ ζ into the expression /1.26/ and utilizing /1.27/, we will obtain the following law for the action of the wave force in the initial locking period:

$$P_b = \frac{Q'(0)}{g(\omega_k - \omega_c)} \gamma W \left\{ 1 - \frac{1 + 2\bar{l}_1}{2\bar{l}_k} + \right.$$

$$\left. + 2 \sum_{n=1}^{\infty} \frac{A_{3n} - A_{2n}}{\nu_n^2 \bar{N}_n} \cos \frac{c_c}{l_c} \nu_n t \right\}. \qquad /2.8/$$

11. THE PROBLEM OF OSCILLATIONS IN THE BOAT - CARRYING TANK OF AN INCLINED SHIP ELEVATOR.

Oscillations of the water surface and of the boat in the tank of an inclined ship elevator may be investigated on the basis of two assumptions:

1. the acceleration or stoppage of the tank occurs during some finite time interval;
2. the moving tank stops in such a brief interval of time, which may be considered as instantaneous (sudden stoppage).

The solution of the problem of an instantaneous chamber stoppage is of interest for the clarification of maximally possible undulations of the surface in emergency cases. It is treated in article /5/ and therefore is not presented here. We wish to note, however, that for this case, when the assumed operating speeds of the tank are of the order of 1 m.per sec, the undulatinns are quite admissible (this conclusion has later been confirmed experimentally). Now let us turn to the more general first problem.

3. Approximate Differential Equations of Water Surface Oscillations in the Chamber.

In this case differential equations are derived in a manner similar to the method given above for locks. The complication consists in the following: in utilizing dynamic equations of fluid motion we have to regard as mass forces not only gravity, but also the inertia due to the transition of the system since it is expedient to examine this problem in a moving system of coordinates rigidly connected with the tank.

With relation to the shape of the tank we will make the same assumptions as above in the case of the lock-chamber. We shall assume that the tank is moving along a straight rail-line, inclined at an angle Θ. The motion of the fluid and of the boat in the chamber we shall refer to a moving system of coordinate xyz (Fig. 3).

Since in the ship elevator tank may be permitted undulations only of a small height, the theory of long waves of small amplitude may be used as a basis for the solution of the problem in this case also.

Now let us write down the dynamic equations for the fluid in motion:

$$-j_x - \frac{1}{\rho}\frac{\partial p}{\partial x} = \frac{\partial u_x}{\partial t}, \qquad /3.1/$$

$$g + j_z + \frac{1}{\rho}\frac{\partial p}{\partial z} = 0 \qquad /3.2/$$

where $j_x = j\cos\Theta$, $j_z = j\sin\Theta$, a $j(t)$ - acceleration of the tank. The component of the acceleration j_z is usually practically insignificant as compared with the acceleration of gravity g; therefore, we will disregard it in the equation /3.2/. Then for a pressure p we will again obtain the formula /1.3/.

Instead of /1.4/ we will now have

$$\frac{\partial U_x}{\partial t} = -\left(j_x + g\frac{\partial \zeta}{\partial x}\right). \qquad /3.3/$$

The continuity equation, derived with the same assumptions as for the lock, will result in

$$b_k\frac{\partial \zeta}{\partial t} = -\frac{\partial (u_x \omega)}{\partial x}. \qquad /3.4/$$

Excluding u_x from /3.3/ and from /3.4/ we get (1)

$$b_k \frac{\partial^2 \zeta}{\partial t^2} = \frac{\partial}{\partial x}\left[\omega\left(j_x + g\frac{\partial \zeta}{\partial x}\right)\right], \qquad /3.5/$$

while at ω = constant

$$\frac{\partial^2 \zeta}{\partial t^2} = C^2 \frac{\partial^2 \zeta}{\partial x^2} \qquad /3.6/$$

where C, the celerity of wave distribution, is determined by the former expression /1.16/, /1.17/ and /1.18/.

In the extreme cross-sections of the tank the boundary conditions are

$$u_x(0,t) = u_x(l_k, t) = 0,$$

due to which

$$j_x + g\frac{\partial \zeta(0,t)}{\partial x} = 0, \qquad j_x + g\frac{\partial \zeta(l_k,t)}{\partial x} = 0 \qquad /3.7/$$

For intermediate cross-sections $x=l_1$ and $x=l_1$ by analogy with /1.21/ we now will obtain:

$$\zeta_i(l_i,t) = \zeta_{i+1}(l_i), \qquad \omega_i\left[j_x + g\frac{\partial \zeta_i(l_i,t)}{\partial x}\right] =$$

$$= \omega_{i+1}\left[j_x + g\frac{\partial \zeta_{i+1}(l_i,t)}{\partial x}\right] \quad (i=1,2) \qquad /3.8/$$

If the fluid in the chamber is in a state of relative rest in the initial instant of time t=O, then the initial conditions take on the shape /1.23/.

4. Forces Acting Upon the Boat

In regard to the boat placed in a moving boat-carrying tank, amongst

(1) Here g again an assumption is made that $u_x \frac{\partial \omega}{\partial t}$ is small.

the forces which must be taken into account in determining the tension in the mooring ropes, by which the ship is fastened to the tank are:

1) the force of inertia (the transition inertia);
2) the wave force (the wave pressure);
3) the force of friction between the fluid and the ship (the surface resistance). As the analysis indicates, it is negligible.

If we disregard as negligible the inertia of the fluid mass perturbed by the ship (the so-called virtual mass), then the inertial force may be considered equal to (1)

$$P_u = -j_x \rho W = -\frac{\bar{j}^x}{g} \gamma W. \qquad /4.1/$$

The wave force is determined by formula /1.25/ and /1.26/. The total longitudinal force acting upon the ship will be equal to

$$P = P_u + P_b \qquad /4.2/$$

5. A Solution for the Simplest Cases.

Let us present here the results obtained for two simplest cases:

1) in the tank there either is no boat at all, or the boat is of such small dimensions that it does not influence to any considerable degree water fluctuations ($c = c_k$).
2) the length of the boat is close to the tank length ($l_c \approx l_k$), and the cross-section of its submerged portion does not change throughout ($C = C_c$).

In these cases the equation /3.6/ is applicable. Let us accept the initial conditions in the form of /1.23/, the boundary conditions - in the form of /3.7/.

(1) Tests conducted by us on a ship elevator model have shown that in calculating P_u the virtual mass may be omitted.

We shall consider the motion to be uniformly accelerated : j = constant. Integrating by the method of Fourier, we will obtain the following solution:

$$\zeta(x',t) = -\frac{jx}{g}\left\{x' - \frac{4l_K}{\pi^2}\sum_{n=1,3,5,\ldots}^{\infty}\frac{(-1)^{\frac{n-1}{2}}}{n^2}\cos\frac{n\pi c}{l_K}t \cdot \sin\frac{n\pi}{l_k}x'\right\} \qquad /5.1/$$

where $x' = x - \frac{l_K}{2}$

The second solution may be found by the method of D'Alembert:

$$\zeta(x',t) = -\frac{jx}{g}\left\{x' - \frac{1}{2}\left[f(x'-ct) + f(x'+ct)\right]\right\} \qquad /5.2/$$

where

$$f(t) = \begin{cases} \tau - 2l_K & \text{at} \quad -\frac{5l_K}{2} \le \tau \le -\frac{3l_K}{2}, \\ -\tau - l_K & \text{at} \quad -\frac{3l_K}{2} \le \tau \le -\frac{l_K}{2}, \\ \tau & \text{at} \quad -\frac{l_K}{2} \le \tau \le \frac{l_K}{2}, \\ -\tau + l_K & \text{at} \quad \frac{l_K}{2} \le \tau \le \frac{3l_K}{2}, \\ \tau + 2l_K & \text{at} \quad \frac{3l_K}{2} \le \tau \le \frac{5l_K}{2}, \end{cases}$$

and so forth, with either the increase or the decrease of τ .

It follows from formula /5.1/ and /5.2/ that the period of oscillations T_o and the duration of the oscillation phase τ_o are determined by the relation

$$\tau_o = \frac{T_o}{2} = \frac{l_K}{C}, \qquad /5.3/$$

however, when there is a boat in the tank then evidently the following relation will be more precise:

$$\tau_o = \frac{T_o}{2} = \frac{l_c}{C_c} + \frac{l_K - l_c}{C_K} \qquad /5.4/$$

For individual time instants the longitudinal profile of the free surface is presented on Fig. 4:

O-O - at instants t=O and T_o,
1-1 - at instants $\frac{1}{8} T_o$ and $\frac{7}{8} T_o$,
2-2 - at instants $\frac{1}{4} T_o$ and $\frac{3}{4} T_o$,
3-3 - at instants $\frac{3}{8} T_o$ and $\frac{5}{8} T_o$,
4-4 - at the instant $\frac{1}{2} T_o$.

Thus, in the process of uniformly accelerated motion of the chamber the fluid surface oscillates about the position (profile 2-2 on Fig. 4), which it occupies in the case of relative rest. In that position the surface is a plane, inclined to the horizon under an angle φ, where

$$\tan \varphi = - \frac{j_x}{g}. \qquad /5.5/$$

In the extreme positions the free surface also has the form of planes - a horizontal and an inclined, under an angle φ_{max} to the tangent

$$\tan \varphi_{max} = - \frac{2 j_x}{g}. \qquad /5.6/$$

The extreme position of the surface 4-4 (Fig. 4) will be reached, and in that connection the formula (5.6) will also have a meaning only in the case when the time of acceleration

$$T \geq \tau_0 \qquad /5.7/$$

Due to the smallness of accelerations, which may be conveyed to the boat carrying tank under normal operating conditions, because of the need of restricting the tension of the mooring ropes, the value of the acceleration period T will be quite considerable; therefore, T will meet the condition /5.7/ .

Correspondingly the greatest oscillations of the surface at both the front and rear tank gates will be equal to

$$\zeta_{max} = \mp \frac{l_K}{2} \quad \tan\varphi_{max} = \mp \frac{j_x}{g} l_K \qquad /5.8/$$

By expressing j through the time T, in which the acceleration or stoppage of the tank takes place, and through the speed of uniform motion v, we will get

$$\zeta_{max} = \mp \frac{v l \cos\theta}{gT} \qquad /5.9/$$

The maximum value of the wave force will be reached at such instants of time, which correspond to the odd number of phases of oscillation τ_0, when the free surface attains the maximum incline, determined by the formula /5.6/. Here it follows from /1.26/ and /5.8/ that

$$P_{b\ max} = 2\gamma \zeta_{max} \omega_c = 2 \frac{j_x}{g} \gamma W. \qquad /5.10/$$

At the beginning of the period of acceleration (or instant corresponding to the even number of phases τ_0) the longitudinal force acting on the ship is reduced to the single inertial component

$$P = P_u = - \frac{j_x}{g} \gamma W. \qquad /5.11/$$

In the process of acceleration at the instant $t = \tau_0$ (or the corresponding odd number of phases τ_0)

$$P = P_u + P_{b\ max} = - \frac{j_x}{g} \gamma W + 2 \frac{j_x}{g} \gamma W = \frac{j_x}{g} \gamma W. \qquad /5.12/$$

But if the accelerated motion of the chamber ceases at such an instant, then the action of the wave force is displayed fully:

$$P = P_{b\ max} = 2\frac{j_x}{g}\gamma W \qquad /5.13/$$

Of all the possible magnitudes of the longitudinal force this one is the greatest.

The allowable longitudinal tension of mooring ropes, by which the boat is fastened to the tank, may be determined for normal operating conditions with the aid of A. V. Mikhaylov's formula, which he received on the basis of an analysis of the conditions of ship stay in lock chambers:

$$P_{allow.} = \frac{\gamma W}{n_{allow.}},$$

for which Mikhaylov gives both a formula and a diagram for the value of $n_{allow.}$. In setting up the value of $n_{allow.}$ the allowable tensioning of ropes was lessened by introducing the coefficient $K_2 = 0.9$, which takes into account the increase of the capacity of the lock-filling system as compared with the data of their model tests (reaching in some cases 10%).

Since this has no relation to ship elevator operation the coefficient K_2 must be excluded from the results.

The allowable (in calculations and model investigations) longitudinal tension of mooring ropes in application to ship-elevator conditions may be presented in the form

$$P_{allow.} = \frac{\gamma W}{n'_{allow.}} \qquad /5.14/$$

where

$$n'_{allow.} = K_2\, n_{allow.} = 0.9\, n_{allow.}$$

If we disregard the damping of oscillations and assume that the tank acceleration ends at the instant, which corresponds to the odd number of phases τ_o, then equating expressions /5.13/ and /5.14/, we will receive the maximum allowable normal working acceleration

$$j_{allow.} = \frac{g}{1.8\, n_{allow.} \cos\theta} \qquad /5.15/$$

6. A More General Solution

If the assumption $l_c \approx l_k$ is not introduced in the presence of a boat in the tank, then the equation /3.5/ should be integrated for boundary conditions /3.7/ and /3.8/ and initial conditions /1.23/. Considering that the acceleration is constant ($j =$ constant) and integrating by the G.A. Grinberg method, we will get for $t \leq T$:

$$\zeta = \frac{2jx}{g} \frac{l_c}{\sigma^2} \sum_{n=1}^{\infty} \frac{K_n}{\nu_n^2 \bar{N}_n} \left(1 - \cos \frac{c_c}{l_c} \nu_n t\right) X_n(\bar{x}) \quad /6.1/$$

or

$$= -\frac{jx}{g} l_c \left\{ \left(\bar{X} - \frac{\bar{l}_k}{2}\right) + \frac{2}{\sigma^2} \sum_{n=1}^{\infty} \frac{K_n}{\nu_n^2 \bar{N}_n} \cos \frac{c_c}{l_c} \nu_n t X_n(\bar{x}) \right\} \quad /6.2/$$

at $t \geq T$:

$$\zeta = \frac{4jx}{g} \frac{l_c}{\sigma^2} \sum_{n=1}^{\infty} \frac{K_n}{\nu_n^2 \bar{N}_n} \sin \frac{c_c}{l_c} \nu_n \frac{T}{2} \sin \frac{c_c}{l_c} \nu_n \left(t - \frac{T}{2}\right) \bar{X}_n(\bar{x}). \quad /6.3/$$

Here

$$K_n = 1 + (1-\sigma^2)(A_{3n} - A_{2n}) - (A_{3n} \cos \sigma \nu_n \bar{l}_2' + B_{3n} \sin \sigma \nu_n \bar{l}_2'),$$

while $\bar{N}_n$, $X_n(\bar{x})$ and A_{in}, B_{in} are determined by the previous expressions. Natural frequencies are also subjected to the previous expressions /2.6/ and /2.7/.

Applying /1.26/ and /1.27/, we will get the following law of action of the wave and total forces. For $t < T$ the wave force:

$$P_b = \frac{2jx}{g} \frac{\gamma W}{\sigma^2} \sum_{n=1}^{\infty} \frac{K_n (A_{2n} - A_{3n})}{\nu_n^2 \bar{N}_n} \left(1 - \cos \frac{c_c}{l_c} \nu_n t\right), \quad /6.4/$$

or

$$P_b = \frac{2jx}{g} \gamma W \left\{ \frac{1}{2} - \frac{1}{\sigma^2} \sum_{n=1}^{\infty} \frac{K_n (A_{2n} - A_{3n})}{\nu_n^2 \bar{N}_n} \cos \frac{c_c}{l_c} \nu_n t \right\} \quad /6.5/$$

the total force along /4.1/, /4.2/ and /6.5/ is

$$P = P_u + P_b = -\frac{2 j x}{g} \frac{\delta W}{\sigma^2} \sum_{n=1}^{\infty} \frac{K_n (A_{2n} - A_{3n})}{\nu_n^2 \bar{N}_n} \cos \frac{c_c}{l_c} \nu_n t .$$

/6.6/

At $t > T$:

$$P = P_b = \frac{4 j x}{g} \frac{\delta W}{\sigma^2} \sum_{n=1}^{\infty} \frac{K_n (A_{2n} - A_{3n})}{\nu_n^2 \bar{N}_n} \sin \frac{c_c}{l_c} \nu_n \frac{T}{2} \sin \frac{c_c}{l_c} \nu_n \left(t - \frac{T}{2}\right).$$

/6.7/

7. Brief Data Relating to Experimental Investigations On a Model of an Inclined Ship Elevator.

In the years 1957 - 1958 in the Moscow Kouybishev Institute of Civil Engineering the author was in charge of experimental investigations on a model of an inclined ship elevator. A self-propelled boat-carrying tank model running along a section of the railroad was built to a scale 1 : 50. Here the data of the prototype were assumed to be: $l_k = 110$ m, $b_k = 18$ m, $h = 3.65$m, $\tan\theta = 0.05$, the speed of uniform motion ranging from 0.8 to 1.2 m/sec., acceleration in the range of 0.2 to 4 cm/sec.^{2}. Instantaneous (practically, very rapid) chamber stoppages were also effected on the model. The boat was represented by model of a barge of 3,330 t.displacement, and $l_c = 85$m, $b_c = 14$m.and $s = 3.2$ m. Modelling was conducted in accordance with the laws of gravitational similarity.

In the course of the tests synchronous records were made on an oscillograph - of the speed of chamber motion (with the aid of a tachometer), of water surface oscillations (with the aid of an electrolytic resistance wave meters), of variation of the longitudinal force acting on the ship (with the aid of a inductive measurer).

The test data indicates that the theoretical calculations of the water surface oscillations in the tank and of the longitudinal force acting upon the boat are practically exact.

DENOMINATIONS

l_k - chamber length,
b_k - chamber width (or approach channel width), along the free water surface,
h - depth of water in the chamber (or channel),
ω_k - area of the cross-section of the fluid in the free chamber (or channel),
l_c - length of ship,
b_c - width of ship along the water line,
s - ship settlement,
ω_c - cross-sectional area of the submerged portion of the ship,
W - Voluminal ship displacement,
p and p_o - pressure in the fluid and at its free surface
g - acceleration of gravity,
ϱ and γ - mass density and specific weight of water,
t - time,
Q - volume rate of flow entering the lock chamber (or channel)
q - volume rate of flow entering the lock chamber (or channel) through the distributional system (the longitudinal culvert) per unit of length,
Θ - incline angle of the shipways,
v - running speed of the boat-carrying tank (chamber),
j - acceleration of tank motion,
j_x, j_z - horizontal and vertical components of the acceleration of tank motion,
ζ - ordinate of the free fluid surface,
ω - cross-sectional area of fluid,
P_b - wave force acting upon the ship,
P_u - force of inertia acting upon the ship (in the ship-carrying tank),
C_k and C_c - celerity of wave diffusion in the free sections of the chamber and in the section occupied by a boat respectively,

$$\bar{x} = \frac{x}{l_c}, \quad \bar{l}_1 = \frac{l_1}{l_c}, \quad \bar{l}_2 = \frac{l_2}{l_c}, \quad \bar{l}_2' = \frac{l_2'}{l_c}, \quad \bar{l}_K = \frac{l_K}{l_c},$$

$$\sigma = \sqrt{\frac{\omega_K - \omega_c}{\omega_K}}$$

- dimensionless parameters.

BIBLIOGRAPHY

1. Mikhaĭlov A. V., The head filling system of navigation locks and their calculation. Rechizdat, Moscow, 1951.
2. Mikhaĭlov A. V., The navigation locks. Gosstzoĭizdat, Moscow, 1955.
3. Pavlenko G. E., The oscillations of ships. Gostransizdat, Leningrad, 1935.
4. Makkaveev V. M., Hydromechanical processes accompanying the locking through of boats and methods of laboratory research. Sbornik Leningradskogo instituta ingenerov puteĭ soobscheniya, V. 107, 1930.
5. Vasiliev O. F., The oscillations of water in the boat-carrying chamber of an inclined ship elevator after its instantaneous stoppage. Nauchnye doklady vysshe ĭ shkoly, seriya "Stroitelstvo", N 1, 1958.
6. Grinberg G. A., Select problems of the mathematical theory of electric and magnetic phenomema. Published by the Academy of Sciences of the USSR, Moscow-Leningrad, 1948.

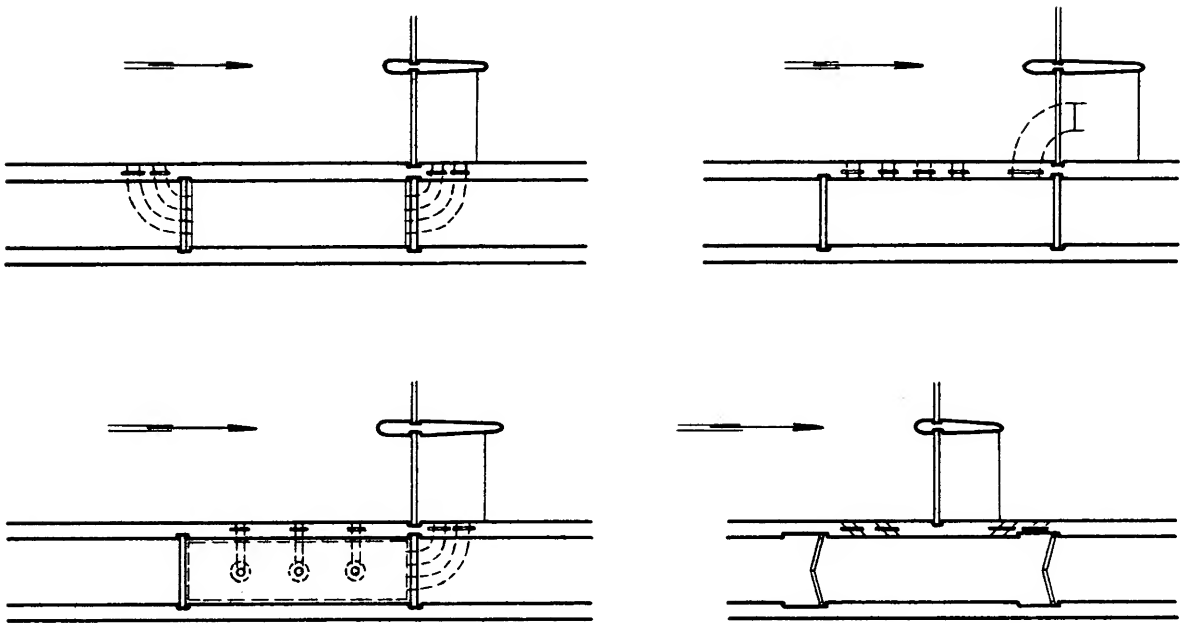

Fig. 1

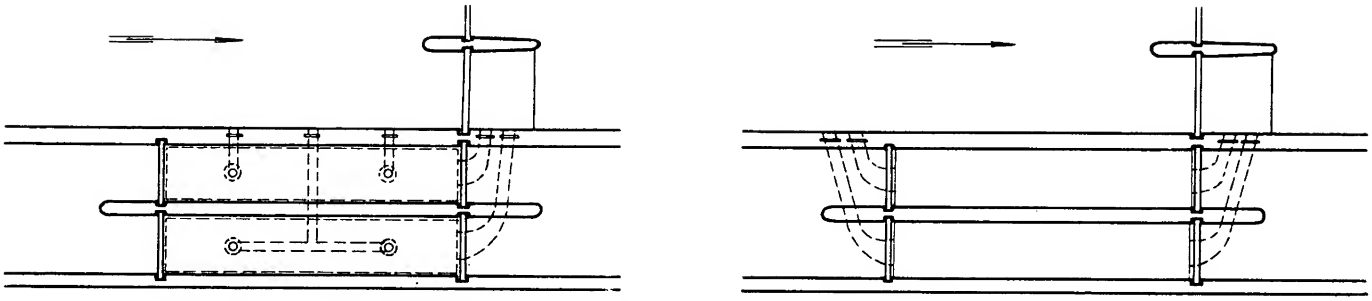

Fig. 2

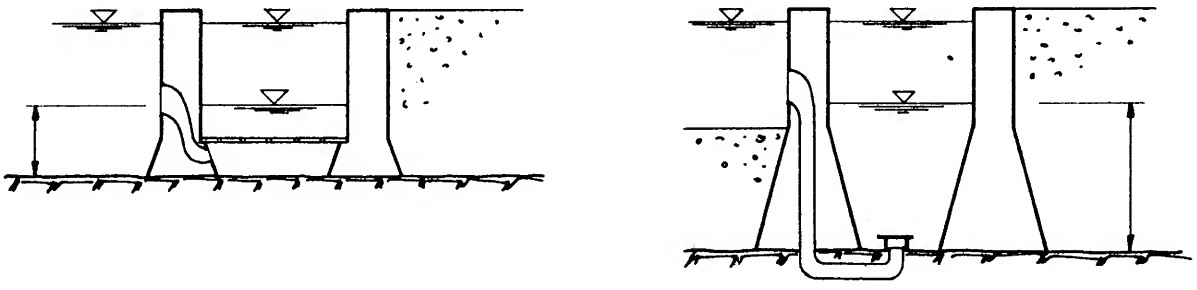

Fig. 3

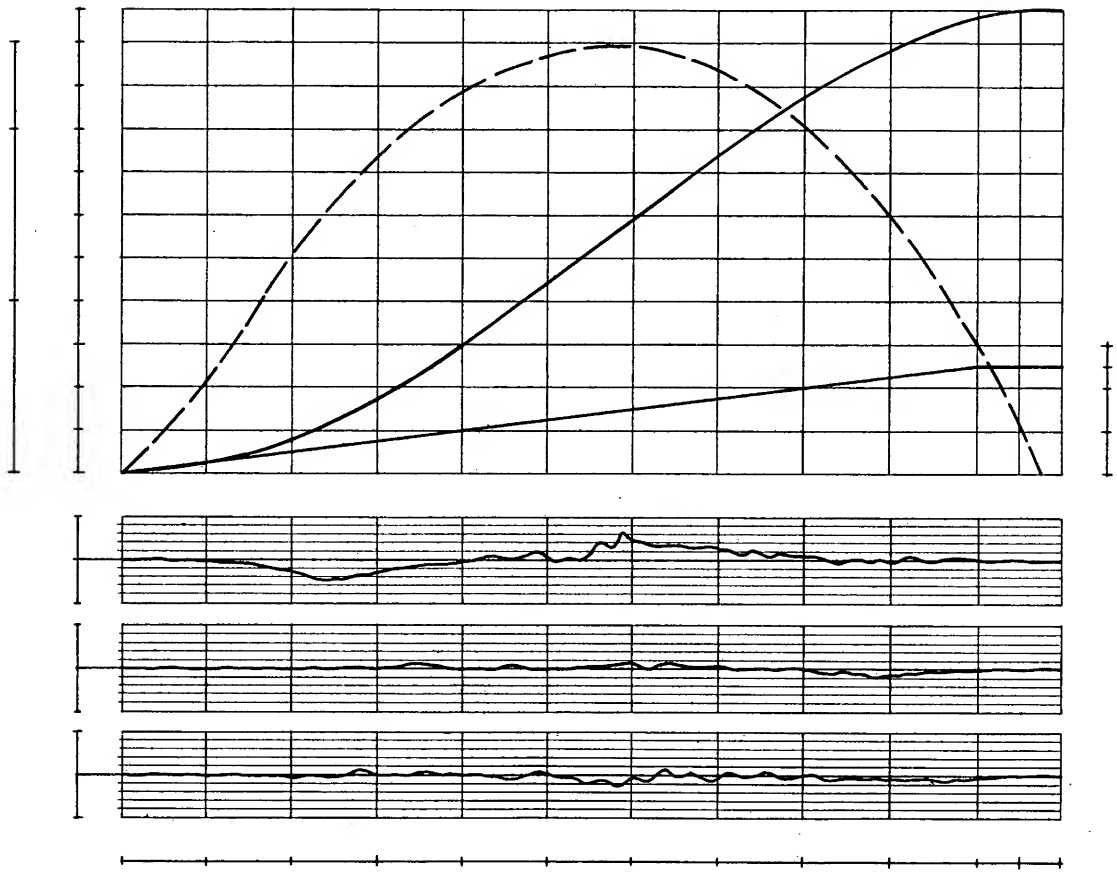

Fig. 4

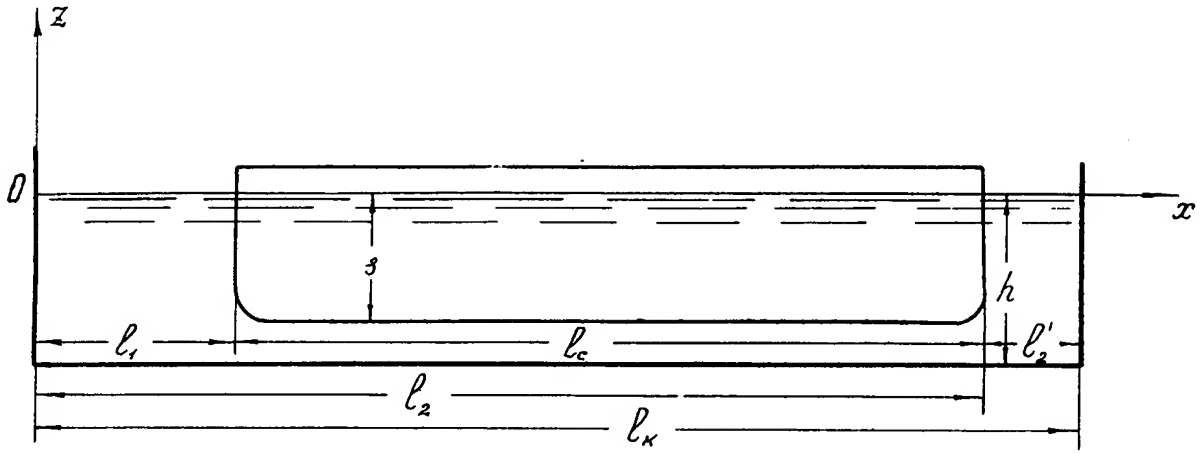

Фиг. 1.

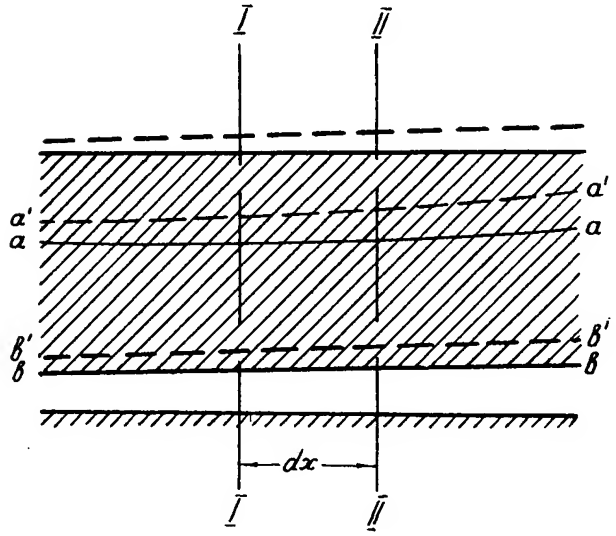

Фиг. 2.

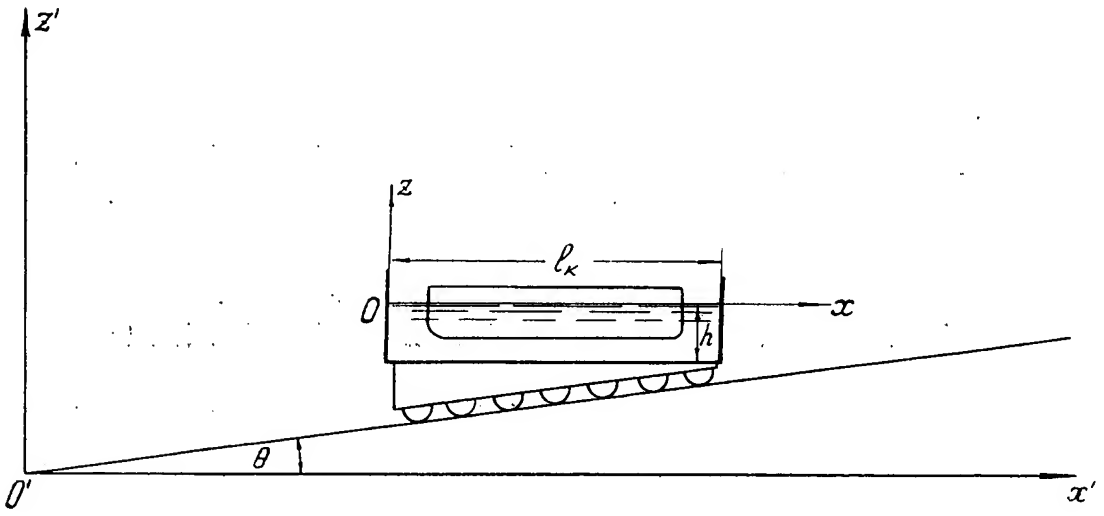

Фиг. 3.

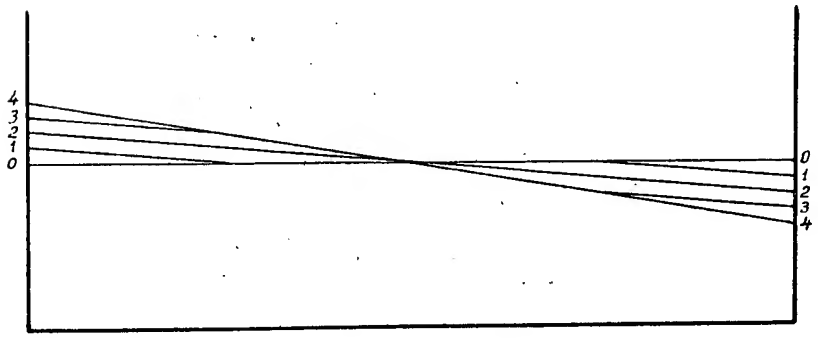

Фиг. 4.

25X1

A STUDY OF ECONOMICAL NAVIGATION LOCKS FOR HIGH LIFTS

* * *

WALENTY JAROCKI

* * *

SUMMARY

This paper describes the investigations on pneumatic chamber locks, requiring small amounts of water for sluicing and utilizing compressed air to raise the tank. This lock is designed for use on those reaches of navigable canals where a water deficiency appears, as well as in cases of considerable lift heights.

In order to learn the principles and the functioning of pneumatic chamber locks, computations were made for and laboratory investigations carried out on a model of a mobile tank in a chamber using compressed air for raising the tank.

The analytical study of the working conditions in a pneumatic chamber lock was based on the dynamic equilibrium condition resulting from d'Alembert's principle. According to this principle, a dynamic equilibrium equation between engaged forces was established. Having solved this equation, the relations were found which permitted the computation of air pressure in the chamber required to raise the tank, etc.

For laboratory investigations a model chamber and a mobile tank with all the connecting devices was built. Particular emphasis

was paid to the problem of providing a suitable tightening in order to reduce compressed air losses and to prevent the seepage of water into the chamber containing air. This would occur near walls where the air is in contact with water.

On the basis of laboratory model tests, diagrams were plotted showing the relation between time, tank motion, velocity and the pressure of the compressed air in the chamber for various water depths in the tank and for different values of tightening pressure.

SOMMAIRE

Ce mémoire décrit l'étude faite sur des écluses pneumatiques. Celles-ci ne nécessitent qu'une petite quantité d'eau pour l'éclusage, utilisant de l'air comprimé pour élever le réservoir. Ces écluses sont particulièrement utiles dans les biefs où l'eau n'est pas abondante ou aux endroits où la hauteur de chute est considérable.

Afin de mieux saisir les principes et le fonctionnement des écluses pneumatiques, des calculs ainsi que des expériences furent effectués sur un modèle réduit de réservoir mobile et un sas contenant de l'air comprimé nécessaire à élever ce réservoir.

Les calculs d'analyse de conditions de fonctionnement des écluses pneumatiques ont été effectués à l'appui de la condition d'équilibre dynamique s'ensuivant du principe de d'Alembert. Selon ce principe, une équation d'équilibre dynamique entre les forces agissantes a été établie. Cette équation étant résolue, on a trouvé les relations permettant de calculer la pression d'air nécessaire dans le sas pour élever le réservoir, etc.

Pour effectuer les essais de laboratoire, un modèle du sas et du réservoir mobile fut construit. On a prêté une attention toute particulière à l'étanchement qui doit prévenir les fuites d'air et également la pénétration de l'eau dans le sas. Ceci se produirait près des murs où l'air est en contact avec l'eau.

D'après les expériences de laboratoire faites sur le modèle, des graphiques furent tracés montrant la relation entre le temps, la vitesse de mouvement du réservoir et la force de pression de l'air comprimé dans le sas, pour différents niveaux de remplissage du réservoir et pour différentes pressions d'étanchéité.

1. INTRODUCTION

On some navigation channels, where water is lacking, or where the lift is great, the construction of navigation locks requiring small water amounts for sluicing is desirable. Included with this type are the pneumatic chamber locks, which seem to have the most advantageous construction for the above mentioned conditions.

Pneumatic chamber locks may be divided into 2 types: first - those that work on the pneumatic clock principle, and second - actual pneumatic locks (fig. 1). The first type of pneumatic chamber lock (Dulton, Morawek) is rather expensive - a strong foundation as deep as the fall height being required. It seems, however, that the second type, one designed by Schancer (fig. 1b) and another by Tillinger (fig. 1,c,d) is more suitable.

The latter type consists of two chambers filled with compressed air. A moving tank filled with water is placed in each chamber. When any vessel enters the tank a certain amount of water is added and the valve is opened. As the air passes from one chamber to the other, one of the two tanks rises, while the other falls.

While the tank is in its upper position, the chamber walls are under relatively small air pressure, approximately equal to the water pressure of 3,5 m. of depth, and does not increase with the increase in fall height. In normal chamber locks, however, pressure increase is proportional to depth. That means that pressure in pneumatic chamber locks is less than in normal chamber locks which require a greater wall thickness.

It was reckoned that in pneumatic chamber locks the sluicing procedure requires about 0.3 m. depth of water, independent of the height.

So with a 10 m. fall height, and using economical basins, the amount of water required by a pneumatic chamber lock will be about 6% of that used by a normal chamber lock. With a fall as high as 12 m. it decreases to 5%, and to 3% in case of a 20 m. fall height.

The Schancer pneumatic chamber lock has a moving water-filled tank, while in Tillinger's system this tank is turned upside down (fig. 1). In the second case the walls may be high, and tightening between tank and chamber walls ought to be placed as low as possible. Tillinger affirms that the pressure exerted by a column of water on the tightening must exceed the compressed air pressure in the chamber, otherwise air can escape from the chamber.

2. ANALYSIS OF THE WORKING OF THE PNEUMATIC CHAMBER LOCK

In order to obtain an analytical picture of the conditions under which pneumatic chamber locks work, the movements of the tank in a chamber filled with compressed air were observed.

As a starting point of this discussion we will consider equilibrium as the condition not only the equilibrium of weight of the tank filled with water remaining under compressed air pressure, but also the setting of this bed in motion.

The condition of dynamic equilibrium resulting from d'Alambert's principle is a differential equation of the second degree, motion acceleration being the second derivative of distance against time.

The equation of dynamic equilibrium between acting forces will be as follows:

$$-Q - F\gamma H - fd + kF = \frac{Q + F\gamma H}{g} \frac{d^2y}{dt^2}$$

where:

Q = weight of tank,
H = depth of water column,
γ = unit weight of water,
F = a cross section through the chamber on the level of the tank bottom,
d = pressure in tightening,
f = friction coefficient,
k = compressed air pressure,
g = acceleration due to gravity,
y = stroke or travel of the tank,
t = time of tank motion.

In this equation the negative factors represent forces acting downwards, while the kF factor, the pressure force directed upwards, has the plus sign.

The dynamic equilibrium equation after transformation may be written in the following form:

$$\frac{d^2y}{dt^2} = -\frac{(Q + F\gamma H + fd - kF)}{Q + F\gamma H} g = \left(-1 + \frac{-fd + kF}{Q + F\gamma H}\right) g$$

Assuming

$$A = -1 + \frac{-fd + kF}{Q + F\gamma H} \tag{1}$$

we shall obtain a differential formula of tank motion:

$$\frac{d^2y}{dt^2} = Ag \tag{2}$$

In this equation an unknown factor is the travel of the tank in function of time i.e. $y = f(t)$. After obtaining the solution of the differential equation, we determine the distance in function of time, according to boundary and initial conditions. It may be noted, that the initial conditions are relative to that moment when the movement begins, while the boundary conditions are the beginning and the end of the stroke.

The integral of the differential equation of the motion, has the following form:

$$y = \frac{Agt^2}{2} + Bt + C$$

Thus, in order to fix two optional constants B and C, it is assumed that $y(O) = O$, and $y'(O) = O$, that means, that in the initial moment, distance and velocity are equal to zero. With such an assumption the tank movement will begin without any jerk at the initial moment ($t = O$).

Under such initial conditions the form of the integrate is

$$y = \frac{A g t^2}{2} \tag{3}$$

Considering that T_o is the time required for the rise of the tank to the entire height L_o, with the value of A corresponding to the known parameters Q, γ, H, d, k, F. Substituting those values in the equation (3) we obtain:

$$L_o = \frac{1}{2} A g T_o^2 = \frac{1}{2} T_o^2 g \left(-1 + \frac{kF - fd}{Q + F\gamma H} \right) ;$$

$$kF = fd + \left(1 + \frac{2L_o}{g T_o^2} \right) (Q + F\gamma H) \tag{4}$$

This final equation includes all parameters. Let us assume the value we try to determine is the pressure k required for the elevation of the tank under given conditions. The following formula thus results:

$$k=\frac{f}{F}\,d+\left(1+\frac{2\,L_o}{g\,T_o^2}\right)\left(\frac{Q}{F}+\gamma H\right) \qquad (4a)$$

As we are not interested in the analysis of the phenomenon of tank motion expressing the relation between stroke and time, therefore, developing the equation (4a) parameter y/gt^2 was written in the $L_o/g\,T_o^2$ form. An essential problem is the determination of the pressure of raising the tank in T_o period required for reaching the final height L_o.

Dividing equation (4a) by $(\frac{Q}{F}+\gamma H)$ we shall obtain the relation:

$$\frac{K}{\frac{Q}{F}+\gamma H}=\frac{f}{F}\;\frac{d}{\frac{Q}{F}+\gamma H}+\frac{2\,L_o}{g\,T_o^2}+1 \qquad (5)$$

The above equation, if compared with equation (4) does not give any new solution, as it is synonymous. Equation (5), however, is of a great value for investigators as it shows which dimensionless parameters are governing the tank motion phenomenon in the chamber, and which are the similarity parameters in model tests.

The dimensionless parameter $\frac{k}{\frac{Q}{F}+\gamma H}$ represents the relation between air pressure K in the chamber and the pressure exerted by the rising chest. The parameter $\frac{d}{\frac{Q}{F}+\gamma H}$ is the quotient of tightening pressure to the pressure of the same kind as in above mentioned parameter. This parameter includes the numeral coefficient f:F. The third parameter is connected with the tank motion phenomenon.

When the parameters $\frac{f}{F}d=$ constant and $\frac{Q}{F}+\gamma H=$ constant

the formula (4a) can be expressed by the hyperbola equation

$$k=C_1+C_2\;\frac{L_o}{g\,T_o^2}$$

This equation confirms that if the time required for the entire tank rise, T_o, is not constant, then with the increase of the duration phenomenon, the air pressure maintaining the motion will decrease.

It is evident (eq. 3) that the tank is moving with uniformly accelerated motion without initial motion. A rapid braking might be extremely undesired after the tank reaches the height L_o. Previous braking should be applied thus reducing the air pressure in the chamber.

Let us assume the uniformly accelerated tank rising motion in 0,9 T_o period, with $v = y' = A\,g\,t$ velocity, is followed by braking procedure within 0,2T_o period. This may be made by reducing the compressed air pressure in the chamber.

Assuming that the second phase of motion (retarded motion) from 0,9 T_o moment, the motion velocity will decrease linearly so that after 0,2 T_o period it will be equal to zero (fig. 2). Under such conditions the duration of the tank motion will be 1, 1 T_o of the period adopted.

During 0,9 T_o period (fig. 3) the tank will travel the following distance:

$$L_1 = \frac{1}{2}\, g\, A\, (0,9\, T_o)^2 = \frac{0,81}{2}\, g\, A\, T_o^2 \qquad (6)$$

The remaining distance is:

$$L_o - L_1 = \frac{0,19}{2}\, A\, g\, T_o^2 \qquad (7)$$

In order to obtain the zero velocity of the uniformly retarded motion at the end of $\frac{0,19}{2}\, A\, g\, T_o^2$ distance, when the starting velocity was 0,9 $Ag\, T_o$, the question arises of adopting a suitable acceleration value $y'' = -A_o g$.

The retarded motion equation has the following form:

$$y = -\frac{1}{2}\, A_o\, g\, t^2 + Bt + C \qquad (8)$$

Since the motion velocity and acceleration are:

$$y' = -A_o g\, t + B \qquad (9)$$

$$y'' = -A_o g \qquad (10)$$

The following values might be applied in order to determine the 3 constant parameters (A_o, B, C) in motion equation (8);

a) The coordinates of point I (eq. 8)

$$(t = 0,9\, T_o,\ L_1 = \frac{0,81}{2}\, A\, g\, T_o^2),$$

b) The coordinates of point II

$$(t = 1,1\ T_o,\ y = L_o = \frac{1}{2}\ A\ g\ T_o^2)\ ,$$

c) The coordinates of point III

$$(t = 0,9\ T_o,\quad v = y^1 = 0,9\ A\ g\ T_o)$$

By substituting in equation (9) the coordinates of the point III, we obtain the relation:

$$-\ 0,9\ A_o\ g\ T_o + B = 0,9\ A\ g\ T_o \qquad (11)$$

The coordinates of the points I and II might be substituted in the equation of stroke (8):

$$-\ \frac{0,9^2}{2}\ A_o\ g\ T_o^2 + 0,9\ B\ To + C = \frac{0,81}{2}\ A\ g\ T_o^2 \qquad (12a)$$

$$-\ \frac{1,1}{2}\ A_o\ g\ T_o^2 + 1,1\ B\ T_o + C = L_o = \frac{1}{2}\ A\ g\ T_o^2 \qquad (12b)$$

Subtracting by sides the equations (12a) and (12b) we eliminate C and obtain the following relation:

$$-\ \frac{1}{2}\ (1,1^2 - 0,9^2)\ A_o\ g\ T_o^2 + 0,2\ BT_o = L_o - \frac{0,81}{2}\ A\ g\ T_o^2,$$

$$-\ 0,2\ A_o\ g\ T_o + 0,2\ B = \frac{0,19}{2}\ A\ g\ To.$$

The above equation forms with the equation (11) the following system:

$$-\ 0,2\ A_o\ g\ T_o + 0,2\ B = \frac{0,19}{2}\ A\ g\ T_o\ ;$$

$$-\ 0,9\ A_o\ g\ T_o + B = 0,9\ A\ g\ T_o$$

Multiplying the upper equation by (-5), and adding it to the second one, we eliminate the unknown factor B:

$$0,1\ A_o = \frac{0,85}{2}\ A$$

Since the value A_o might be computed:

$$A_o = 4,25\ A \qquad (13)$$

In order to evaluate the B constant, we substitute the value of A_o in equation (11) obtaining:

$$B = 0,9\ (4,25+1)\ A\ g\ T_o = 4,725\ A\ g\ T_o \qquad (14)$$

By substituting A_o and B in equation (12b) we obtain the C value:

$$C = A\ g\ T_o^2\ (2,5713-5,1975+0,5) = -2,126\ A\ g\ T_o^2 \qquad (15)$$

Subsequently the constants A_o, B and C are substituted in the retarded motion equation (8) thus:

$$y = -\frac{4,25\ A\ g\ T^2}{2} + 4,725\ A\ g\ T_o\ t - 2,126\ A\ g\ T_o^2$$

The above obtained retarded motion equation is adopted in such a form, that in the moment $t = 0,9\ T_o$ when the braking begins, the tank will be in point I. It will stop on the L_o level when $t = 1,1\ T_o$.

Let us take, for verification, the derivative of the tank motion velocity:

$$y' = -4,25\ A\ g\ t + 4,725\ A\ g\ T_o$$

This velocity value must be equal to zero, when $t = 1,1\ T_o$. Substituting, we obtain:

$$-4,25 \times 1,1\ A\ g\ T_o + 4,725\ A\ g\ T_o = (4,725-4,675)\ A\ g\ T_o = O.$$

3. THE PRELIMINARY STUDIES ON TIGHTENING AND TANK MOTION IN THE CHAMBER

In order to carry on some laboratory experiments on pneumatic chamber locks, a model chamber was constructed. It has the form of a reinforced concrete tank 100 cm. high. The general appearance of the devices applied for tank motion tests in the chamber is shown on the Fig. 4. A 3 mm. thick, metal mobile tank was stiffened with angle plates. The compressed air was conducted to the chamber.

As it is difficult to obtain suitable tightness between water and compressed air, a special attempt was made to the problem of tightening between mobile tank walls and chamber walls. Several types of tightening with a rubber pipe filled with water were designed and tested. The water pressure in this pipe was varying with the variation of water-level in a water reservoir joined to the water-supply network and the rubby tightening pipe. This pipe was settled in a steel sheath welded to the tank, with an outlet along it 1/3 circuit wide.

It was found that the most suitable tightening is a rubber pipe 2,6 cm. of diameter settled in sheath covered with leather tape retained by thin leather straps fastened to the borders of the sheath (fig. 5). This tightening was applied in the preliminary investigations consisting of 45 tests,

In general the whole device was working in a quite satisfying manner, except some cases when the tank moved headlong.

It was confirmed, according to the preliminary investigations, that the projected tightening fulfilled the designed purposes, and the other elements worked well. Only the chamber depth was found to be insufficient for certain research proceedings.

4. SOME DETAILED INVESTIGATIONS ON WATER-FILLED TANK MOTION IN AN AIR-CHAMBER

The detailed investigations began after a supplementary chamber of 0,3 m. height was constructed, and after the rubber pipe filled with water was applied as the tightening.

The investigations involved the following measurements:

H - depth of water in the tank (cm.),
d - water pressure in the tightening pipe (m.H_2O),
p - pressure before the Venturi meter (mm.Hg),
h - pressure on the Venturi meter (mm.Hg),
k - pressure in the chamber (cm.H_2O),
z - air-pressure on the manometer (atm.),
L - differences of levels between the upper and the lower tank positions (cm.),
T_1 - tank rising time (min.),
T_2 - tank falling time (min.),
t - air temperature (C^o),
b - barometric pressure (mm.Hg).

The main purpose of our investigations was to establish a relation between water depth in the tank, air pressure in the chamber, water pressure in the tightening pipe, and tank motion in an air chamber.

The investigations were conducted with the temperature of the environment varying from 16,5° to 24°C., and barometric pressure being about 1 atm.

The height of the pressure applied in our investigations varied from 0,5 to 4,0 m. of water column in the tightening pipe, while the depth of water in the channel was from 5 to 25 cm. (every 5 cm. subsequently).

Pressure p on the conduit was changed within 5 to 80 cm. of Hg (every 5 cm. approximately). There was 40 cm. of difference between the upper and the lower tank positions.

A negligible air flight was observed, and it was found that a certain minimal amount of water was leaking from the tank to the chamber.

A total of 23 test series were made, which included 338 measurements. According to data thus obtained, the $T_1 = f/p/$ relation was shown by 23 diagrams. These diagrams (which are not presented in this paper) were used to procure 5 synthetical diagrams $T_1 = f(p)$ for 5 measurement groups. Every diagram considered measurements made under the same water depth in the tank, and involved all pressure values applied in the tightening pipe under these conditions. On the basis of results above obtained, 5 synthetical diagrams $v = f(p)$ were deduced. Fig. 6 and 7 show diagrams of time and rising velocity for a tank filled with water to H = 15 cm. and H = 20 cm. of depth.

These diagrams prove that when the time of tank rise increases, the pressure in the chamber required for the existence of the motion phenomenon decreases, and vice versa. Equation (4) leads to the same conclusion.

Diagrams showing the variations of air pressure, K, in the chamber required for different pressure values in the tightening pipe are drawn on Fig. 6-7. The lines obtained on these diagrams are generally parallel, this solution being in conformity with equation (1). These diagrams suggest that, as the pressure in the tightening pipe increases, a greater air pressure in the chamber might be necessary in order to raise the tank (eq. 4).

Fig. 8 shows the relation curves for $T_1 = f(p)$ and $v = f(p)$ plotted for different amounts of water in the tank. According to these curves, and to the equation (4) it is evident that a greater pressure is required for raising a heavier tank up within the same time.

In table 1 are collected the values of dimensionless parameters, k:c, resulting from the many computations arising from the different pressure, d, in the tightening pipe and for different weights of tank filled with water -c. According to the above mentioned table, a diagram was plotted (Fig. 9). It shows that as water pressure in the tightening pipe increases, the value of the dimensionless parameter, k:c, also increases; thus a higher air pressure might be applied in the chamber.

Fig. 9 shows an agreement between experimental records and an analytical solution expressed by equation (5). According to Fig. 5, it is evident that if the pressure in the tightening pipe decreases to zero, the value of the k:c ratio will be greater than one; the equation (5) implies the same solution. If in this equation (which is the straight line equation) an assumption is made that d = 0, the k:c ratio will become equal to the two remaining components, the last being equal to one.

TABLE 1.

Computation of the dimensionless parameters

N	Pressure d in the tightening m	Depth of water in the chest H cm	Pressure of the chest kg/cm^2	Air pressure in the chamber kg/cm^2	Dimensionless parameters k : c
1	0,5	10	0,0237	0,0312	1,32
2	0,5	15	0,0287	0,0383	1,33
3	0,5	20	0,0337	0,0469	1,39
4	0,5	25	0,0387	-	-
				The average	1,35
5	1,0	10	0,0237	0,0342	1,44
6	1,0	15	0,0287	0,0403	1,40
7	1,0	20	0,0337	0,0467	1,40
8	1,0	25	0,0387	0,0533	1,38
				The average	1,40
9	1,5	10	0,0237	0,0375	1,58
10	1,5	15	0,0287	0,0470	1,64
11	1,5	20	0,0337	0,0509	1,51
12	1,5	25	0,0387	0,0571	1,48
				The average	1,55
13	2,0	10	0,0237	0,0399	1,68
14	2,0	15	0,0287	0,0460	1,60
15	2,0	20	0,0337	0,0549	1,63
16	2,0	25	0,0387	-	-
				The average	1,64
17	3,0	10	0,0237	-	-
18	3,0	15	0,0287	-	-
19	3,0	20	0,0337	0,0620	1,83
20	3,0	25	0,0387	0,0780	2,01
				The average	1,92

5. CONCLUSIONS

As a conclusion to the analytical computations and the laboratory experiments performed on a model device utilizing the principle of a pneumatic chamber lock, the following remarks may be stated:

a) There is full agreement between the analytical solution and the laboratory model experimental results.
b) As the total tank rising time increases the compressed air pressure maintaining the movement decreases.
c) Tank rising velocity rises with an increase of air pressure in the chamber.
d) Increasing the water pressure in the tightening pipe, requires greater air pressure in the chamber in order to raise the tank at the same time.
e) Tank motion in the chamber remains smooth (without shocks), providing that the position of the mobile tank is absolutely horizontal.
f) As the tank rising in the chamber proceeds with a uniformly accelerated motion adequate braking should be applied.
g) Required tightness can be obtained at the confluence of water and compressed air.
h) Established formulas afford the possibility of the calculation of the required factors such as friction coefficient, compressed air pressure in the chamber lock in the initial and final motion periods, etc.
i) Because of the small model size, it was impossible to state the advantage of Tillinger's method, which proposes the solution of the tighting problem on the lower borders of an upside down turned tank. For the same reason we were not able to determine the condensed air losses in relation to the tonnage, time of sluicing and temperature of the environment.
j) It appears from what studies we have made, that the application of the pneumatic chamber locks is quite possible and economic. It is probable, however, that in practice, several difficulties will arise at the time when details of construction of such a sluice are being worked out.

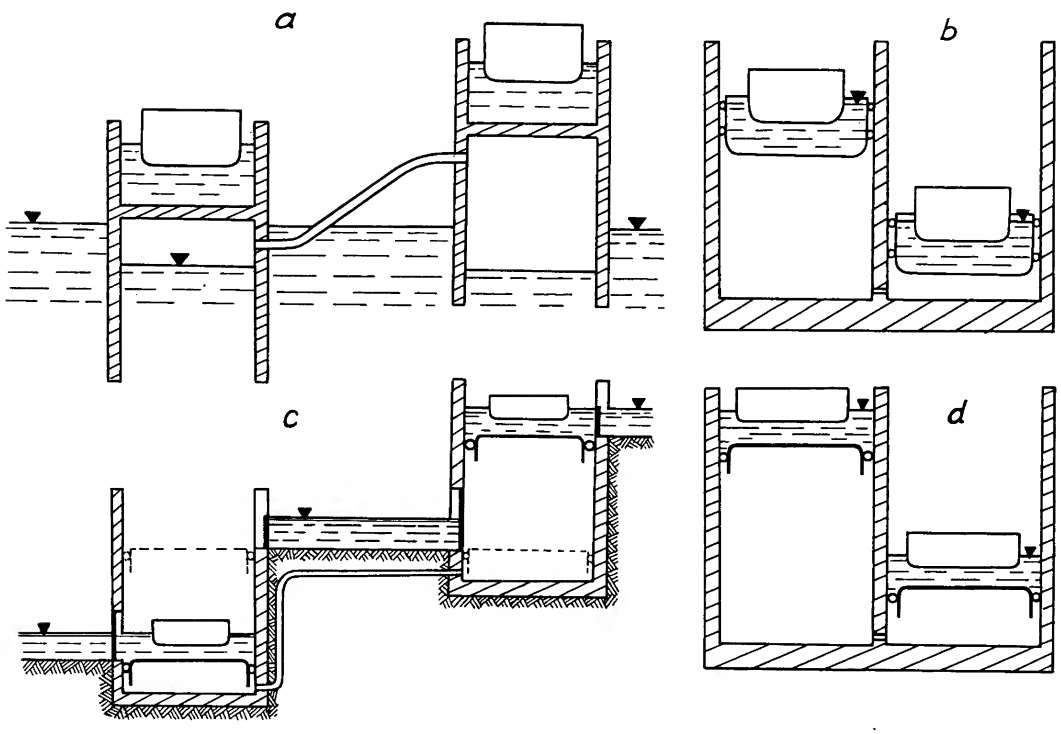

Figure 1 - Pneumatic chamber locks schemes.

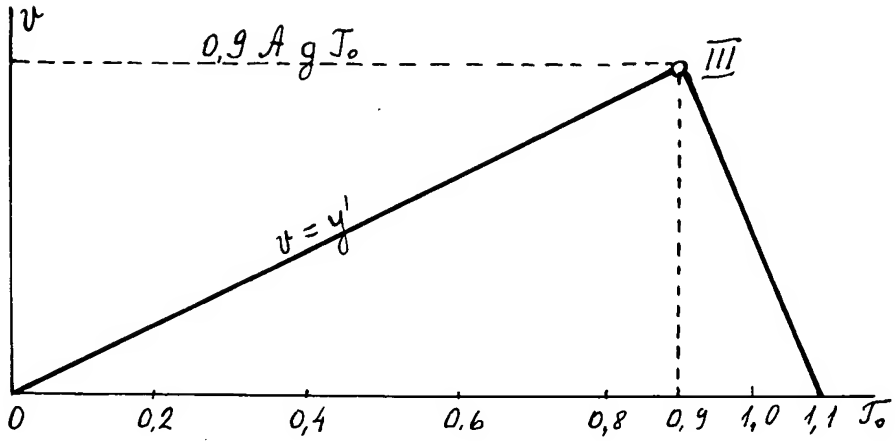

Figure 2 - The diagram of tank motion velocity.

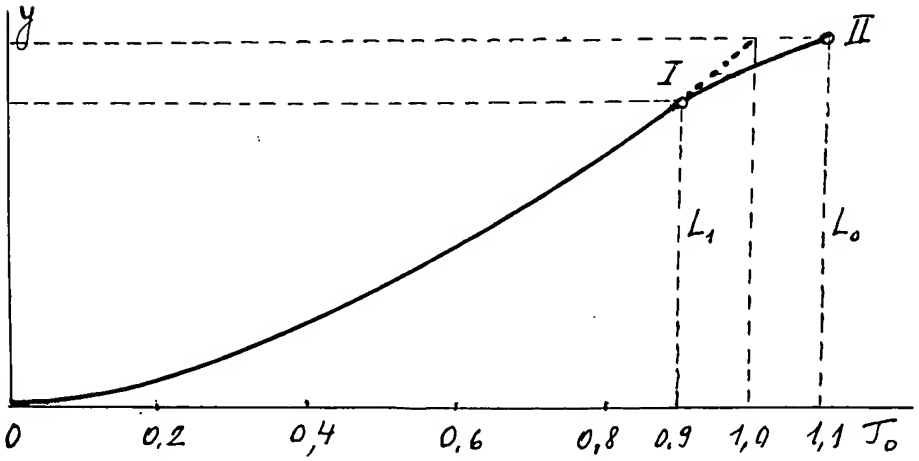

Figure 3 - The Diagram of Tank Stroke

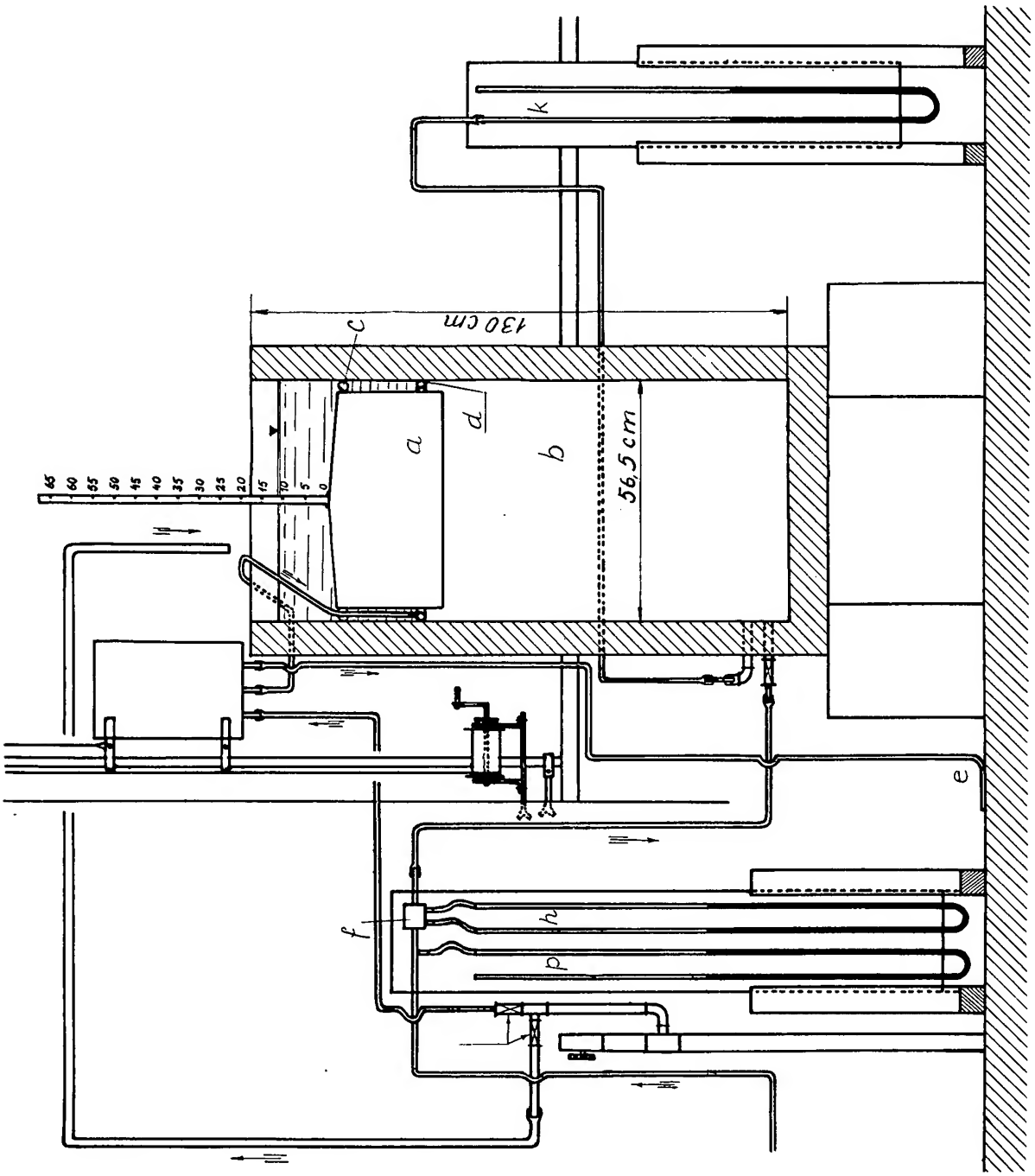

Figure 4 - The cross-section through the chamber and the tank, and the general appearance of the devices.

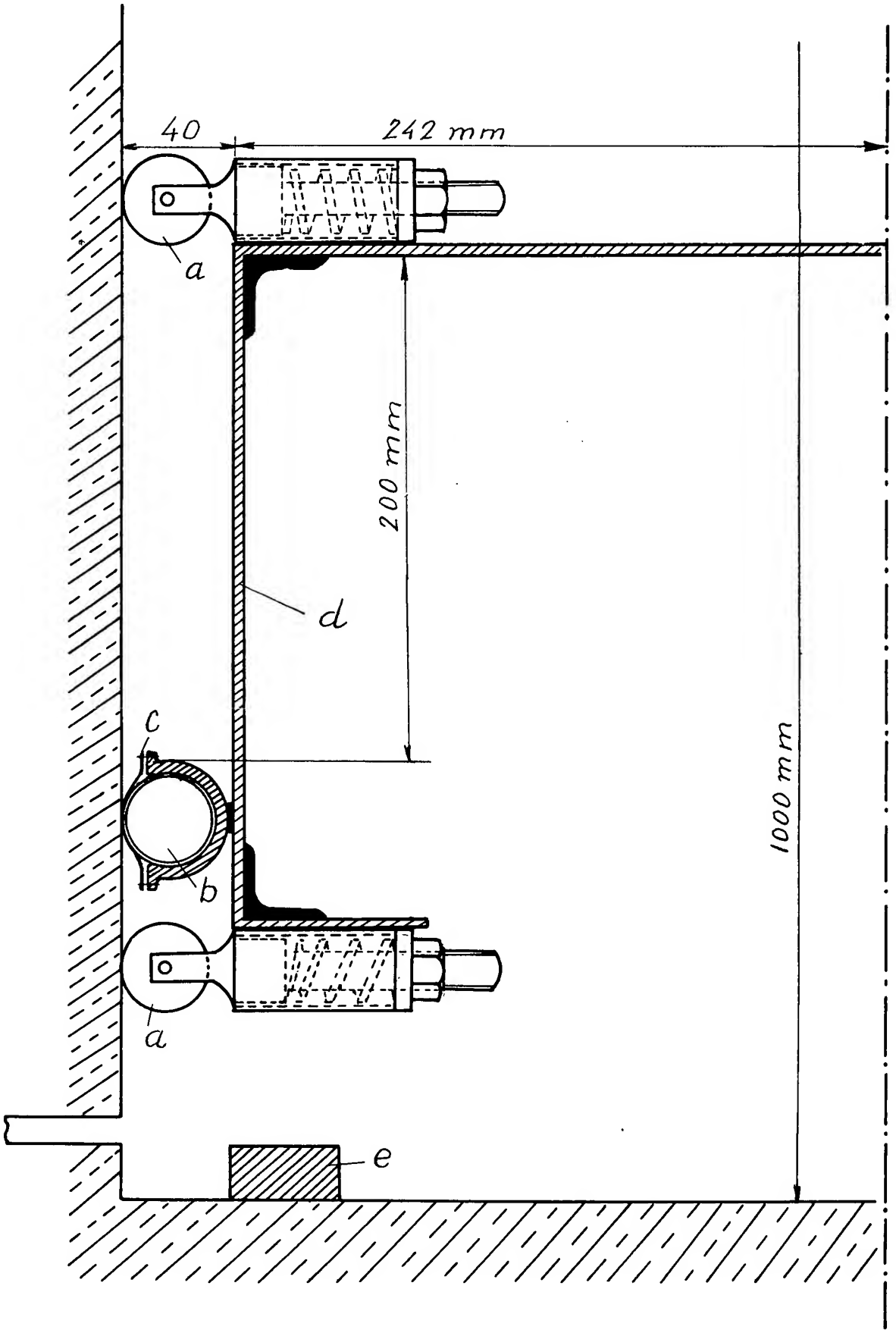

Figure 5 - The cheme of the tank construction in the chamber.

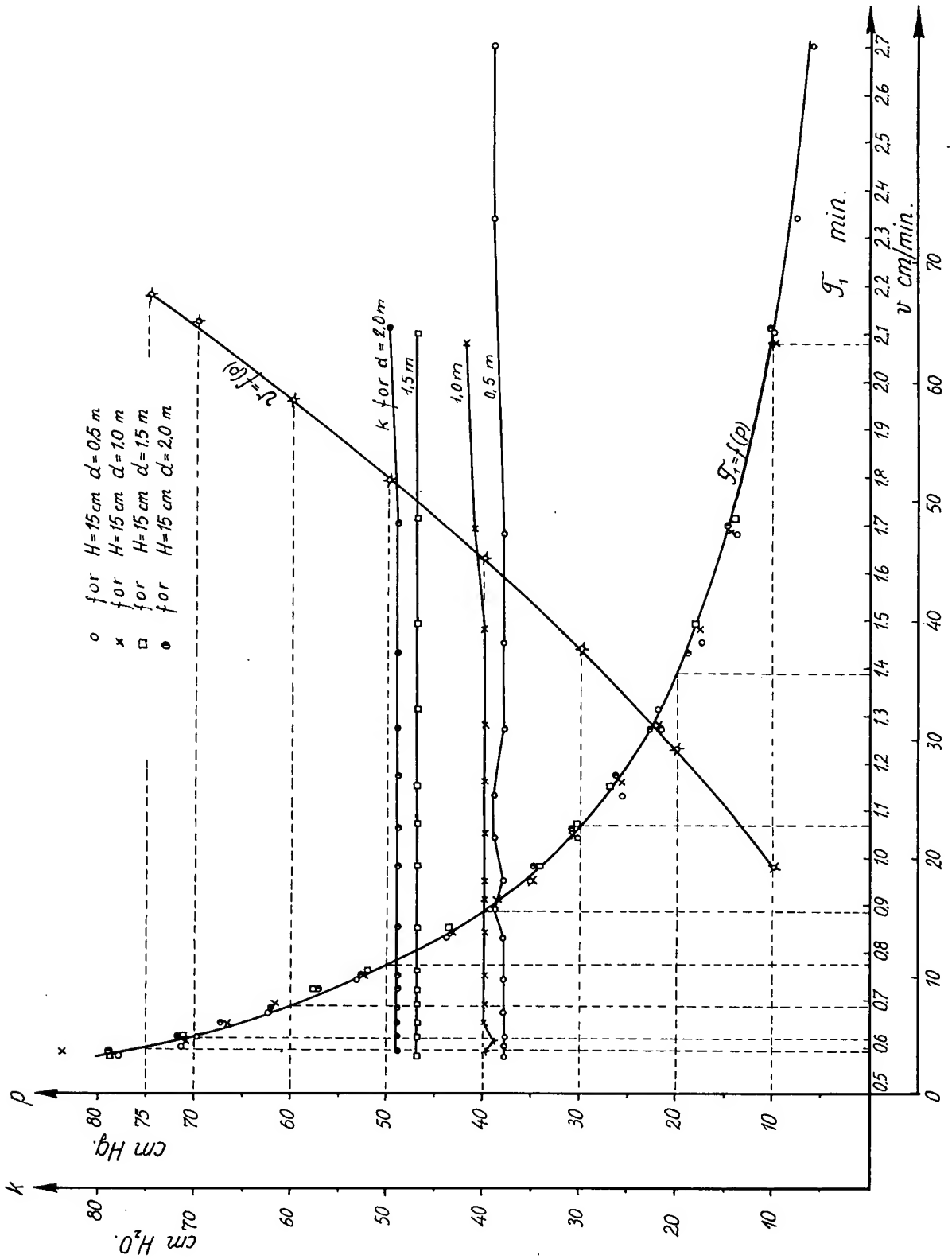

Figure 6 - Time and rising velocity diagrams for the tank filled. Water up to 15 cm. depth, when pressure d in tightening varies from 0.5 to 2.0 m of water column.

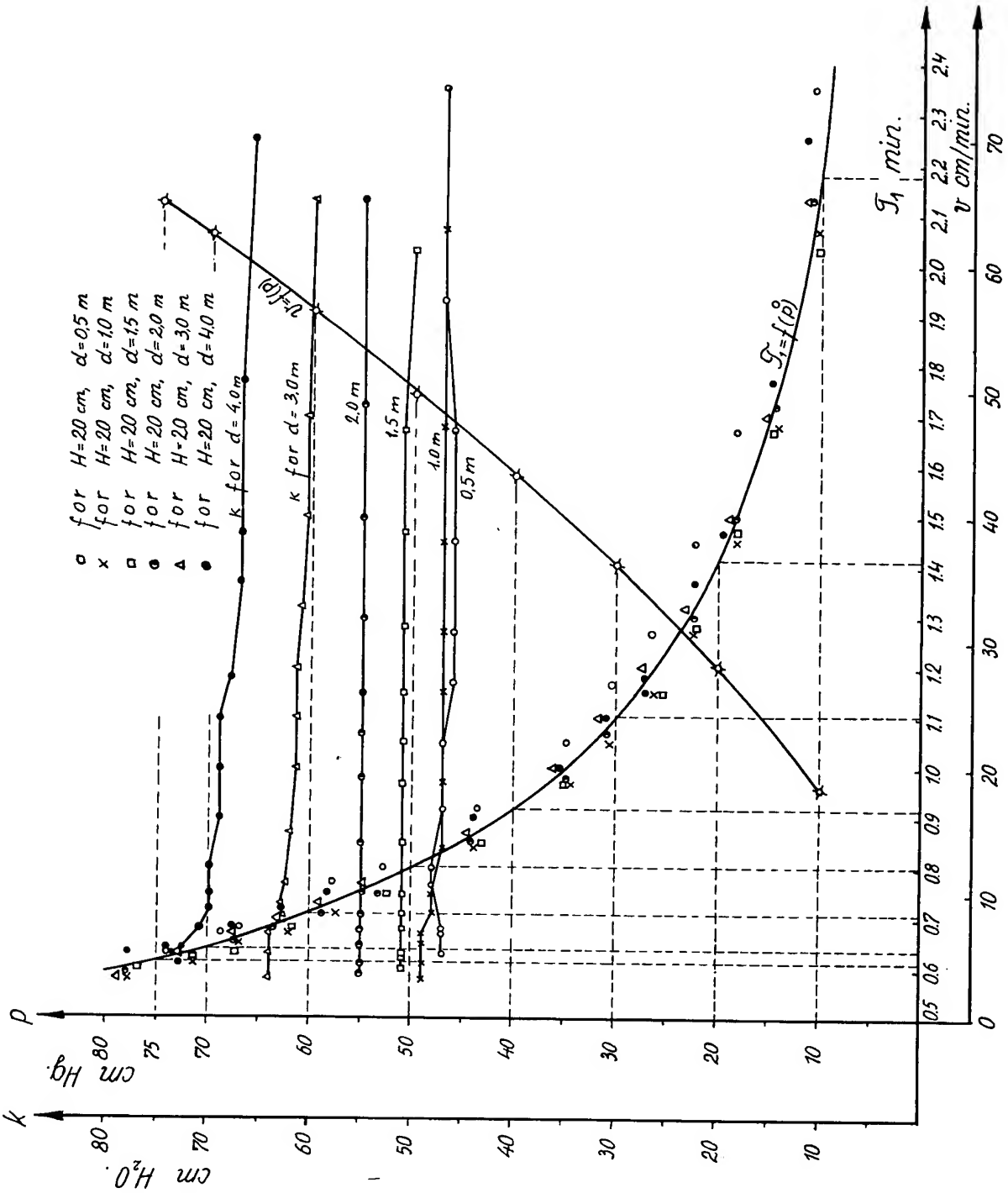

Figure 7 - Time and rising velocity diagrams for the tank filled. Water up to 20 cm. depth, when pressure d in tightening varies from 0.5 to 4.0 m. of water column.

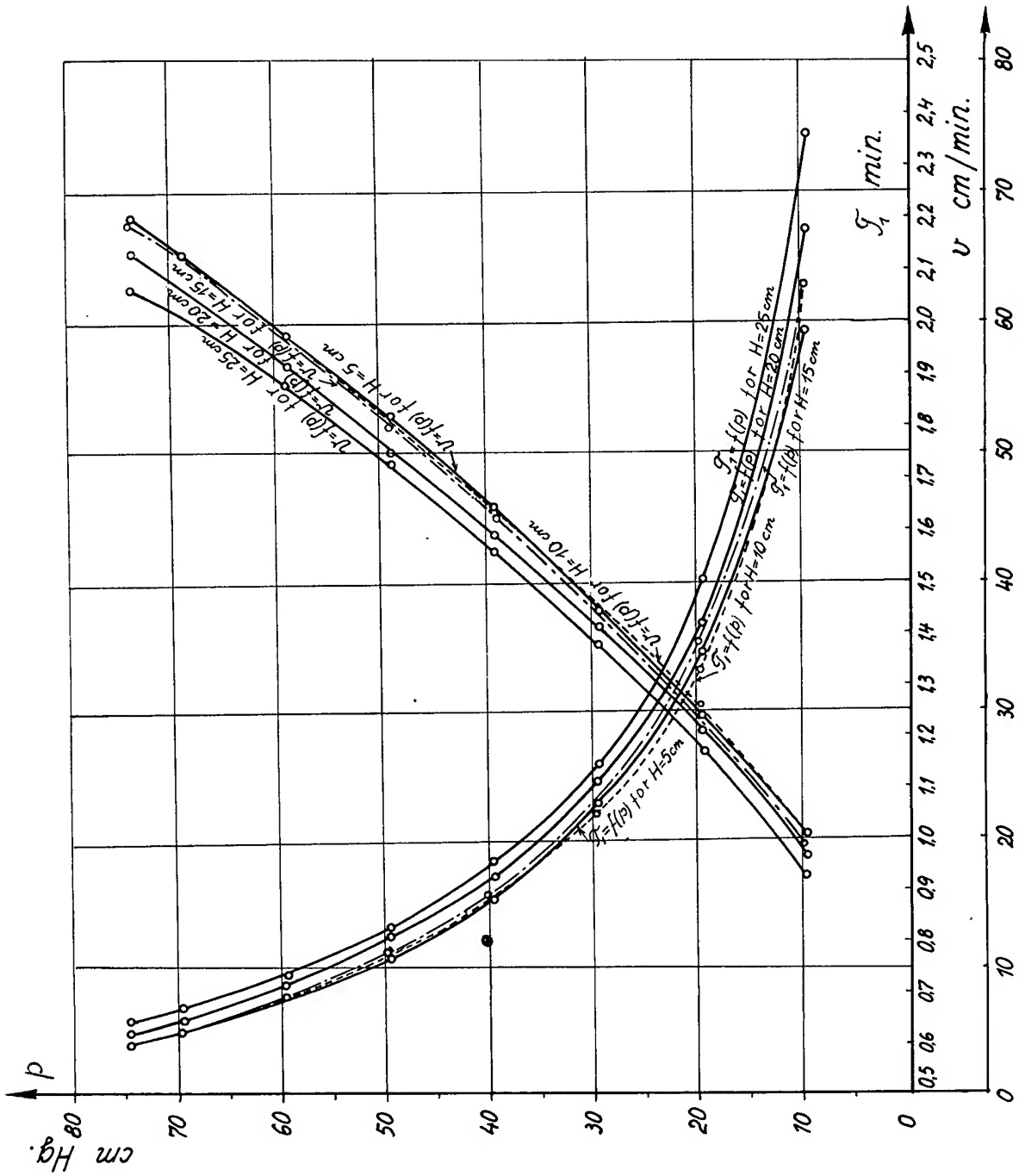

Figure 9 - The relation between pressure d in the tightening and the dimension less parameter.

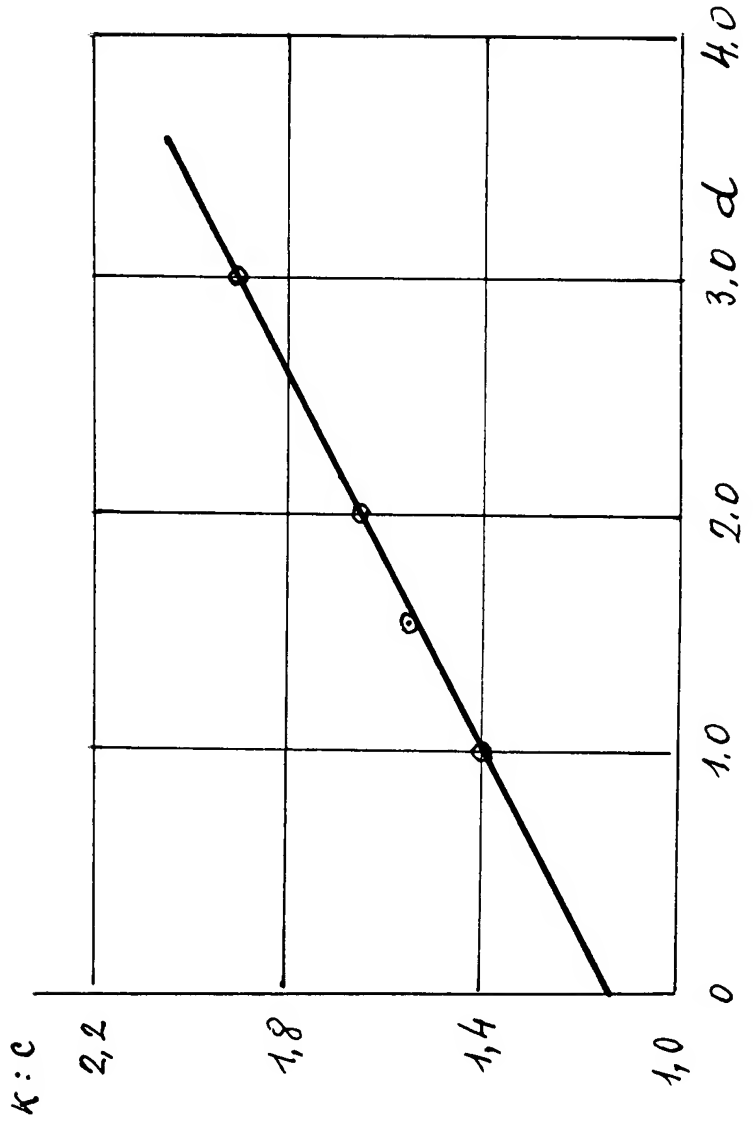

Figure 8 - The synthetical diagrams of time and tank rising velocity for different depths of water varying from 5 to 25 cm.

25X1

INVESTIGATIONS OF THE TOTAL PULSATING HYDRODYNAMIC LOAD ACTING ON BOTTOM OUTLET SLIDING GATES AND ITS SCALE MODELLING

* * *

A. S. ABELEV
Master of Science, Senior Research Engineer
of the All-Union Scientific Research Institute
of Hydrotechnics named for B. E. Vedeneyev

* * *

SUMMARY

The paper presents a brief description of laboratory investigations of the total hydrodynamic pulsating load on bottom outlet sliding gates. The problem of scale-modelling of this phenomenon is also considered.

The investigations showed that pulsations are unperiodical oscillations recorded as a number of positive and negative impulses different in form, value and duration. The oscillations are considerably dependent on head pressure and hydraulic conditions as well as on the vortex zone forming behind the gate. The value of maximum amplitude of the total hydrodynamic pulsating load pertaining to the average hydrodynamic loads can reach 55-60% and higher. For the investigated scheme of gate location the value of pulsation under study reached the highest magnitude with full gate opening ($n = 1.0$). When the lower edge of the gate is raised above the top of the conduit, i.e. when $n > 1.0$ the magni-

tude of pulsation first sharply increases reaching the maximum at n = 1.13 - 1.14, then gradually decreases and finally drops to zero at n = 1.35 - 1.40.

The paper presents the universal design diagrams for determination of the total hydrodynamic pulsating load.

Investigations of scale-modelling of the total hydrodynamic pulsating load upon sliding gates has been carried out on models built to different scales (the scale series). The investigations showed that the basic principles of this theory relative to the automodel region completely proved out. Within the range of Reynolds numbers adopted in the experiments with the three scale models ($2760 \leq Re_R \leq 80000$) in the case of transition from one model to another the absolute magnitude of the maximum amplitude of pulsation varies in proportion to the cube of linear scale coefficient while the dominant pulsation frequencies vary inversely proportional to the square root of the linear scale coefficient.

SOMMAIRE

Le présent rapport comporte une brève description des résultats des recherches expérimentales sur la charge de pulsation sommaire hydrodynamique sur les vannes à glissière de fond. Le problème des études sur les modèles est aussi traité.

Les recherches ont demontré que les pulsations étudiées représentent les oscillations désordonnées, enregistrées comme un nombre des impulsions positives et négatives, différentes en leurs formes, valeurs et durée.

Ces oscillations dépendent considérablement de la chute, ainsi que du régime hydraulique de comportement de l'ouvrage et de la position de zone tourbillonaire qui se forme derrière la vanne. En rapport aux charges hydrodynamiques moyennes la valeur de l'amplitude maximum de la charge de pulsation hydrodynamique sommaire sur les vannes à glissière peut atteindre 35-60% et même davantage. Pour le schème de la position de vanne

étudié le valeur de pulsation atteint son maximum à l'ouverture totale de la vanne (n = 1.0). Quand le bord inférieur de la vanne est monté au-dessus de la paroi supérieure de la conduite d'eau, c.-à.-d. quand n > 1.0, la valeur de pulsation au début s'accroît brusquement et au n = 1.13 - 1.14 atteint la grandeur maximale, après quoi elle commence à se reduire et au n = 1.35 - 1.40 elle baisse jusqu'à zéro.

Dans le rapport sont présentés les graphiques universels de calcul pour la détermination de pulsation de la charge sommaire hydrodynamique.

Les études sur modèles réduits de la charge sommaire hydrodynamique sur les vannes à glissière de fond ont été exécutées sur plusieurs modèles avec différentes échelles (la série d'échelles).

Les études ont prouvé que pour le phénomène étudié les principes fondamentaux de la théorie d'expérimentation sur les modèles concernant le domaine d'automodèle, sont entièrement confirmés. Dans les limites des valeurs des nombres de Reynolds existant dans les trois modèles de la série d'échelles ($2760 \leqslant Re_R \leqslant 80000$) en passant d'un modèle à l'autre, la valeur absolue de l'amplitude maximum de pulsation étudiée varie proportionnellement au cube du coefficient linéaire d'échelle, tandis que les fréquences de pulsation prédominantes varient en proportion inverse de la racine carrée du coefficient linéaire d'échelle.

1. INTRODUCTION

The experience gained from hydraulic structures now in service as well as the data obtained from model and field investigations show that gates are subject to a vibration which is due to the pulsation of hydrodynamic loads acting upon them.

Under conditions of ever increasing head pressures and diameters of outlets closed by gates, the problem of vibration appears to be of considerable importance.

However, up to the present moment, the state of development of theoretical and experimental research of gate vibration does not meet the requirements established by common practice of design

and operation of hydraulic structures. In this connection thorough and systematic studies of gate vibration and development of proper measures to prevent or eliminate this phenomenon are of great theoretical and practical interest.

2. ESSENCE OF THE PROBLEM IN QUESTION AND ITS PRESENTATION

As it has already been pointed out in our paper [1], gate vibration in field conditions is an extremely complicated phenomenon which, other factors being equal, depends, as to acting pulsating loads, upon the structure and rigidity of an oscillating system, supports and supporting parts as well as upon external and internal forces of non-elastic resistance.

Theoretical solution of the problem and reliable scale-modelling of the vibration phenomenon with observance of similarity of basic determining parameters is extremely difficult and apparently cannot be obtained practically.

Because of this, when studying the vibration phenomenon in laboratory conditions, the problem is divided in two stages:

a) experimental, comprising investigations of amplitude and pulsation frequency of total hydrodynamic load (exciting force) for different structures and different service conditions of deep gates;
b) theoretical, when main parameters characterizing gate vibration, based on the theory of induced oscillations, are established. Investigations of the exciting force may be carried out on oscillating as well as on fixed gate models.

The systematic investigations carried out at the All-Union Scientific Research Institute of Hydrotechnics since 1953 have been made on oscillating gate models suspended on strain gauges by using highly sensitive measuring apparatus.

This investigational work threw some light on the pulsation of the total hydrodynamic load acting on bottom outlet sliding gates and helped in studying the problem of scale-modelling.

---

1) A. S. Abelev, Basic Problems of Design and Research of Gate Vibration in Hydraulic Structures, Proc. of All-Union Scientific Research Inst. of Hydrotechnics named after B. E. Vedeneyev, vol. 54, 1955.

3. INVESTIGATION OF THE TOTAL PULSATING HYDRODYNAMIC LOAD ACTING ON BOTTOM OUTLET SLIDING GATES

The investigations were conducted on oscillating gate models by using the methods described in our papers [1], [2]. The gate models were suspended on six wire resistance strain gauges (Fig. 1), which enabled recording of the pulsation of the total hydrodynamic load acting on slide gates both in vertical (strain gauges I and II) and horizontal directions (strain gauges III, IV, V and VI).

The tests carried out showed that the pulsation of total hydrodynamic loads represented unperiodical oscillations as a number of positive and negative impulses different in form, value and duration (fig. 2).

The investigation was intended to determine the value of maximum pulsation amplitude P'_{max} of the total hydrodynamic load acting on gates, and the dominant most frequently repeated oscillation frequency of this load for various service conditions of the structure.

The value of the maximum pulsation amplitude P'_{max} was determined by photographic recording of oscillations as well as through visual observations of deflection of a light indicator on an oscillograph screen[3].

To determine the frequency range (spectrum) of recorded oscillations and the dominant frequencies, the experimental data were subjected to statistic analysis. According to the data obtained, curves were plotted of oscillation distribution in periods $\frac{m_T}{\sum m} = f(T)$ or in frequencies

$$\frac{m_N}{\sum m} = f(N)$$

Since the investigations were intended to determine the frequency of maximum pulsation, in the analysis of the experimental data, the oscillations with very small amplitudes were not taken into account and

---

1) See p. 4.

2) A.S. Abelev, Investigation of Total Hydrodynamic Pulsating Loads for Design of Vibration of Bottom Outlet Sliding Gates, Proc. of the All-Union Scientific Research Inst. of Hydrotechnics named after B.E. Vedeneyev, vol. 58, 1958.

3) While investigating pulsating loads, the readings of instruments corresponding to the average hydrodynamic loads were compensated by the electric method.

considered were only those oscillations, of which the amplitudes were not less than (0.5-0.3) $P'max$.

Such curves had a pronounced maximum and enabled to determine the magnitude of a dominant period T_d and its corresponding dominant frequency

$$N_d = \frac{1}{T_d} .$$

It is obvious that the longer the analysed oscillogram is, the more accurate the results obtained by such analysis will be. As a rule, in oscillation frequency tests, the length of each oscillogram was not less than 1500 mm. which corresponds to a filming period of not less than 30 seconds.

It should also be pointed out that the natural oscillation frequency of the system always exceeded considerably (several times) the maximum oscillation frequency and was quite sufficient for measurement of pulsations without introducing an error.

The investigations described below have been carried out with a sliding gate installed in the inlet section of a conduit as shown in fig. 3. The peculiar feature of this installation is that the gate is placed in grooves without any intake beam in front of it.

The gate model was provided with double sided skin plate and bottom seal. The latter was designed so that it did not prevent oscillations of the system[1].

Maximum head pressure upon the gate model above the bottom of the conduit was in the order of 150-155 cm.

The research has been conducted at various openings of the gate

$$n = \frac{a}{h}$$

The investigations showed that the value of maximum amplitude and pulsation frequency of the total hydrodynamic load depend, to a considerable extent, upon the hydraulic conditions in the conduit and location of the vortex zone forming behind the gate. A special series of experiments has been conducted to study this problem, the experiments having been carried out under the conditions of relatively small submerging of the top of the conduit at constant downstream water level (DWL),[2]

---

1) See p. 5, n. 2.

2) The downstream water level (DWL) in the present series of experiments has been determined at a considerable distance from the outlet section of the conduit behind the recovery area.

various gate openings, various upstreams water levels and various air discharges Q_2 behind the gate. The air discharge varied from $Q_2 = 0$ to $Q_2 \neq 0$ i. e. the value corresponding to the unlimited access of air into the conduit[1]. The results of the investigation enabled to outline three characteristic regions of hydraulic conditions in an operating conduit: the region of pressure conditions, with the hydraulic jump roller coming over the bottom edge of the gate, the region of transition condition, with the roller moving away from the gate but located inside the conduit, and finally, the region of pressureless condition, with the roller coming out of the conduit, to which air can get freely from the downstream side[2]. To explain this, fig. 4 shows the relation between the maximum amplitude of the total pulsating hydrodynamic load acting on a gate in the horizontal direction, and the varying upstream level (UWL). The variation of UWL determines the different hydraulic conditions of the operating structure. In these experiments, the DWL remained constant.

The experiments showed that, other factors being equal, the value of pulsating load under the pressure condition exceeds that of the pressureless condition, while the pulsation frequency increases as a rule in the course of transistion from the pressure condition to the pressureless one. In case of vacuum, air delivery behind the gate results in considerable changes of hydraulic conditions and in reduction of the pulsation amplitude of the total hydrodynamic load for all those cases when the conduit works under the pressure condition; if the conduit operates under pressureless conditions, free access of air below the gate determines the tendency towards a certain increase in pulsating loads. The experiments show that with a given gate opening and constant downstream water level, the value of maximum amplitude of the total hydrodynamic pulsating load is the greatest either on the boundary line between pressure and transition conditions (at heads lower than maximum) or at maximum head pressure in the region of pressureless condition (fig. 4).

In this connection, when estimating pulsating load and expected gate vibration, particular attention should be paid to the hydraulic condition of operating structure as well as to the value of acting head pressure; in certain cases an increase in effective head pressure results in changes in hydraulic condition, thus considerably reducing

---

1) Since aeration of the flow is not scaled up, it is obvious that, in the experiments with air discharge behind the gate, it is possible on the basis of model investigations to evaluate only the quantitative aspect of the problem - the influence of air discharge on pulsating load and expected vibration.

2) See p. 5, n. 2

the pulsating load and the possibility of development of dangerous vibration.

With respect to averaged hydrodynamic loads, the value of maximum pulsation amplitude of the total hydrodynamic load can reach 35-60% and higher. It should be kept in mind that for the design values of total pulsating loads, one should take account not of the amplitude value P'_{max} but of the corresponding deviation of hydrodynamic load from its total averaged value. However, since this deviation is not the same on either side and the location of the averaged load line is not known, the load, equal approximately to $\approx(0,65-0,75)\ P'_{max}$ may be assumed for a tentative design value. This, however, needs further verification.

The results obtained from these investigations have refuted the general opinion that vibration is most dangerous at partial gate openings, that is, with $0 < n < 1,0$ and becomes negligible when the gate is lifted up to the full height of the conduit, i.e. at $n = 1,0$. For the installation that has been tested by the author (fig. 3) with the gate located in the conduit inlet section and with the bottom seal provided, the value of maximum pulsation amplitude of total hydrodynamic load reaches the highest magnitude at full gate opening ($n = 1,0$).

When the bottom edge of the gate is raised above the conduit top, that is, with $n > 1,0$ the value of maximum pulsation amplitude of total hydrodynamic load first sharply goes up and with $n = 1,13-1,14$ increases, compared to $n = 1,0$, by 2,5 - 4 times, then starts decreasing and drops to zero at $n = 1,35-1,40$. A more detailed consideration of the problem was given in our paper [1]. This paper also gives recommendations to reduce pulsating loads at $n = 1,0$ and $n > 1,0$.

The next extensive cycle of experiments conducted by the author was aimed at establishing the criteria for determination of P'_{max} and N_d under different operating conditions of deep sliding gates.

As the above described experiments have shown, other factors as to the design and scheme of gate location within the conduit being equal, the unknown values P'_{max} and N_d depend to a considerable extent upon the hydraulic conditions of operating structure. In this connection, we adopted the following approach to the problem in question. The search for design criteria has been determined for a certain fixed hydraulic condition of the operating structure; then were determined the correction factors (condition coefficients) which enabled to evaluate pulsation loads for other hydraulic conditions of

---

1) See p. 5, n. 2.

the operating structure.

The pressure condition, i.e. such a condition in which the longitudinal boundaries of the flow represent rigid walls, was assumed as a characteristic hydraulic condition, for which the design relations were determined[1].

In the design charts for the determination of $P'max$ shown in figs. 5 and 6 the results obtained from investigations are presented in terms of dimensionless coordinates A and n the dimensionless parameter A being taken as equal to the following characteristic values:

$$A = \frac{P'max}{\gamma \omega H} \qquad (1)$$

where ω is the area to which the pulsating load is applied. It is evident that $\omega = b_1 h_1$ for the pulsating load acting in horizontal directions (see fig. 5) and $\omega = b_1 \delta$ for the pulsating load acting in vertical direction (see fig. 6).

It can easily be determined from equation (I) that dimensionless parameter A is the mean value of maximum strain of pulsating load $(p'max)_{mean} = \frac{P'max}{\omega}$ expressed by the corresponding liquid column $(h'_{pmax})_{mean} = \frac{(p'max)_{mean}}{\gamma}$ and related head pressure H, that is

$$A = \frac{(h'_{pmax})_{mean}}{H} = \frac{(p'max)_{mean}}{\gamma H} = \frac{P'max}{\gamma \omega H} \qquad (2)$$

The investigations showed that the relations $(P'max)_h = f(H)$ and $(P'max)_v = f(H)$ are the <u>linear</u> functions of H for all gate openings; in this connection, by introducing the dimensionless parameter A containing H in the denominator, it is possible to replace the design charts plotted for the determination of $(P'max)_h$ and $(P'max)_v$ by the two universal curves respectively

$$A_h = \frac{(P'max)_h}{\gamma b_1 h_1 H} = f(n) \quad \text{and} \quad A_v = \frac{(P'max)_v}{\gamma b_1 \delta H} = f(n)$$

(figs. 5 and 6).

In investigations of the bottom outlet gate position, knowing its dimensions h_1, b_1, δ and head pressure H we can determine, by using the above

---

1) In this series of experiments the downstream water level elevations were measured by the piezometer established in the outlet section of the conduit.

curves, the values of $(P'max)_h$ and $(P'max)_v$ for pressure condition of the operating structure at any gate openings $0 < n \leqslant 1,0$.

The experiments have shown that for pressure condition of the operating conduit the value of relative submergence of the conduit top from the downstream side does not influence the value of $P'max$ and the nature of oscillations under study.

A special series of experiments was aimed at studying the above-mentioned condition coefficients, that is, relative variation of the maximum hydrodynamic load for the case of transition from pressure condition, for which the design relations have been obtained (figs. 5 and 6), to other hydraulic conditions of operating structure.

The investigations have shown that for the most unsatisfactory hydraulic state within the range comprising the pressureless and pressure conditions the value $(P'max)_h$ can increase, in comparison with corresponding loads fixed for pressure condition, more than three times while $(P'max)_v$ increases more than twice.

At the same time in the case of transition from pressure condition to the pressureless one the values of $(P'max)_h$ can decrease almost four times and those of $(P'max)_v$ more than thrice. Thus, from the above it is possible to draw a very important practical conclusion to the following effect: to reduce pulsation loads and, therefore, possible vibration of a gate, efforts should be made to provide a pressureless condition for an operating structure. If it is not possible, measures should be taken to ensure a steady pressure condition. It is not recommended to operate structures under intermediate hydraulic conditions which cause a considerable increase in pulsation loads.

To conclude the paragraph it should be mentioned that the extensive experimental data, relative to the frequency characteristic of the phenomenon under investigation, require more accurate definition and additional analysis prior to publication.

4. SCALE-MODELLING OF THE TOTAL PULSATING HYDRODYNAMIC LOAD ACTING ON BOTTOM OUTLET SLIDING GATES

When studying total pulsating hydrodynamic load on oscillating gate models, the problem of scale-modelling of this phenomenon should be investigated. This would make it possible to examine the scale effect, that is, the distorting effect of small dimensions of the model, and to develop reliable formula for applying scale laws to the prototype.

In other words, the problem involves the examination of the theory of scale-modelling of this complicated phenomenon and the determination of the boundaries of the automodel region. This paper gives a description of investigations carried out by the author in 1955-1956, with regard to the problem of scale-modelling of maximum amplitudes and dominant frequencies of the total hydrodynamic pulsating load. It should be mentioned that this problem, as far as we know, had never been studied before either for the conditions of flow around the gates or for any other boundary layer conditions.

The papers published on the subject deal with the problem of scale-modelling of the pulsating pressure in separate points of a streamlined profile located on pressure gallery walls behind the gate[1] and on the dam's apron[2].

In the investigations described below the problem of scale-modelling of the total pulsating hydrodynamic load has been studied by carrying a special series of model experiments, the models being built to different scales (scale series).

The investigations were carried out on three geometrically similar models of slide gates made to scales 1, 1:1,5 and 1:3 which are further referred to as M_1, $M_{1/1,5}$ and $M_{1/3}$. The experiments were carried out for the pulsating load acting in horizontal direction with various openings of sliding gates installed in the inlet section of rectangular conduits according to the scheme, being as shown in fig. 7. In addition to the similarity of the gate models, there was ensured the complete geometrical similarity of acting pressures in headrace, of grooves, conduits and tailrace. The basic dimensions of the experimental installation shown in fig. 7 refer to the largest model made to scale M_1.

For the two remaining models the above mentioned basic dimensions of conduits, gates, heads etc. were reduced by 1,5 and 3 times respectively.

---

1) D.I. Kumin, N.A. Preobrazhensky and G.A. Yuditsky, Scale-Modelling of the Pulsating Pressure on Pressure Gallery Walls, Proceedings of the All-Union Scientific Research Institute of Hydrotechnics named after B.E. Vedeneyev, vol. 52, 1954.

2) M.S. Fomitchev, Studies of Scale-Modelling of the Pulsation and Hydrodynamic Pressure, USSR Academy of Science, Proceedings (Isvestiya AN USSR, OTN) Technological Series, No. 11, 1956.

The frequency of natural oscillation of the system for the three models of the scale series considerably (several times) exceeded the maximum frequency of oscillations under study and was quite sufficient for pulsation measurements without introducing an error. Investigations were conducted under pressure conditions without admitting air behind the gate.

1°. SCALE-MODELLING OF THE MAXIMUM AMPLITUDE OF THE TOTAL HYDRODYNAMIC LOAD. - To obtain reliable experimental data, testing of the three models was repeated for most of the gate openings and in some cases was carried out three to four times.

To investigate the problem of scale-modelling of the maximum pulsation amplitudes of total hydrodynamic load P'_{max} the experimental points, obtained for the three scale models, were plotted in the diagram (fig. 8) where the ordinates give n and the abscissas give the dimensionless numbers A, the values of the latter being computed by means of the formula (2) according to which for a load acting in horizontal directions A equals to

$$A = \frac{P'_{max}}{\gamma \omega H} = \frac{P'_{max}}{\gamma b_1 h_1 H} \qquad (3)$$

As can be seen from this diagram the experimental points of the three models of the scale series lie within a single curve with an acceptable degree of accuracy. As to the scatter of experimental points, it is not the result of systematic deviations due to the scale effect and can be entirely attributed to the measurement error lying within the limits of ± 15%.

The results obtained show that for the three models of the scale series

$$A = \text{idem} \qquad (4)$$

Equation (4) shows that the phenomenon under study for the three models is taking place in the automodel region.

It should be pointed out that since the gravity effect of liquid in pressure condition is negligible while it is nil in horizontal conduit, similarity of the phenomena in this case is determined, as is known, by the identity clause of Reynolds criterion, conformance to which ensures identity of the values of Euler criterion connecting pressures and velocities in similar flows.

Since the turbulent disturbances in the flow under consideration developing in the zone of gate location and causing hydrodynamic pulsating load

are large in magnitude and intensity, the automodel region, that is, the zone of quadratic resistance, within which similarity is taking place despite nonconformance, the identity clauses of Reynolds criterion, is accomplished with relatively small numbers Re.

To confirm the aforesaid and establish the boundaries of the automodel region, fig. 9 gives the relations $A = f(Re_R, n)$. The diagram (fig. 9) is plotted by using the experimental data obtained on the three scale models for various n adopted as a parameter. The numbers have been computed by means of the formula

$$Re_R = \frac{v\ R}{\nu}$$

The analysis of the data given in fig. 9 shows that within the range of Reynolds numbers in the experiments for the three models of the scale series ($2760 \leq Re_R \leq 80000$) the value of the dimensionless parameter:

$A = \frac{P'max}{\gamma b_1 h_1 H}$ practically does not depend upon Re, which corresponds to the automodel region. In this connection the pulsation similarity determined for the three models with respect to their maximum magnitudes and dominant frequencies (see parag. 4, 2°), is found out with relatively small values of Re. This enables us to draw an important practical conclusion that the investigations involving studies of the total pulsating hydrodynamic load acting on sliding gates can be conducted on models of relatively small scale.

Proceeding from equation (4) and denoting all the components of equation (3) by index "f" for the larger model and by index "m" for the smaller model we can write

$$\frac{(P'max)_f}{\gamma_f b_{1f} h_{1f} H_f} = \frac{(P'max)_m}{\gamma_m b_{1m} h_{1m} H_m} = A = idem$$

Since density of liquid is considered to be constant and thus $\gamma_f = \gamma_m$ it is not difficult to obtain from equation (3) the following expression for the ratios of the maximum amplitudes of total pulsating hydrodynamic load in the case of transition from one scale model to the other

$$\frac{(P'max)_f}{(P'max)_m} = \alpha_{P'max} = \frac{b_{1f} h_{1f} H_f}{b_{1m} h_{1m} H_m} = \alpha_e^3 \qquad (6)$$

therefore

$$\alpha_{P'max} = \alpha_e^3 \qquad (7)$$

Then

$$(P'max)_f = (P'max)_m \alpha_e^3 \qquad (8)$$

The result obtained shows that with respect to the maximum amplitudes of the phenomenon under investigation, the general principles of the

scale-modelling theory relative to the automodel region are completely proved. Within the range of the Reynolds numbers used in tests on the three models of the scale series ($2760 \leq Re_R \leq 80000$) in the case of transition from one model to the other the absolute value of the maximum amplitude of total pulsating hydrodynamic load acting on deep sliding gates varies in proportion to the cube of the linear scale coefficient and, thus, the scale effect for relative values of the amplitude may be considered as being equal to zero.

Let us compare now the results obtained with respect to the scale coefficient $\alpha_{P'max}$ for maximum amplitudes of total pulsating hydrodynamic load, with the data of corresponding investigations intended to study the problem of scale-modelling of the pulsating hydrodynamic pressure in separate points of a streamlined profile[1), 2)]. From equation (7), we obtain

$$\alpha_{P'max} = \alpha_e^3$$

if we go now from P'_{max} to corresponding average stresses of pulsating load $(P'_{max})_{mean} = \frac{P'_{max}}{\omega}$ the scale coefficient $\alpha_{(P'max)mean}$ for the above stresses will be apparently equal to:

$$\alpha_{(p'max)mean} = \frac{\alpha_{P'max}}{\alpha_\omega} = \frac{\alpha_e^3}{\alpha_e^2} = \alpha_e \qquad (9)$$

which is in full agreement with the results obtained from the investigations of scale-modelling of the hydrodynamic pulsating pressure in separate points of a streamlined profile placed in the flow region with intensive turbulent mxing[1), 2)].

2°. SCALE-MODELLING OF THE TOTAL PULSATING HYDRODYNAMIC LOAD BY FREQUENCY. - In test of scale series was also investigated the problem of scale-modelling of the total pulsating hydrodynamic load by frequency. To this end the pulsations were recorded on film and the curves of oscillation distribution by pulsation impulses in periods or in frequencies have been plotted on the basis of statistical analysis of oscilligrams as described above (see 3). To obtain the reliable research data, pulsation recording in each experiment has been repeated not less than three times.

Fig. 10 presents some of the results obtained from the statistical analysis of the oscillograms recorded for the three models by measuring cell $\overline{V}$ at $n = 0,2$. The curves of oscillation distribution in periods

1) See p. 11, n. 1.

2) See p. 11, n. 2.

$\frac{m_T}{\sum m} = f(T)$ presented in this fig. show that the maximums of the above curves are shifted in the direction of larger periods with increasing scale of the model and thus the dominant frequencies of oscillations under study $N_d = \frac{1}{T_d}$ are reduced respectively. Such curves plotted for all experiments enabled to determine regularity in variation of the characteristic frequencies depending on model scale.

It should be pointed out that the condition of pulsation similarity according to frequency is determined, as is known, by the identity of the criterion of homochronism which is also called the Strouhal number. According to this, the further analysis of the experimental data consists in determining the Strouhal number for all scale series experiments. Comparison of different Strouhal numbers for models made to different scales enable to establish similarity of total pulsating hydrodynamic load by frequency and determine the scale coefficient for the dominant frequencies.

The Strouhal number has been determined by using the equation

$$Sh = \frac{N_d h}{v_1} \qquad (10)$$

in which the height of the conduit "h" was adopted for the characteristic linear dimension of pressure flow[1].

The dominant frequencies and the corresponding Strouhal numbers for the total pulsating hydrodynamic load applied to the upper and lower parts of the gate were determined by strain gauges III (or IV) and V (or VI) respectively[2].

The Strouhal numbers computed for pulsations are plotted in diagram shown in fig. 11 where the abscissas give the Strouhal numbers and the ordinates give "n".

As the diagram shows, all experimental points corresponding to pulsations, recorded by strain gauges III (or IV) irrespective of the model scale, lie within a single curve with an acceptable degree of accuracy

---

1) It is known that in kinematically similar flows the scale of turbulence which influences the frequency of pulsation under study is proportionate to the linear dimensions of the flow.

2) The symmetrically located strain gauges III and IV gave absolutely identical pulsation recordings. The same can be said about symmetrically located strain gauges V and VI.

while the points corresponding to pulsations recorded by strain gauges V (or VI) lie within the other curve. As to some scatter of the experimental points, this, as the diagram (fig. 11) shows, resulted not from the systematic deviations due to the scale-effect but from the measuring error lying within the limits of ± 15%.

The result obtained shows that the Strouhal numbers for all three scale models may be assumed as being constant

$$Sh = idem \qquad (11)$$

On these grounds we could admit that the phenomenon in question for all three models is taking place in the automodel region. To confirm this and to determine the boundaries of the automodel region figs. 12 and 13 give relations $Sh = f(Re_R, n)$ for pulsations recorded by strain gauges III (or IV) and strain gauges V (or VI).

The above relationships have been plotted according to the experimental data obtained for the three scale models with various n taken as a parameter.

It can be seen from the above diagrams (figs. 12 and 13) that within the range of Reynolds numbers adopted in the experiments for the three scale models ($2760 \leq Re_R \leq 80000$)[1] the Strouhal numbers are practically independent of Re_R which corresponds to the automodel region.

Proceeding from equation (11) and denoting the components of equation (10) by the index "f" for the larger model and by the index "m" those for the smaller model, we can write the following:

$$\frac{N_{d.f}\, h_f}{v_{1f}} = \frac{N_{d.m}\, h_m}{v_{1m}} = Sh = idem \qquad (12)$$

Then it is not difficult to obtain the relation of the dominant frequencies of total hydrodynamic pulsating load in the case of transition from one model to the other:

$$\frac{N_{d.f}}{N_{d.m}} = \alpha_{N_d} = \frac{v_{1f}}{v_{1m}} \cdot \frac{h_m}{h_f} \qquad (13)$$

Since the pressure conduits in scale models connect the two open water

---

1) The values of Re_R have been computed as explained above, see page 13.

levels, the elevations of which were predetermined as being proportionate to the linear dimensions of the conduits, and the discharge coefficients of the conduits, as it follows from the experimental data, practically did not depend upon Re_R, then as is known, in the case of transition from one model to another we have

$$\frac{v_{1f}}{v_{1m}} = \alpha_v = \alpha_e^{\frac{1}{2}} \tag{14}$$

Further, if we take into consideration that

$$\frac{h_m}{h_f} = \frac{1}{\alpha_e} \tag{15}$$

and substitute equations (14) and (15) for equation (13), we obtain

$$\alpha_{Nd} = \alpha_e^{-\frac{1}{2}} \tag{16}$$

In compliance with this we have

$$N_{d.f} = \frac{N_{d.m}}{\sqrt{\alpha_e}} \tag{17}$$

The result obtained shows that, as to the frequency characteristics of the phenomenon in question, the basic principles of the scale-modelling theory relative to the automodel region proved out with sufficient degree of accuracy.

Within the range of Reynolds numbers adopted in the experiments for the three scale models ($2760 \leqslant Re_R \leqslant 80000$) in the case of transition from one model to the other the dominant frequency of the total pulsating hydrodynamic load upon sliding flat gates varies inversely proportional to the square root of the linear scale coefficient and thus the scale effect for relative values of frequencies is equal to zero.

It must be noted that a similar result has been obtained in the investigations mentioned above[1), 2)] when studying the scale laws for the characteristic frequencies of hydrodynamic pressure pulsation in separate points of a streamlined profile in flow regions with intensive turbulent mixing.

---

1) See p. 11, n. 1.

2) See p. 11, n. 2.

3°. Some additional investigations and conclusions. The additional investigations showed that the above scaling-up formulas for the total hydrodynamic pulsating load obtained under pressure condition and expressing the scale laws of the phenomenon under study are true not only for pressure conditions but can apparently be used in the case of pressureless and intermediate conditions.

It follows from the above data that scale-modelling of the total hydrodynamic pulsating load on bottom outlet sliding gates and hydrodynamic pulsating pressure in separate points of a streamlined profile placed in flow regions with intensive turbulent mixing are dependent on Froude's law of gravitation similarity. The scale laws of pressure pulsation in separate points which are in good agreement with model results were proved out by the corresponding field investigations[1]. This suggests that the scale laws of pulsation of the total hydrodynamic load, proved out by testing the scale model series, could be applied to the prototype with sufficient degree of accuracy.

5. GENERAL CONCLUSIONS

The problem of the total hydrodynamic pulsating load on bottom outlet sliding gates and scale-modelling of this phenomenon has been for the first time studied in the investigational work carried out by the writer.

The results obtained enable us to draw a number of important conclusions and generalisations which are of interest both from the viewpoint of finding out some common regularities of the phenomenon under investigation and with respect to their practical application in the design practice to evaluate the dynamic loads and expected vibrations. The investigations did not expose any particular circumstances which would prevent the use of sliding gates for operation under high head pressure both at full or partial openings. Taking account of the acting averaged and pulsating loads as well as of the above remarks, the sliding gates can be designed for high head pressure and will offer reliable service, provided they are properly made. At the present moment similar investigations with other schemes of location of sliding gates have been completed and investigations of tainter and throttle type gates are under way.

---

1) See p. 11, n. 2.

LIST OF SYMBOLS

A - is a dimensionless parameter

a - denotes height of gate lifting above the bottom of the conduit

b - denotes width of the conduit

b_1 - " part of gate to which load is applied

H - " $\nabla UWL - \nabla DWL$ - acting head pressure

h - " height of the conduit

h_1 - " working height of the gate

h'_p - " excessive piezometric height

M - " scale of the model

m_T - " number of pulsating impulses of equal duration or equal period

m_N - " number of pulsating impulses of equal frequencies

Σm - " summation of impulses considered in frequency analysis of oscillograms

N [1] - " pulsating frequency

N_d - " dominant pulsating frequency

$n = \frac{a}{h}$ - " relative gate opening

---

1) In our preceding papers the pulsating frequency was denoted by symbol ν which, however, appeared to be inconvenient since it is known that in hydraulics and hydromechanics this symbol denotes generally the kinematic viscosity. That is why from now and on we shall denote the pulsating frequency by symbol N .

$P'_{max} = P_{max} - P_{min}$ - denotes maximum amplitude of total pulsating hydrodynamic loads

P_{max} and P_{min} - " averaged total hydrodynamic loads, acting on the gate in different periods of time

$(P'_{max})_{III+IV}$ and $(P'_{max})_{IV+VI}$ - " maximum pulsation amplitudes of total hydrodynamic load acting in horizontal direction upon the upper lower parts of the gate

$(P'_{max})_h$ and $(P'_{max})_v$ - " maximum amplitudes of total pulsating hydrodynamic load acting on the gate in horizontal and vertical directions respectively

$(P'_{max})_{mean} = \frac{P'_{max}}{\omega}$ - " mean value of maximum strain of pulsating load

Q_1 - " flow discharge

Q_2 - " air discharge behind the gate

R - is hydraulic radius

$Re_R = \frac{\upsilon R}{\nu}$ - " Reynolds number

Sh - " Strouhal number

T - " duration or period of pulsating impulse

T_d - " dominant pulsating period

υ - " mean flow velocity in conduit behind the point where the jet is widening

υ_1 - " mean flow velocity in section I-I under the gate, jet compression being ignored (see fig. 11)

α_e - " linear scale efficiency

α_{Nd} - denotes scale efficiency of dominant pulsating frequencies of total hydraulic load

$\alpha_{P'max}$ - " scale efficiency of maximum amplitudes of total pulsating hydrodynamic load

$\alpha_{(P'max)mean}$ - " scale efficiency of average values of strain of pulsating load

α_v - " scale efficiency of velocity

α_ω - " scale efficiency of area

γ - " volume weight of water

δ - " thickness of the gate

ν - " kinematic viscosity

ω - " area

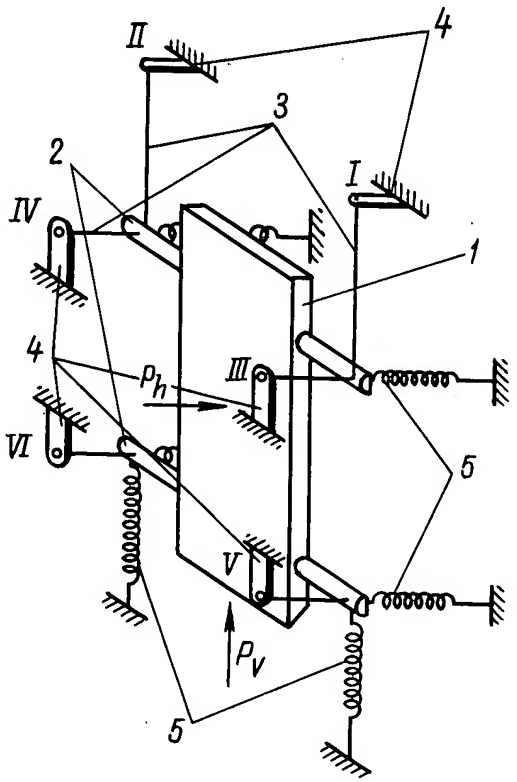

Figure No. 1

Schema of an oscillating model of the sliding gate. 1 - gate; 2 - rods; 3 - strings; 4 - cantilever beams for the wire resistance strain gauges; 5 - tension springs; P_h and P_v hydrodynamic loads acting upon the gate in horizontal and vertical directions.

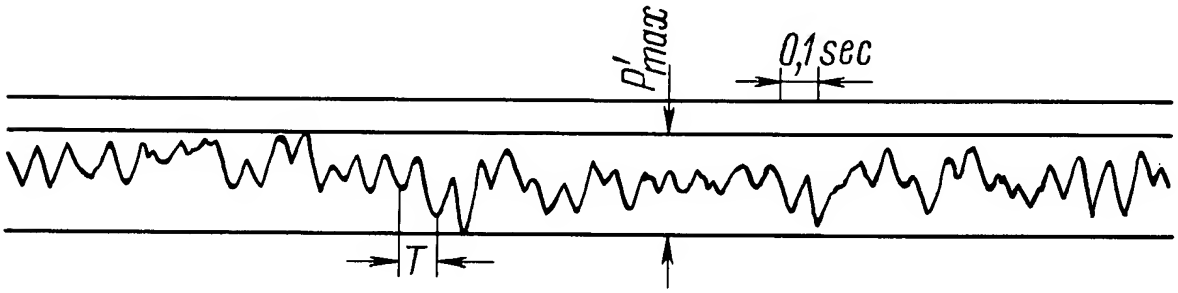

Figure No. 2

A typical recording of total hydrodynamic pulsating load.

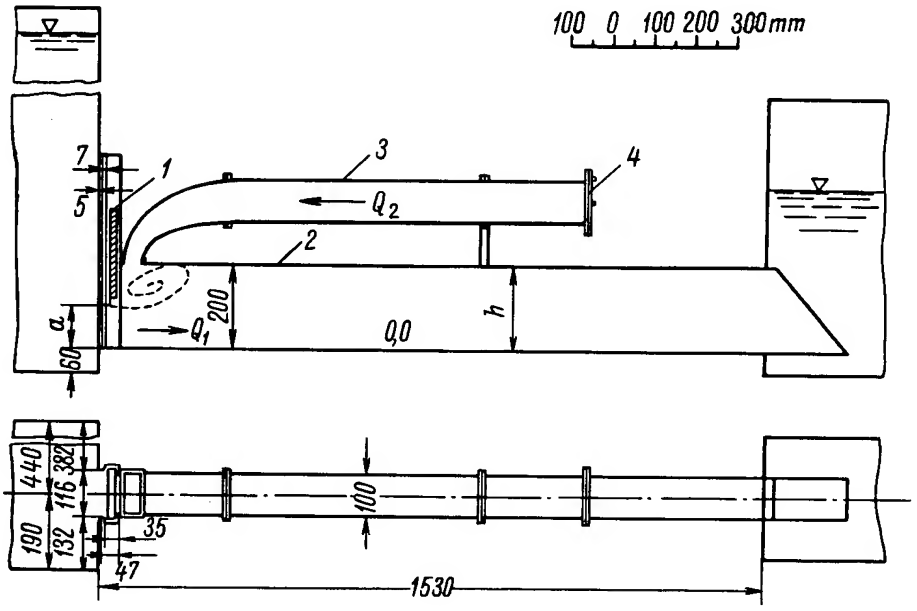

Figure No. 3

Plan and longitudinal section of the experimental installation. 1 - gate; 2 - conduit; 3 - aeration tube; 4 - diaphragm for measurement of air discharge.

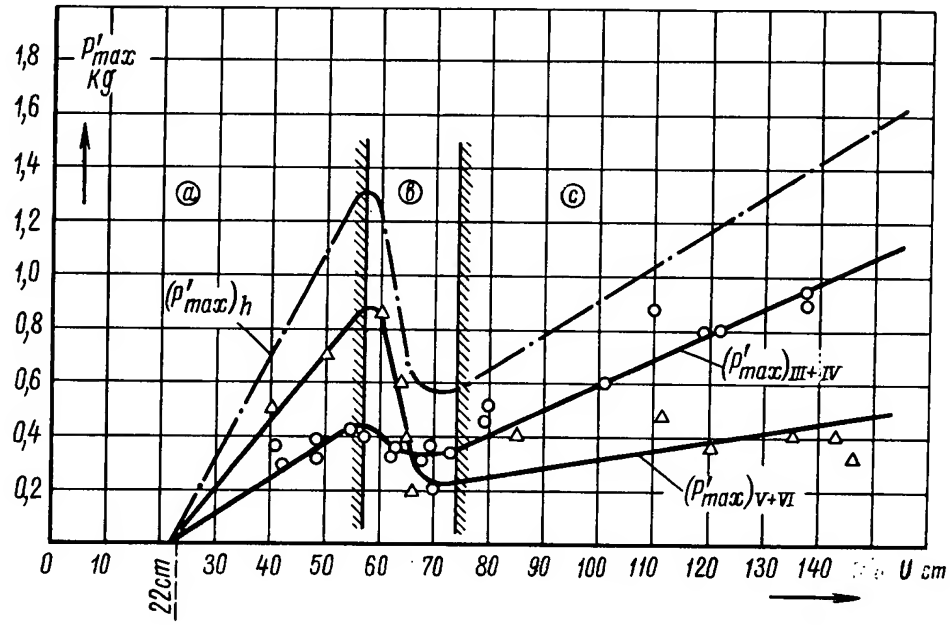

Figure No. 4

Relations $(\bar{P}'_{max})_{\overline{III}+\overline{IV}} = f(u)$, $(\bar{P}'_{max})_{\overline{V}+\overline{VI}} = f(u)$ and $(\bar{P}'_{max})_h = f(u)$ at downstream water level 22.0 cm; $n = 0.2$; $Q_2 \neq 0$; u upstream water level; ⓐ - region of pressure condition; ⓑ region of transitional regime; ⓒ - region of pressureless regime.

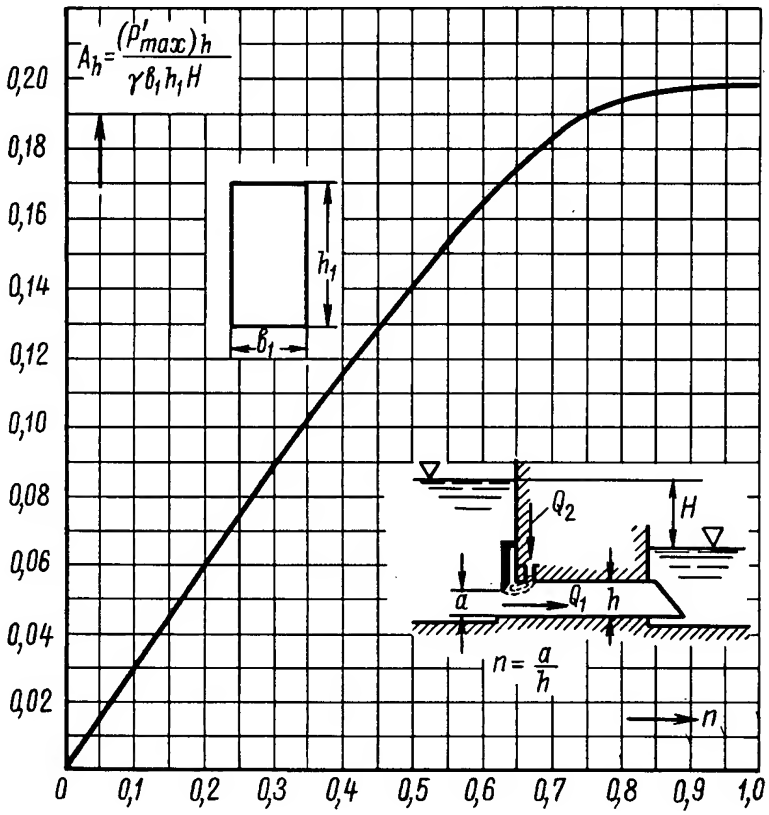

Figure No. 5

Universal design relation $A_h = f(n)$ for pressure condition of operating structure.

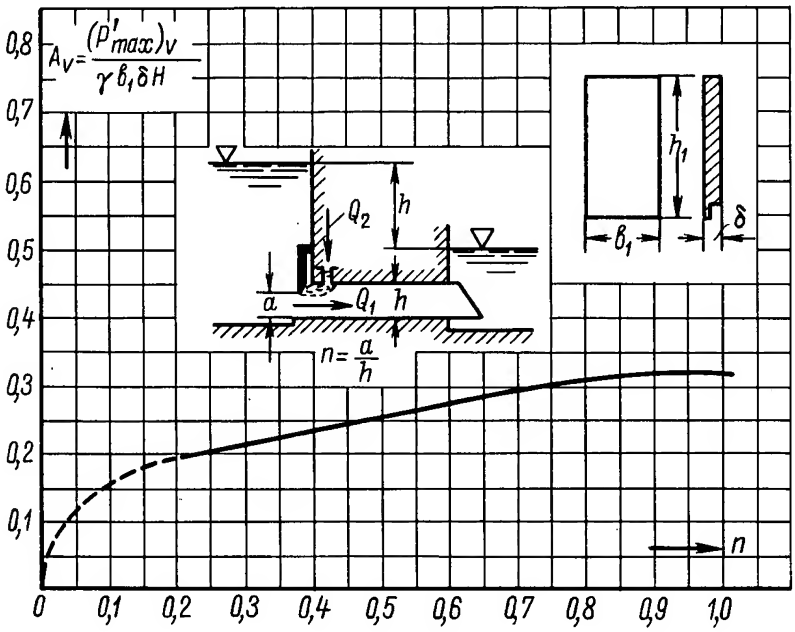

Figure No. 6

Universal design relation $A_V = f(n)$ for pressure condition of operating structure.

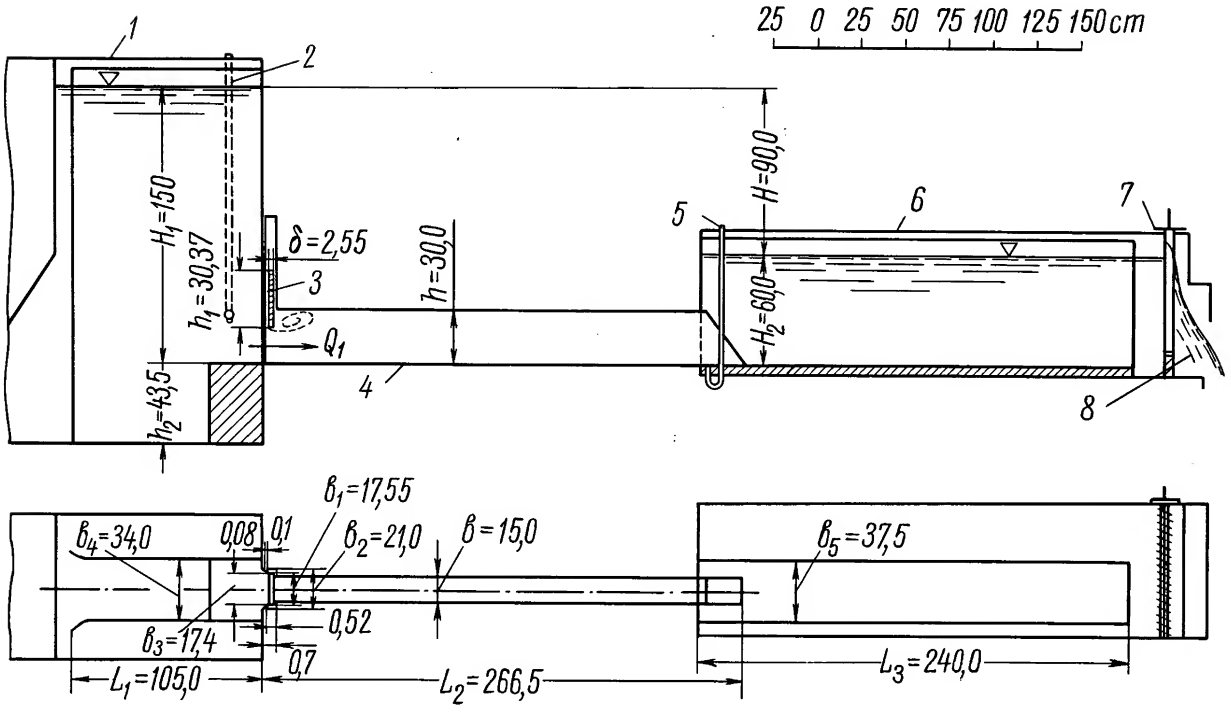

Figure No. 7

Plan and longitudinal section of a scale series experimental installation. Model made to scale M_1. 1 - pressure tank; 2 - gauge glass; 3 - gate; 4 - conduit; 5 - piezometer; 6 - tail race flume; 7 - shutter; 8 - discharge.

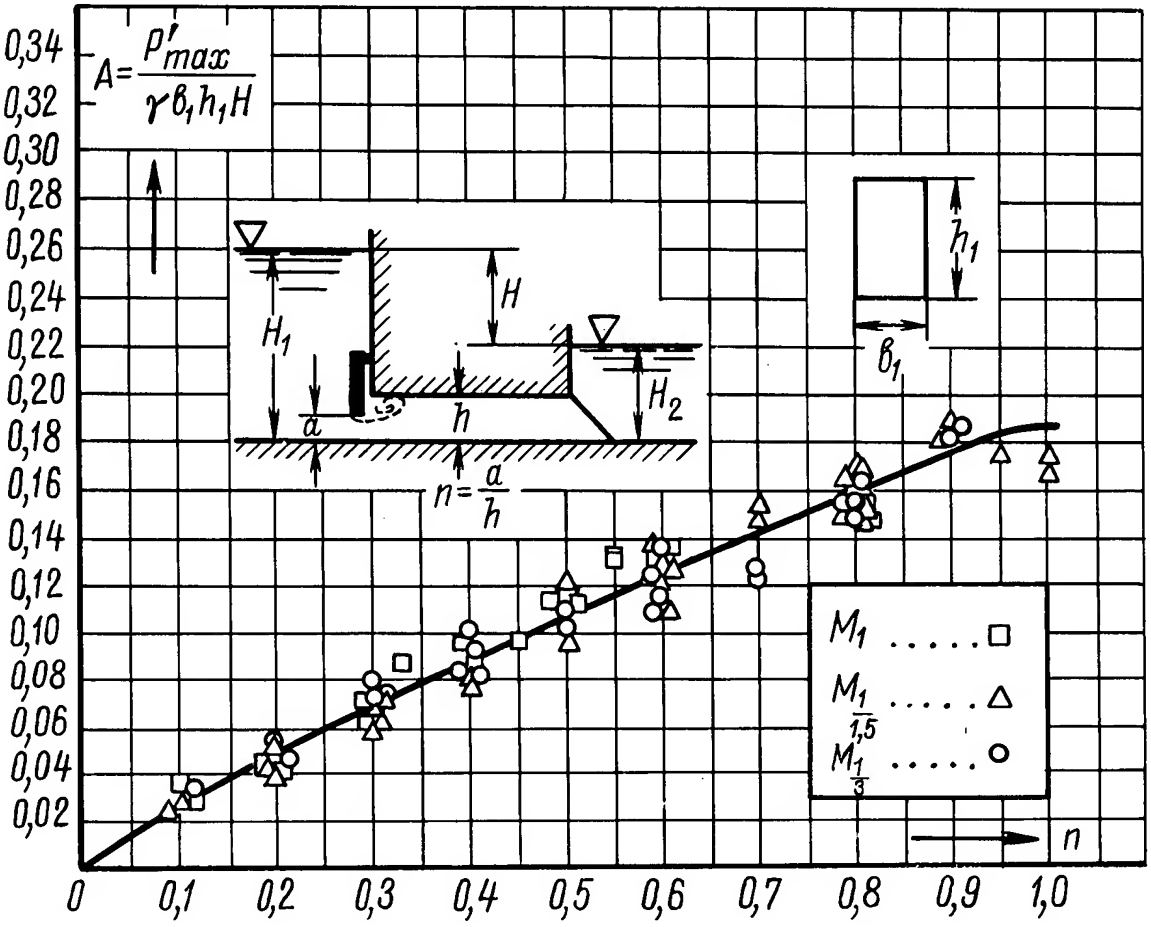

Figure No. 8

Relations A = f (n) plotted according to the experimental data.

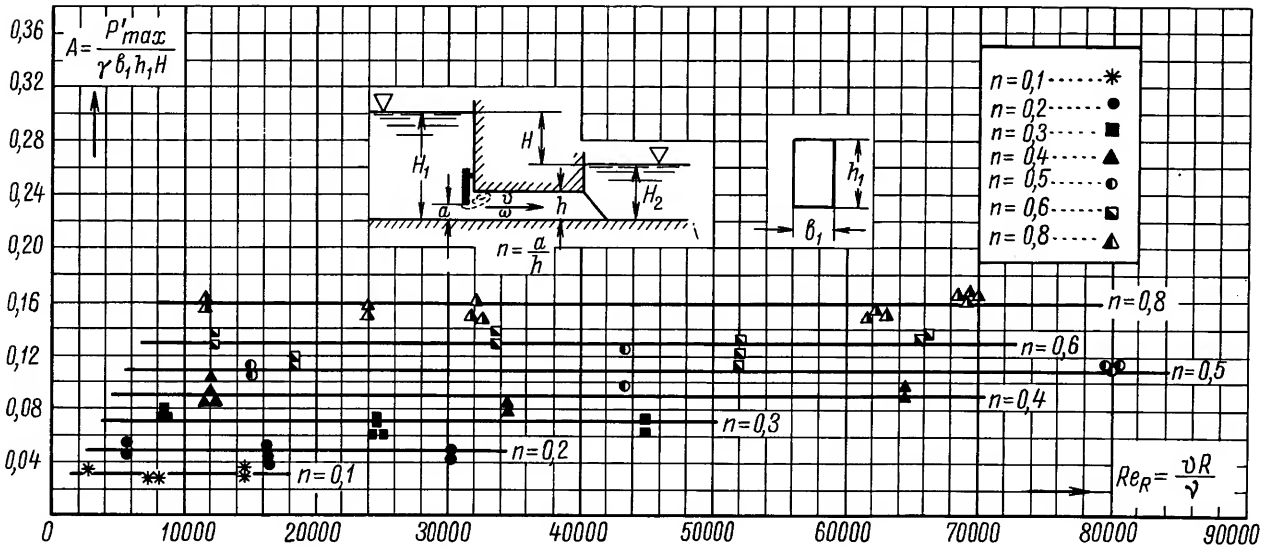

Figure No. 9

Relations $A = f(Re_R, n)$ plotted according to the experimental data.

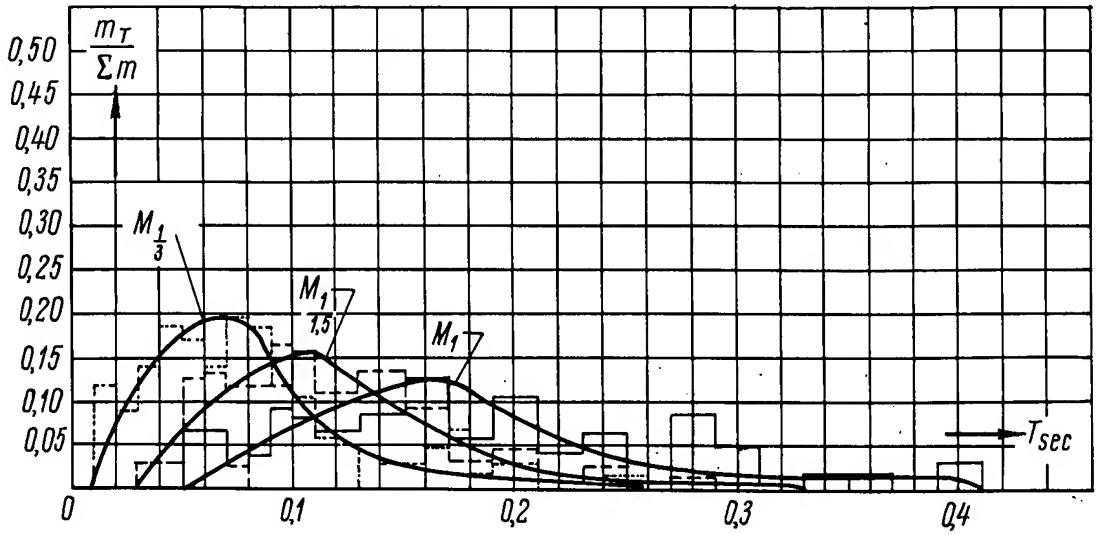

Figure No. 10

Curves of oscillation distribution in periods for pulsations recorded by strain gauges V.

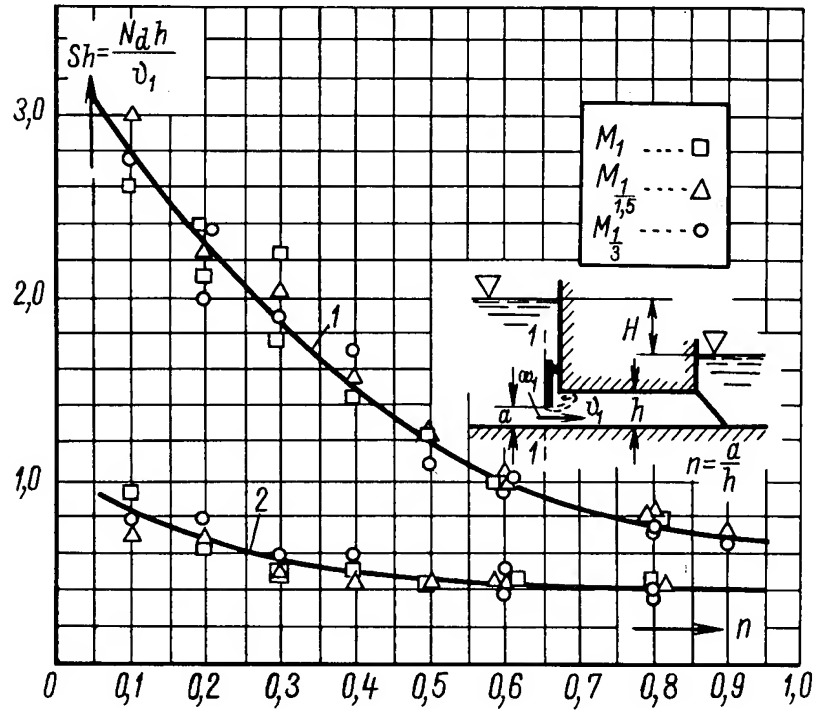

Figure No. 11

Relations Sh = f (n) for pulsations recorded by strain gauges III (or IV); and V or (VI). 1 - pulsations recorded by strain gauges III (or IV); 2 - pulsations recorded by strain gauges V (or VI).

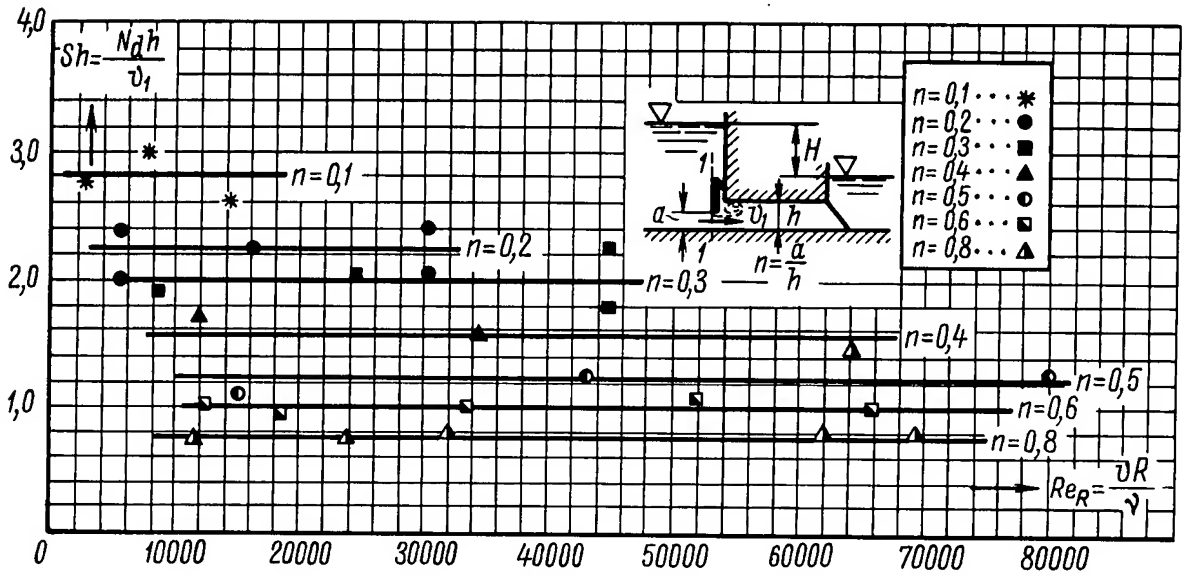

Figure No. 12

Relations Sh = f (Re_R , n) for pulsations recorded on scale models by strain gauges III (or IV).

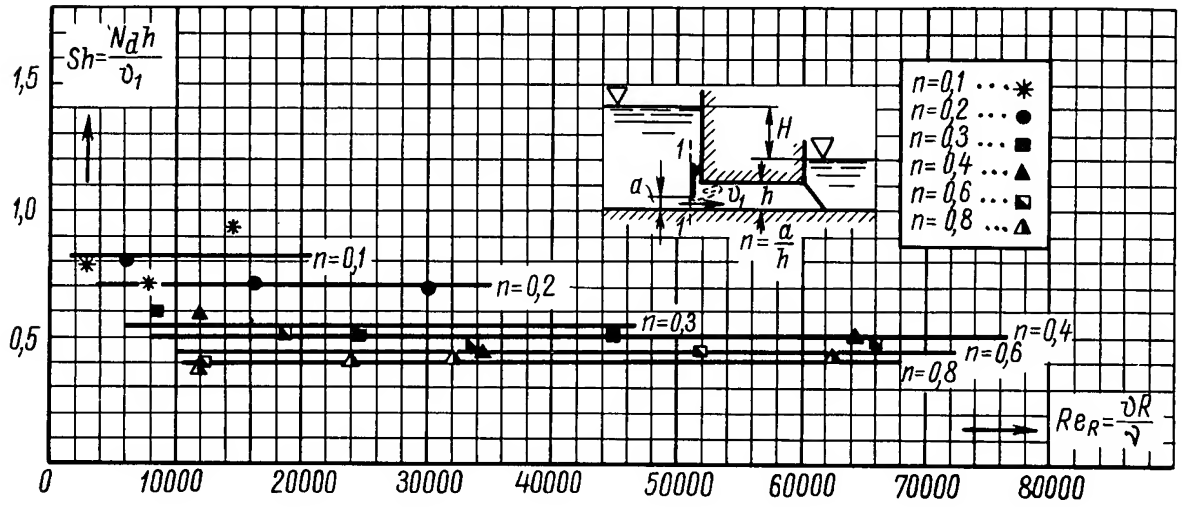

Figure No. 13

Relations Sh = f (Re_R , n) for pulsations recorded on the scale models by strain gauges V (or VI).

Next 18 Page(s) In Document Denied